FURTHER EXPERIMENTS ON THE SEISMIC PERFORMANCE OF STRUCTURAL CONCRETE BEAM-COLUMN JOINTS DESIGNED IN ACCORDANCE WITH THE PRINCIPLES OF DAMAGE AVOIDANCE

A thesis submitted in partial fulfilment of the requirements for the
Degree of Master of Engineering in Civil Engineering
at the University of Canterbury

by

Luoman. Li

Supervised by

Professor John B. Mander

Chair of Structural Engineering

Department of Civil Engineering
University of Canterbury
Christchurch, New Zealand

2006

ABSTRACT

Recent research on jointed unbonded post-tensioned precast concrete frames has demonstrated their superior seismic resistance. Inelastic rotation generated during large earthquake motions is accommodated through gap opening and closing at the beam-to-column connections in the frame. By applying the principles of Damage Avoidance Design (DAD), a steel-steel armoured connection has been demonstrated to be effective in protecting the precast elements from damage. The re-centring ability of the unbonded prestressed post-tensioned system allows the building to return to its original undeformed position after the earthquake with negligible residual deformations.

This research experimentally assesses the biaxial performance of the unbonded precast beam-to-column joint and simplifies the steel-steel armoured connection details in the joint. The experimental results of both quasi-static unidirectional lateral loading tests and biaxial lateral loading tests conducted on a 80% scaled unbonded jointed beam-to-column joint are presented. The performance of the proposed simplified steel-steel connection is assessed.

A theoretical model is developed based primarily on rigid body kinematics and is validated using the test results. A formulation is also developed based on St Vennants' principle, to estimate the effective stiffness of the precast concrete beams under bidirectional rocking. Based on the experimental findings, improvements to the steel-steel armoured connection and joint details are proposed.

ACKNOWLEDGEMENTS

This research was performed at the University of Canterbury Civil Engineering Department, New Zealand, under the guidance of Professor Mander.

I would like to express my sincere gratitude to Professor Mander, my academic and thesis supervisor, for his invaluable guidance and motivation during my research. I also would like to thank him for making available some funding to support my studies. This was provided through the FRST funded "Future Buildings" research project.

I must also thank the laboratory technicians at the University of Canterbury for their help and friendship, especially Tim Perigo, Russell McConchie, John Maley, Stuart Toase, Richard Newton and Kevin Wines.

Thanks to my fellow post-graduate students: Ming Wei Bong; Sue Jian Ji; Darren Yang; Kevin Solberg, Naoto Mashiko, Kathryn Robertson; Brendon Bradley; Lanford Sue and the many others who have been extremely helpful whenever a problem was encountered.

Thanks Firth Industries for donation of concrete for the experimental portion of this project.

I wish to thank my family for their love and support.

TABLE OF CONTENTS

1 Section One: Introduction and Literature Review

1.1 Introduction:

There has been an increase in the use of precast concrete for structural components in buildings in New Zealand over the past 30 years. This is primarily due to precast elements having high quality control, reduction in site formwork, site possession time and a marked increased in speed of construction. Significant increases in the use of precast concrete in moment resisting frames and structural walls started in the mid to late 1980s. Today, precast seismic frames, walls, and flooring system have become the norm for use in buildings throughout New Zealand.

However, outside New Zealand, it has been reported that moment resisting frames and structural walls incorporating precast concrete elements have performed poorly in earthquakes (Hall, 1994; Wyllie and Filson, 1989). It is believed that the poor seismic performance in these precast frames and walls is due to brittle (non-ductile) behaviour of connection details between the precast concrete elements, inadequate detailing of components and outdated design concepts.

To ensure that adequate ductility may be achieved in structures, the capacity design for monolithic concrete structures was developed by New Zealand engineers and researchers and summarised in report by the New Zealand National Society for Earthquake Engineering in the 1970s (Park, 2002). The primary objective of the capacity design of structures for earthquake resistance is to ensure that the structure displays a dependable capacity to accommodate large earthquake imposed displacements and therefore prevent collapse even under severe earthquakes.

In the 1980's, there was a gradual transition away from cast-in-place construction to precast construction. The New Zealand form of precast construction mostly emulates

monolithic (cast-in-place) construction. Plastic Hinge (PH) zones are at beam-ends, away from precast connections.

While recent earthquakes such as Northridge 1994, Kobe 1995, have confirmed the adequacy of capacity design techniques in preventing structural collapse, they have also highlighted the extensive damage levels that can be expected. As a consequence of this extensive damage on building and infrastructure, significant economic losses were incurred due to repair of damage and down-time. There is now much greater demand from clients and the public for engineers to provide structural systems which are designed for preservation of life-safety as a predominant objective. There is also an emphasis on limiting the cost of repairing/reinstating the damaged structure.

In 1990, research commenced in the United States on prestress seismic structure system (PRESSS). Early results of the PRESSS as reported by Cheok and Lew (1993), Stone et al (1995), Priestley and MacRae (1996), and Priestley et al (1999) have shown that precast concrete frames constructed from prestressed segmental elements performed markedly better than conventional frames when subjected to lateral loading. Structural deformations were accommodated via gap openings at the precast component jointed interfaces. Similar strength and interstorey drift capacities were achieved, however damage to the structural elements was significantly reduced and the frames displayed a re-centring capability that resulted in negligible residual displacement.

Mander and Chang (1997) advanced the ideas of rapid jointed precast construction and introduced the concept of Damage Avoidance Design (DAD). Experiments were conducted on rocking bridge columns that demonstrated that it is possible to armour the member ends with steel thereby mitigating high stress concentration in concrete and avoid crushing and splitting. Cyclic loading experiments

demonstrated that all damage could be largely avoided. Moreover due to the unbonded prestress present, recentring of the system could be achieved.

By applying the DAD philosophy to jointed building frames, Davies (2004) and Arnold (2004) have demonstrated that specially designed steel to steel connections at beam to column interface can successfully prevent damage from occurring to the precast components during loading even at 3% drift level. However, by their design, some extensive welding is needed to secure the steel end plates to the reinforcing bars to allow high contact forces to transfer safely from end steel plate into the concrete during rocking action. Moreover, very little tolerance is permitted in manufacture of these precast segments as a precise length is required to ensure adequate force transfer through the jointed connection.

Research described herein is firstly devoted to attempting to simplify the end steel connection in such frame systems and to develop adjustable beam end connections to accommodate construction tolerances. Second, extend previous research by investigating the behaviour of a jointed beam to column connection under biaxial seismic loading. The concept of the jointed frame system and Damage Avoidance Design (DAD) philosophy will be used to design and construct the physical model of beam-column joint subassemblies.

1.2 Literature review

1.2.1 Rocking Motion:

Housner (1963) was the first to study the rocking motion mechanism. He developed an expression that fully describes the amplitude dependent rocking motion of a rigid block in terms of its weight, the mass moment of inertia about its rocking toe and radius to the centre of gravity. Based on the assumption that no bouncing occurred on impact and that the decay of the rocking motion was the result of successive inelastic collisions, a relationship for the dissipation of energy for the rocking mechanism was developed.

Meek (1975) developed a theory for predicting the response of single degree of freedom system with no-tensile capacity rigid foundations using a time-history dynamic analysis approach. From his study, Meek conclude that for certain structures, uplift of the foundation may have a beneficial effect in reducing the maximum lateral displacement and base shear force.

Elgawady et al (2005) studied the rigid body rocking behaviour of nine blocks with different aspect ratio and interface material. Free rocking motion of the test specimens was investigated. It was found that both aspect ratio and interface material properties have significant influence of the free rocking response. Test results were compared to the prediction using the simple rocking motion equation (SRM) developed by Housner (1963). It is found that SRM equation predicts the free rocking motion well in a limited aspect ratio range. Furthermore, the SRM equation showed slower vibration energy dissipation than the measured energy dissipation from the tests.

1.2.2 Precat Post-Tensioned Walls

Kurama et al. (1999) studied the seismic behaviour of a six-storey precast post-tensioned wall structure. The precast wall panels are jointed horizontally via unbonded post-tensioned steel at each floor level. Two type of responses of the rocking wall under lateral load have been identified: (1) flexural gap-opening and (2) shear slip between individual wall panels. A fibre element computer model was developed and four distinct states of behaviour under lateral load were identified-decompression, softening, yielding and failure. Their results demonstrated such jointed wall have the capacity to undergo large displacements with minimal damage. A performed-based seismic design approach for the wall has been established.

Rahman and Restrepo (2000) studied the seismic behaviour of three half-scaled rocking precast concrete wall specimens. All of the wall specimens were jointed to the foundation via unbonded post-tensioned tendons and able to rock under lateral loads. It has been demonstrated that these walls have large drift capacity and the post-tensioning force in the prestressing provides the precast concrete components with a self-centring capability. Furthermore, though appropriate detailing of the concrete reinforcement post-earthquake damage could be mitigated. Supplementary energy dissipator in the form of tension-compression reinforce rods have been installed at base of the walls. The effectiveness of these energy dissipation devices was proven with and equivalent viscous damping ration of 14 percent being observed.

Holden et al (2002) expanded on the research conducted by Rahman and Restrepo. A jointed wall configuration was investigated and comparison made with the performance of conventional ductile monolithic wall system design in accordance with New Zealand Concrete Standard (NZS3101, 1995). Two geometrically identical half-

scaled wall specimens were constructed- the first consistent with current cantilevered ductile design and the second a rocking wall using the Damage Avoidance Design approach (DAD) with unbonded carbon fibre tendons and steel fibre reinforcing. Quasi-static cyclic testing was performed. As expected, the wall designed to emulate monolithic behaviour suffered significant damage after cycling to 2.5% drift. Eventual failure due to buckling was observed followed by fracture of the longitudinal reinforcing. In contrast, the rocking wall performed exceptionally well with drifts over 6% achieved and little damage recorded.

Sudarno (2003) compared the seismic performance between a conventionally designed thin precast concrete wall panels and rocking walls under dynamic loading. A total of three thin (with a height to thickness ration of 60:1) precast wall specimens were constructed: two conventionally designed thin precast concrete wall panel with a longitudinal reinforcing ratio of 1.27% and 0.54% respectively and a third wall with a rocking base connection designed according to DAD principle. Shake table tests were conducted. It was found that both monolithic walls were suffered significant damage and eventually collapsed. Large out-of-plane deformations were observed. In contrast, the rocking wall performed significantly better than the two monolithic walls with limited damage. Moreover, the rocking wall specimen returned to its original up-right position with no sign of residual deformation both in or out-of-plane.

Ma. et al (2005) studied the dynamic behaviour of a rocking concrete masonry wall. The physical experiment results were then compared with the simulation results obtained through three currently used modelling methods namely: (1) Numerical Simulation method (2) Idealised equivalent single degree freedom system with nonlinear elastic rotational base connection (3) Lumped mass system with fibre elements. Their

results highlighted some of the deficiencies in these current models in particularly the difficulties in achieved an accurate modelling of system damping during the course of rocking.

1.2.3 Prestressed Frames with Rocking Connection

Due to the relatively poor seismic performance of precast concrete structures compared to the cast-in-place structures, a multi-phase research programme was initiated at the National Institute of Standards and Technology (NIST) in 1987. The main objective was to develop guidelines for an economical precast beam-to-column connection for regions of high seismic activity. In the first phase of this research programme, Cheok et al (1991) tested four monolithic and two equivalent post tensioned precast concrete beam-to-column joints. From their results, they showed that the post-tensioned precast concrete beam-to-column joint connections was as strong and ductile as the monolithic connection and was a viable connection for high seismic regions. However the post-tensioned precast concrete beam to column connection show less energy dissipation capacity than that of monolithic specimens. Several methods of increasing the energy dissipation of the precast concrete connection were explored in the second and third phase of the NIST programme (Cheok et al, 1993). Six precast concrete specimens were tested. It is found that after moderate ductility levels had been achieved, these tests specimens suffered excessive loss of stiffness at low displacements. This loss of stiffness was thought to be cause by a reduction of effective prestress clamping force through the column, resulting from inelastic strain of the prestressing tendon at the critical section.

Priestley and Tao (1993) proposed the concept of using partially-unbonded prestressing tendons through the rocking beam-column connections to explicitly provide the restoring force. Several dynamic inelastic analyses were carried out on single degree of freedom oscillators of different initial natural periods and hysteretic characteristics which represented partially bonded jointed construction and monolithic construction. They concluded that for longer period structures (T>1.2 seconds) the displacement demand for the partially prestressed system characterised by a bilinear elastic hysteretic response, was similar to that for equivalent monolithic construction.

Using the concept developed by Priestley and Tao (1993), so-called "Hybrid" precast connection that contained both mild steel and post-tensioning (PT) were studied (Stone et al 1995) in the last phase of the NIST programme. A total of 10 hybrid systems with different mild steel and post-tension steel combinations were tested. It was found that a hybrid precast system can be designed to have a similar flexural strength as a conventionally designed monolithic system, yet the hybrid system will suffer less damage than the equivalent monolithic system and exhibit reasonable energy dissipation capacity as well as undergo very large drifts and have self-centring capability.

An analytical study on the seismic performance of moment-resisting precast concrete frames with hybrid connections was undertaken by Cheok et al (1998). The results form the experimental work done at NIST were used to develop a seven parameter computer model describing the behaviour of hybrid precast connections in terms of stiffness degradation, strength degradation and the observed pinching behaviour attributed to opening and closing of cracks or debonding of the mild steel. This hybrid joint model was then used to develop several jointed precast hybrid frame computer models which were tested under a series of earthquake motions. The study concluded that the seismic response of precast concrete frames with hybrid connections were similar to

or better than the seismic response of the concrete frame with monolithic connections in terms of drift demand and failure modes.

El-Sheikh et al (1999) studied the seismic behaviour of two six-story unbonded post-tensioned frames using a fibre and a spring model. Both models offered good agreement with the observed experimental behaviour in terms of initial stiffness and strength. However, both models were found to underestimate the energy dissipation. Based on the assumption that "plane sections remain plane before and after bending", a tri-linear idealisation of the response of the unbonded post-tensioned beam-column connection was proposed. It was found that this idealised tri-linear response gives a good approximation of the true behaviour of the joint.

Mander and Cheng (1997) proposed a new seismic design and construction philosophy called "Damage Avoidance Design" or (DAD) which intended to force damage to occur only in the replaceable "fuse" components of the structure therefore protect the structural system. They investigated the performance of bridge piers designed to rock at the top and bottom of the pier columns under lateral loading. A generalised displacement-based design methodology was proposed based on energy methods used to evaluate the damping of the system based on the energy radiated during each impact of rocking. A complete force-displacement model of the rocking system was developed considering pre-rocking flexibility, rigid body kinematics and accounting for the effect of post-tensioning the pier to the foundation. Their finding showed that the steel armouring at pier end zones effectively prevents damage to the rocking connection at the top and bottom of the pier. Good agreement between the predicted and experimental behaviour of the system was observed.

A joint U.S-Japan research programme on precast seismic structural systems (PRESSS) performed extensive investigation into jointed unbonded post-tensioned beam to column connections. The programme concluded with a test on a five-storey precast concrete building comprising four different ductile structural frame systems in one direction of response and a "hybrid" structural wall system in the orthogonal direction. Both frames and wall performed extremely well with much less damage than equivalent monolithic frame and subjected to same drift demands. Little residual displacement was observed in both frames and walls. The modelling results agree well with the experimental observations.

Pampanin, et al (2001), proposed a section analysis method for the 'hybrid' beam to column connections called "monolithic beam analogy" method. An iterative procedure required to achieve both section equilibrium and member compatibility to evaluate the neutral axis position and concrete strain in a 'hybrid' section. This allowed the connection to be modelled in a non-linear analysis program using two parallel rotational springs that represents the prestress and dissipator moment rotation behaviour respectively. The "monolithic beam analogy" method was validated against the test data form the 'hybrid' post-tensioned beam-to-column connections tested at NIST (Stone, et al 1995). Good agreement between analytical model and experimental data was reported.

Pampanin, et al (2004) studied the behaviour of a gravity-load-dominated one bay frame consisting of draped unbonded post-tensioning tendons and inclined bars. Two different systems: Brooklyn Cable-stayed solution and Brooklyn Suspended solution were tested. It is found that both type of Brooklyn solutions were very efficient and showed a significant increase in overall strength and stiffness when compared to the similar traditional precast solution. Furthermore, both frames also showed significant displacement ductility up to the ultimate limit state and re-centring capability.

Spieth et al, (2004) developed a multi-spring contact element in the finite element program RUAUMOKO to model rocking behaviour of a joint connection. By using this new model in modelling a jointed structure, the self-centring characteristic, the shift of neutral axis position during rocking and elongation of the unbonded positioning during gap opening can be captured. Up to ten parallel spring elements were studied in this new spring element. Good agreement between the comparisons of analytical results with the experimental results was shown.

Murahidy et al, (2004) performed a uniaxial dynamic test of a quarter scaled multi-story jointed precast concrete building. The jointed unbonded precast testing model was constructed according to the current New Zealand Loading standard (NZS4203). Draped tendon profile was selected to improve the performance under serviceability loading. Flexural type supplemental energy dissipators were installed in the structure. The dynamic behaviour of the building was studied. As expected the structure had negligible residual drift at the completion of each test. Computer modelling of the structure were setup using SAP2000 and RUAUMOKO 3D. Reasonably good agreement was found between the test results and modelling.

1.3 Recent Research Works at University of Canterbury, New Zealand.

Recently, a multi-year research programme-Future Building system was initiated at University of Canterbury, New Zealand to develop a new generation of seismic resisting precast concrete structural system using unbonded post-tensioning to joint precast elements together. Following several paragraphs summarise first, the conceptual design developed for such joint precast structure including: general characteristics under lateral loading, energy dissipation, shear transfer, and construction process and second, the experimental findings from two large scaled tests.

1.3.1 General Characteristics of a Jointed Precast Frame

The use of unbonded prestressing in a precast seismic frame enhances its seismic performance by accommodating all inelastic rotation through gap opening and closing at connections rather than through plastic hinge zones. This protects the precast elements from damage and gives building significant economic benefits over the traditional monolithic buildings. In addition, the structure has limited or no residual drift after an earthquake which allows the building to be immediately functional with minimum or no repair. “Dry” connections are used in jointed precast frames as opposed to the “wet” connection used in the traditional emulation of cast-in-place precast construction. This allows all the precast elements to be made offsite in a controlled manufactured environment and assembled onsite with the minimum of labour and cost.

It is well-accepted that a tri-linear idealisation of the response of a precast frame system with unbonded prestressed tendons as shown in Figure1-1 gives good approximation to the true response of a precast frame. Three behaviour limit states exist: (1) the decompression limit state where the initiation of gapping occurs, (2) the linear

limit state where noticeable softening of the structure occurs, and (3) the "yield" limit state where the initiation of proportionality was reached in the post-tensioning steel.

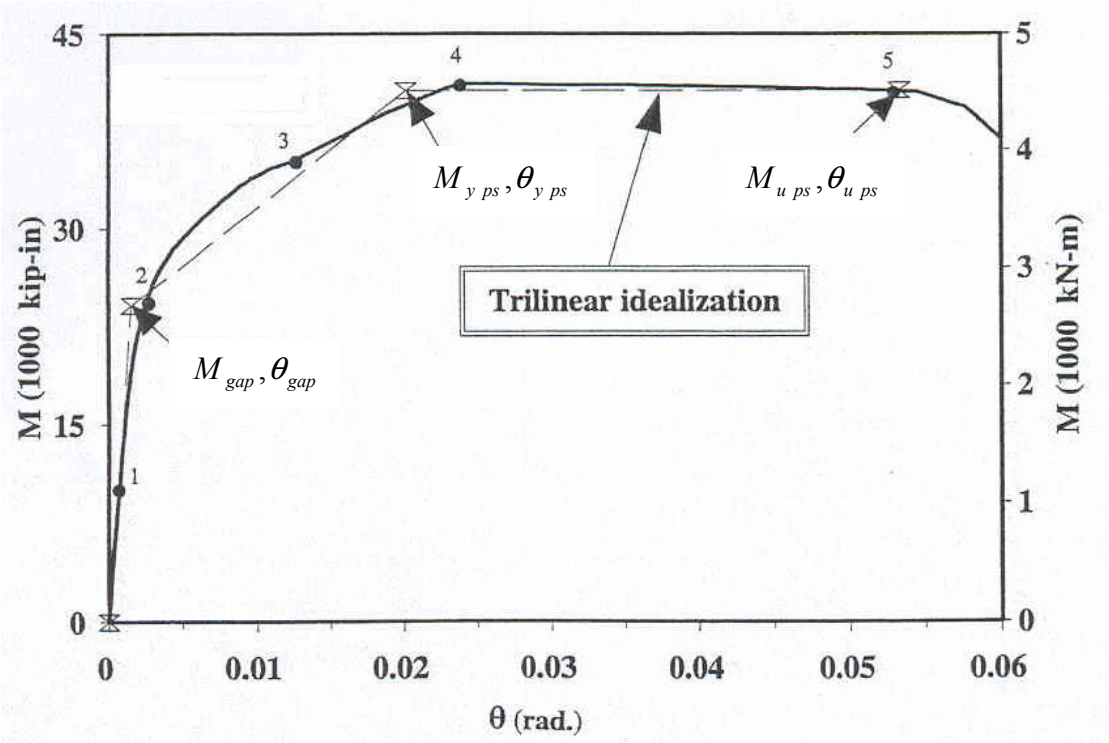

Figure 1-1 An idealised Trilinear moment-rotation behaviour for unbonded post-tensioned beam-column connections. (EI-Sheikh, et al 1999)

1.3.2 Energy Dissipation

Damping provided through hysteretic energy dissipation reduces the maximum response of structures to seismic loading. Large amounts of energy can be dissipated through inelastic rotation of members at the plastic hinge regions in monolithic frames. In jointed precast frame systems with unbonded prestressing steel, the main energy dissipation is through radiation damping of the rocking column surfaces and via friction between the tendon and its ducting. Due to the lesser degree of inherent hysteretic energy dissipation in jointed frame systems, there may be a need to provide supplemental damping to reduce the seismic response. According to Damage Avoidance Design Philosophy (DAD), supplementary energy dissipation should be provided in a way that it does not result in damage to the lateral load resisting system and maintains the re-centring characteristics of unbonded prestressed construction. Therefore, any energy dissipating mechanisms should be either still functional after an earthquake or easily replaceable at a reasonable cost.

Several different types of energy dissipators have been studied such as elastomeric spring dampers (Percassi, 2000), flexural yielding dissipators (Toranzo-Dianderas, 2002), and friction Damper (Morgen and Kurama, 2004). The most common and simple type of the energy dissipator is a threaded fuse rod dissipator (Arnold, 2004). This type of dissipator can be added both externally or internally across a connection (Figure 1-2). The fuse rod will emulate the tension and compression steel layer in a plastic hinge zone of a monolithic frame and yield in tension and compression during rocking, therefore providing extra energy dissipation to the jointed precast frame. It is found that this tension-compression type of dissipator Arnold (2004) is much more efficient than a flexure type of dissipator Davies (2004), due to their relative low stiffness.

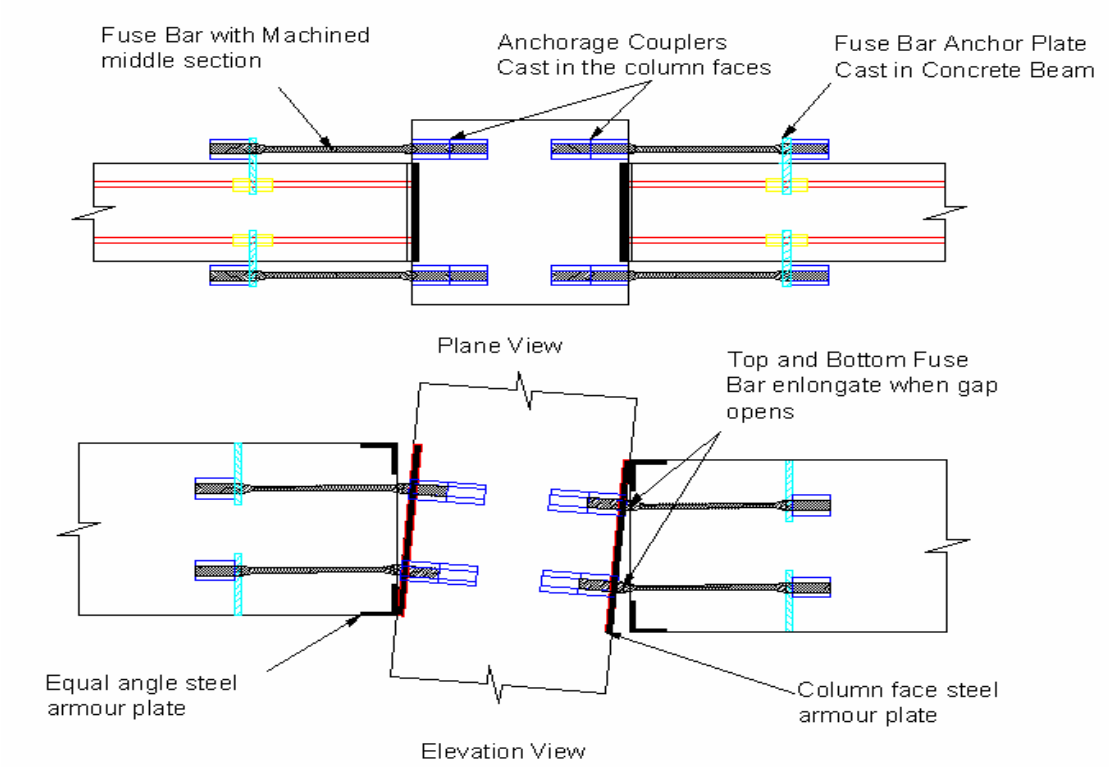

(a) External Fuse Bar Energy Dissipator Layout across connections

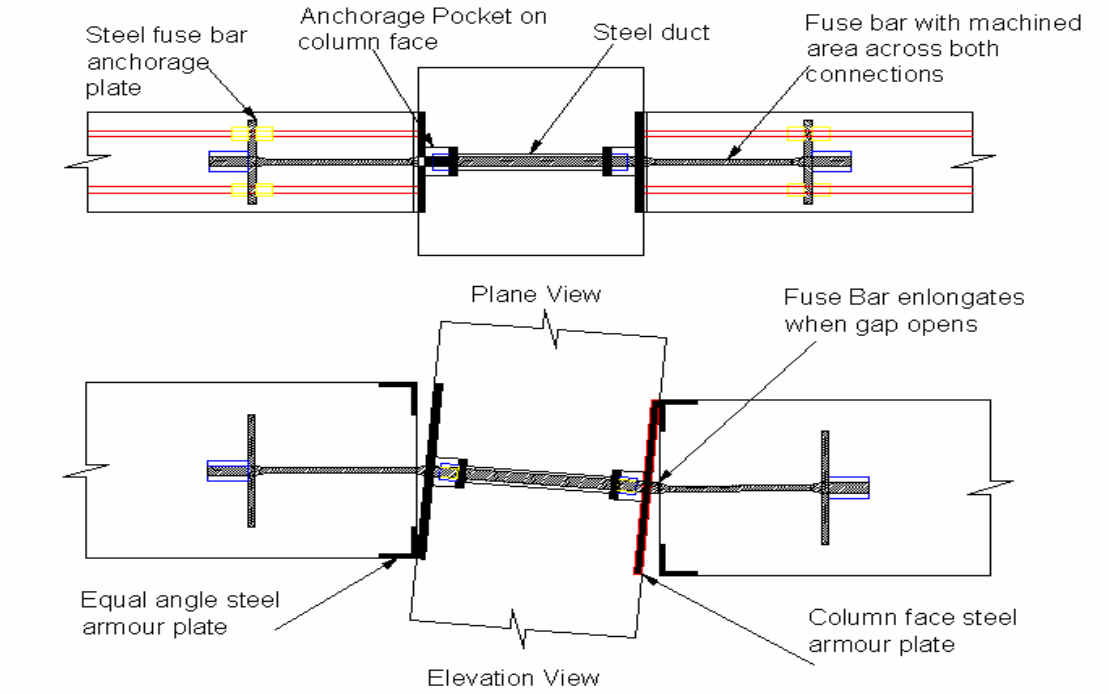

(b) Internal Fuse Bar Energy Dissipator layout across connections

Figure 1-2: **Supplemental energy dissipator layouts in rocking beam to column joint.**

Advantages of threaded fuse rode dissipators are: (1) they can be used as an aid during construction to quickly secure the precast beams into their position. (2) they are capable of adjusting to reduce the need for accurate fabrication. (3) they can be pre-torque to yield in the fuse which will effectively increase their first cycle hysteretic energy dissipation. (4) they are easy to install, replace and inspect.

1.3.3 Shear Transfer

It is important to ensure that adequate shear and torsion can be transferred across the connection, both before and during rocking. In the jointed precast construction, the large clamping force applied across the beam to column connection by the prestress creates reasonably large Coulomb friction forces between rocking interfaces. This can form a primary shear transfer mechanism. However, a contradictory argument has been recently raised up on the possible losses of prestressing due to beam-elongation in multi-storey buildings due to higher mode effects. To eliminate this possible short coming, shear pintles and corbels can be incorporated into connections. With accurate design these shear pintles and coble systems can sustain the self weight of the beam and serve as a temporary supporting system of the beam during construction, therefore eliminating the need of propping and resulting in reduced construction time. Two possible types of shear transfer mechanisms are shown in Figure 1-3.

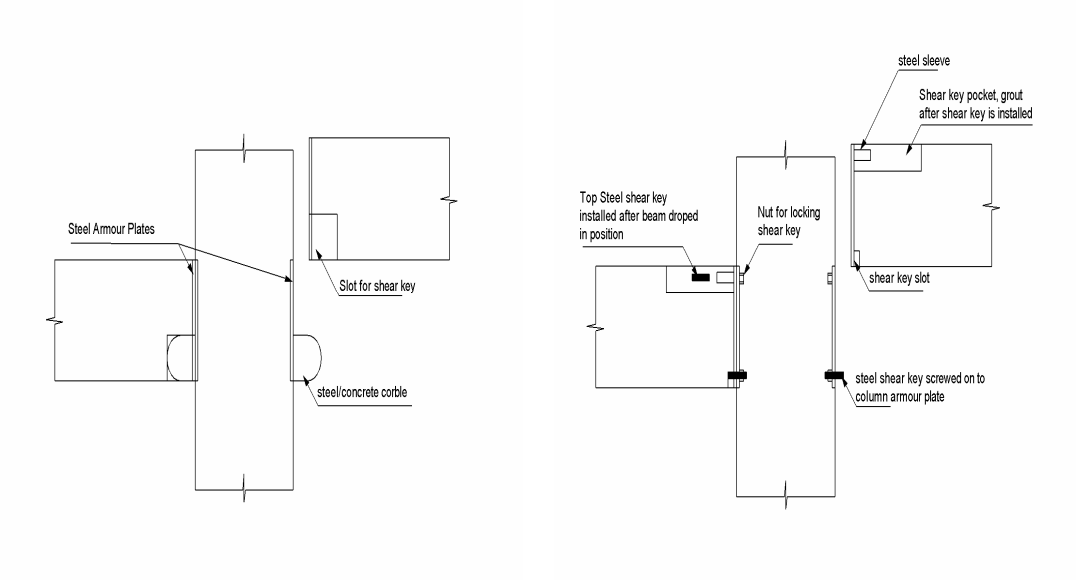

(a) Steel/Concrete Corbel (b) Threaded shear studs.

Figure 1-3: Possible Shear Transfer mechanism for a jointed beam to column joint.

1.3.4 Construction Process

One of the major advantages of using a jointed precast construction over the traditional monolithic construction is the construction speed. With most precast elements manufactured in the factory, minimum amount of on site labour and time is needed to erect the building. Precast seismic designed beams will be dropped between columns and supported by shear keys. Prestress is fed through the frame, and after all precast beams are in place and they are post-tensioned. As like any precast construction a successful jointed precast concrete construction relies on a full understanding of the need for tolerances and the full implications of variation must be developed by designers, fabricators and constructors. One of the critical issues with such jointed construction is to ensure that every beam-to-column connection must be fully engaged after the post-tensioning is applied to ensure the building achieves its designed strength and stiffness. This requires the precast beam element to have very small variation tolerance in their length, thus reducing the construction tolerances of the entire structure. The high requirements needed to manufacture the precast elements may render the mass production impractical and will certainly increase the manufacturing percision and cost. One possible solution is to provide adjustable precast beam elements to accommodate any length variation within the span. An economical way to achieve this is to provide cast-in-situ ends for the beams where steel armour plates and small number of stirrups are installed and cast on-site. In this way any length variation in the manufactured precast beams can be accommodated. To improve the strength of the connections and to also control cracking at the ends of the beam, these cast-in-situ ends should be cast using high strength concrete or fibre reinforced concrete.

1.3.5 Near-full scaled quasi-static tests on jointed precast beam-to-column joint.

To study the seismic performance of jointed precast structural frame systems and to gain the necessary insight and knowledge into the behaviour of such systems to enable provision of future practical design solutions, two large scaled jointed unbonded post-tensioned concrete beam-to-column subassemblies were designed using DAD principles and tested under reversed quasi-static loading at the Civil Engineering Laboratory at University of Canterbury.

The 80% scale beam-to-column subassemblies were selected to represent a typical beam-to-column junction in the seismic-load resisting (Davies, 2004) and gravity load resisting frames (Arnold, 2004) in the lower storey of a 10 storey office building at Christchurch. Both test subassemblies have a column dimension of 600mm square and a beam dimension of 400mm wide by 560mm deep.

In the seismic frame the precast beams were jointed directly on the column face while in the gravity frame the beam-stubs were provided and the rocking connections were set at 600mm away from the column face on both sides of the column. The length of the beam-stubs were selected to represent the width of two typical 1200mm flooring slab sitting side by side and forming a hinging floor plate mechanism.

Steel armour plates were installed at end of precast beams and column face to mitigate high stresses generated during rocking thus protect precast element from damage. A straight tendon profile is provided in the seismic-loading frame while a draped tendon profile is used in the gravity-carrying frame to balance gravity load.

Experimental set-up of both tests is shown in Figure1-4. And more detailed information regarding the two subassemblies was given by Davies (2004) and Arnold (2004).

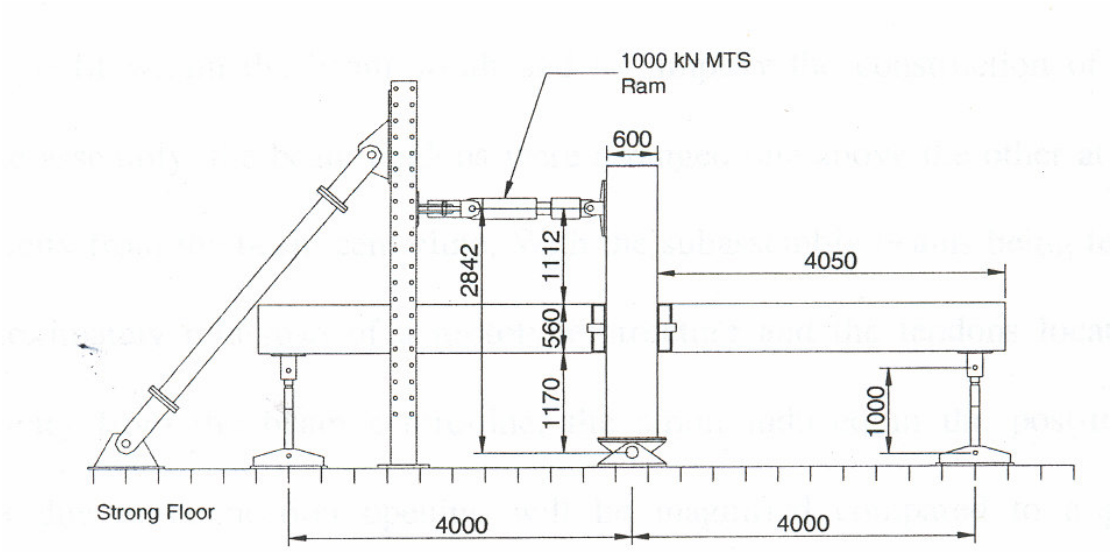

(a) Experiment Setup of the jointed Beam-to-column joint (Davies, 2004)

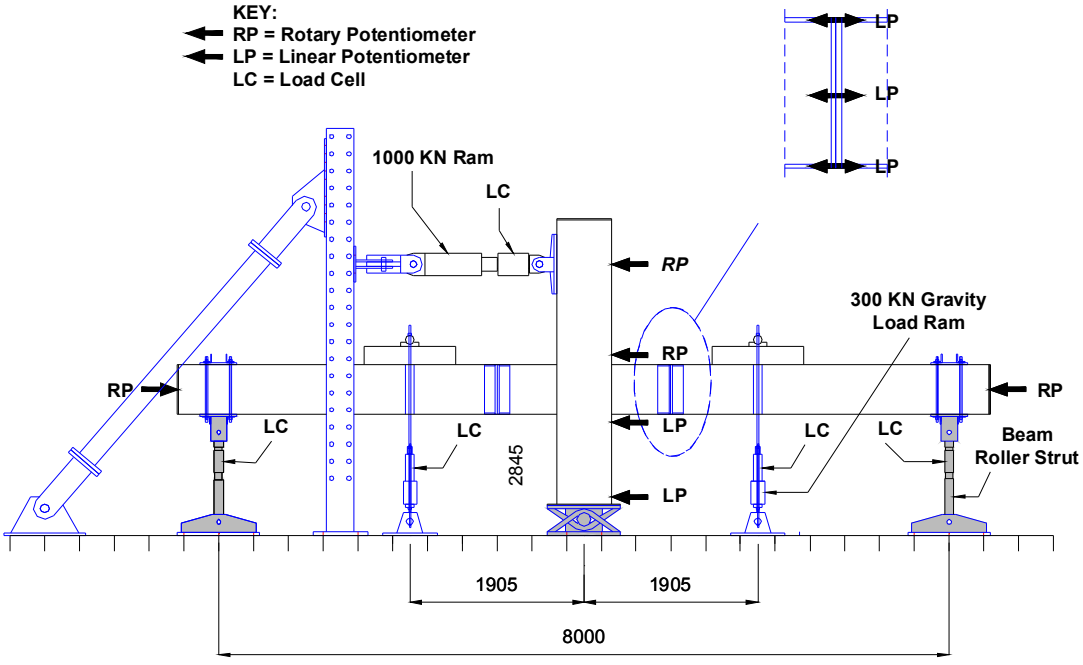

(b) Experiment Setup of the jointed beam-to-column joint (Arnold, 2004)

Figure 1-4 Experiment Set-up of Two armoured unbonded post-tensioned precast beam-to-column joint subassemblies.

Reversed quasi-static tests were performed and test results showed that both subassemblies performed well up to 3% drift level with minor damage. Both subassemblies re-centred with negligible residual drift upon removal of the lateral load. The performance of two types of supplementary energy dissipator namely: tension-compression ('dog-bone') dissipator and flexural ('boomerang') dissipator were investigated using both test subassemblies. A selective summary of their test results are given in Figure1-5.

It was noticed during testing that the small tolerance between the bolt and the slightly oversized holes on the supplementary energy dissipators caused significant pinching in the hysteresis plots (Figure 1-5(c) and (d)) and lowered the total amount of energy dissipation of the joint. To eliminate this misfit between the bolt and the dissipator, the bolts were welded onto the dissipator and subassemblies were tested again. Significant improvement in the subassembly performance was noted (Figure1-5(e) and (f)) It was found that the performance of the systems is very sensitive to the level of contact force at the armoured connection and the tolerances in the connections of the external energy dissipators. The zero tolerance required in construction of such system was recognised as impractical and further study is needed.

The tests demonstrate that tension-compression type dissipator (Figure 1-5 (e) and (f)) seem to perform better (12% equivalent viscous damping at 3% drift) than the flexure type energy dissipator (Figure1-5 (a) and (b))which had a 6% equivalent viscous damping at 3% drift.

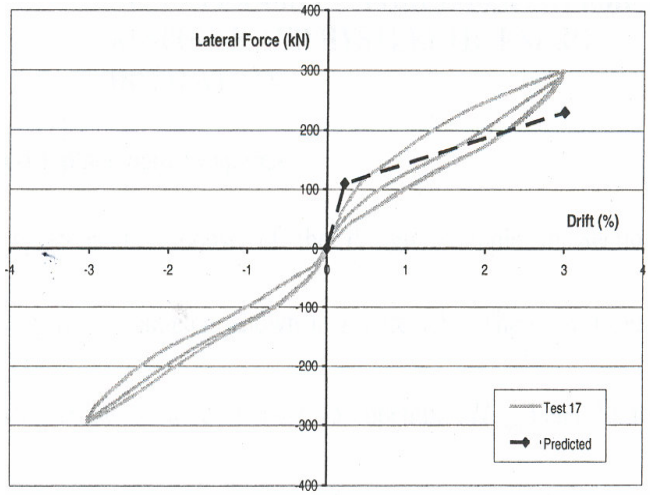

(a) 'Boomerang' Dissipators (Davies, 2004)

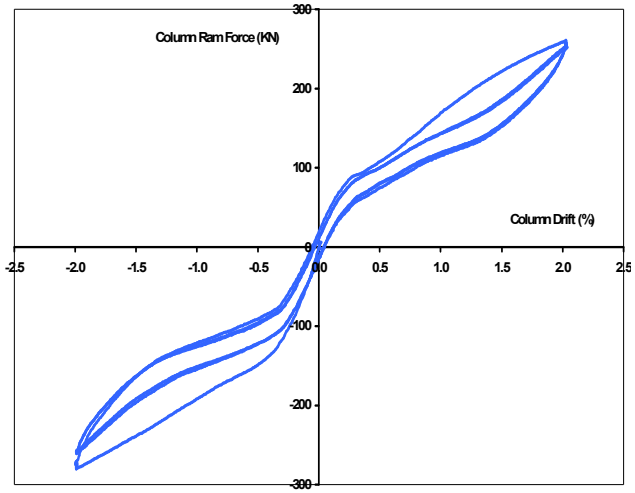

(b) 'Boomerang' Dissipators (Arnold, 2004)

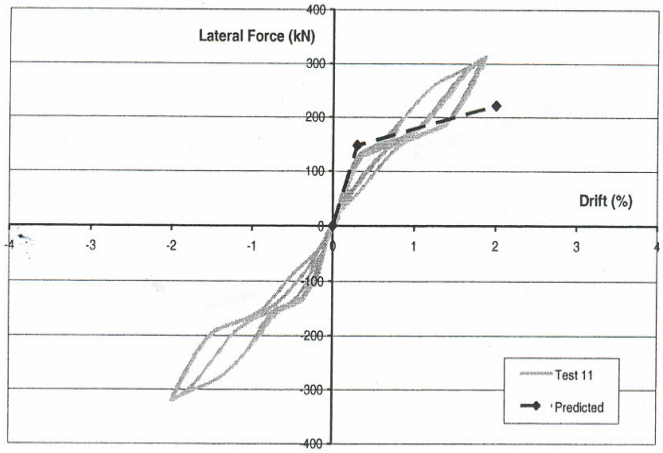

(c) Bolted 'Dog-bone' Dissipator (Davies, 2004)

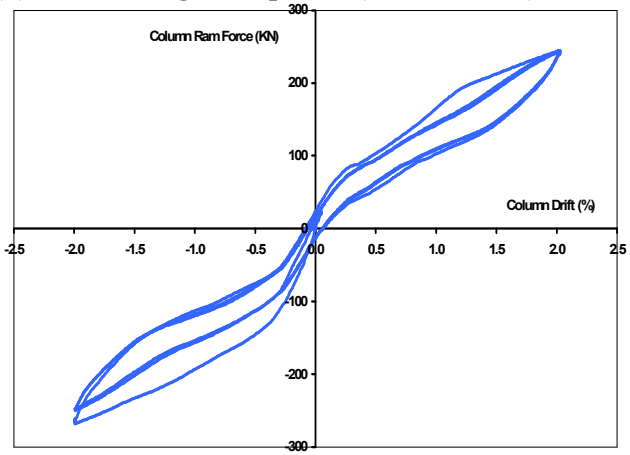

(d) Bolted 'Dog-bone' Dissipator (Arnold, 2004)

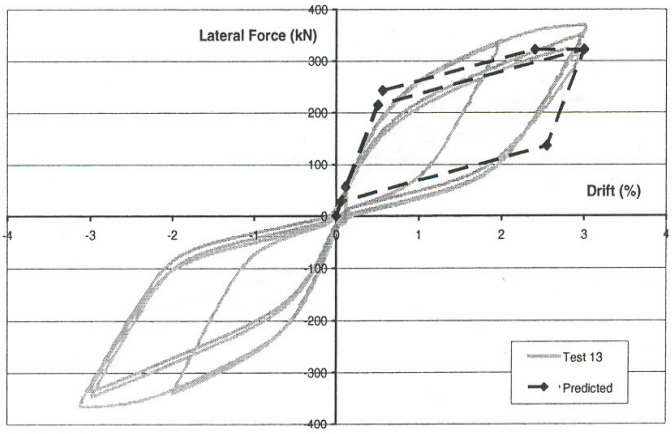

(e) Welded 'Dog-bone' Dissipators (Davies, 2004)

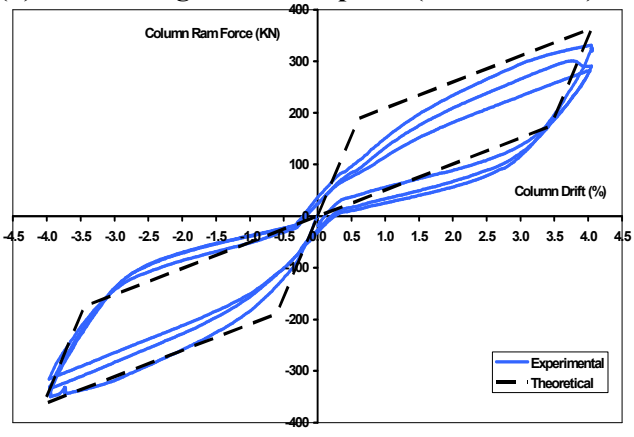

(f) Welded 'Dog-bone' Dissipators (Arnold, 2004)

Figure 1-5: A selective summaries of test results of two jointed unbonded post-tensioned precast concrete beam-to-column joint subassemblies (Davies, 2004 and Arnold, 2004)

Both studies concluded that it was possible to prevent precast elements from damage by using steel armour plate to achieve the DAD requirements in designing a post-tensioned unbonded jointed precast system. However the research also pointed out that a more practical design solution needs to be developed. Such a solution is one of the principal aims of this thesis.

1.4 What's particularly new in this thesis?

As discussed above, many experimental studies have been conducted on jointed unbonded post-tensioned precast concrete beam-to-column joint under unidirectional loading, however, the behaviour of the jointed beam-to-column joint under concurrent bidirectional loading has not been studied.

In this research, quasi-static bidirectional tests are performed on a near full (80%) scaled unbonded post-tensioned precast concrete beam-to-column joint subassembly designed according to the Damage Avoidance Design principle. To simplify the steel-steel connections and to reduce manufacturing costs, equal flanged steel angles are cast at ends of the precast beams. In preventing the potential problems of slip and out-of-plane rotations at the jointed connections, tapered shear keys are installed at column faces. In attempting to ease the construction and lower the tolerance requirements in manufacturing the precast beam, an adjustable beam end is developed.

1.5 Outline of the thesis

The study is separated into four main sections outlined as follows:

Section 1 gives a general introduction on the topic of the unbonded jointed precast concrete construction. Relevant previous research studies are summarised and presented.

Section 2 presents the theoretical development of the rocking connection addressing several issues including: load balancing, shear and torsion transfer mechanisms, energy dissipation, re-centring capacity, and construction tolerances. Five jointed precast seismic frames with different tendon profile and connection details are then proposed based on a seismic Damage Avoidance Design (DAD) philosophy.

Section 3 experimentally investigates the seismic performance of a near full scaled beam-to-column joint under both unidirectional and bidirectional quasi-static lateral loading. The theoretical model developed in section 2 is verified.

Section 4 utilises the experimental results generated in section 3 to attempt to further improve the connection details. A reversed equal flange steel armour end is proposed for the rocking connection. Major future research areas have been discussed.

1.6 Reference:

Arnold, D.M (2004). *Development and Experimental Testing Of a Seismic Damage Avoidance Designed Beam to Column Connection Utilising Draped Unbonded Post-Tensioning* Masters, Thesis, Department of civil Engineering, University of Canterbury, Christchurch, New Zealand.

Cheok, G.S. and Lew, H.S. (1991), *Performance of precast concrete beam to column connections subject to cyclic loading.* PCI journal, Vol. 36 ,No.3, pp56-67.

Cheok, G.S, Stone, W.C. and Kunnath, S.K (1998), Seismic Response of Precast Concrete Frames with Hybrid Connections. ACI Structural Journal, V.95, No5, pp527-539.

Davies, M.N (2004) *Seismic Damage Avoidance Design of Beam-Column Joints using Unbonded Post-Tensioning: Theory, Experiments and Design Example.* Masters, Thesis, Department of civil Engineering, University of Canterbury, Christchurch, New Zealand.

EI-Sheikh, M., Sause, R., Pessiki, S. and Lu, L.-W. (1999), *Seismic Behaviour and Design of Unbonded Post-Tensioned Precast Concrete Frames*. PCI journal, v44, No3 1999, P54-71.

Elgawady, M., Ma, Q., Ingham, J., and Butterworth, J.,(2005) *Experimental Investigation of Rigid Body Rocking* The New Zealand Concrete Industry Conference, Auckland, NewZealand.

Hall, J.F.(Editor) *"Northridge Earthquake of January 17, 1994, Reconnaissance Report Vol.2."*Supplement to Vol.11, Earthquake Spectra, 1995.

Holden, T.J., Restrepo, J.I., Mander, J.B. (2003). *Seismic Performance of Precast Reinforced and Prestressed Concrete Walls,* Journal of Structural Engineering, Vol.129, No. 3, pp 286-296.

Houser, G.W (1963). "*The Behaviour of Inverted Pendulum Structure during Earthquakes*, Bulletin of the Seismological Society of America, vol. 53, No.2, pp. 403-417, February 1963.

Kurama, Y., Sause, R., Pessiki, S., and Lu, W-L (1999) *Lateral load Behaviour and Seismic Design of Unbonded Post-Tensioned Precast Concrete Walls*. ACI structural Journal, vol.96, No.4, pp622-632.

Ma, Q.T. Wight, G.D. Butterworth, J.W. and. Ingham, J.M. (2005), *Predicting the In-Plane Rocking Behaviour of Post-Tensioned Concrete Walls Subjected to Earthquake Excitations*, The New Zealand Concrete Industry Conference, Auckland 2005.

Mander, J.B., and Cheng, C.T. (1997). *Seismic Resistance of Bridge Piers Based on Damage Avoidance Design*, Technical Report NCEER-97-0014, Department of Civil, Structural and Environmental Engineering, State University of New York at Buffalo, New York, USA.

Meek, J.W. (1975). *Effects of Foundation Tipping on Dynamic Response*, Journal of the Structure Division ASCE, vol.101, No. ST 7, July 1975, pp 1297-1311.

Morgen, B.G. and Kurama, Y.C. (2004) *A Friction Damper For Post-Tensioned Precast Concrete Moment Frames,* PCI journal, v49, n 4, July/August, , p112-133.

Murahidy, A.G, Carr, A.J, Spieth, H.A, Mander, J.B and Bull (2004), D.K. *Design, construction and dynamic testing of a post-tensioned precast reinforced concrete frame building with rocking beam-column connections and ADAS elements*. Paper 31, 2004 NZSEE conference.

Park, R (2002) *Seismic Design and Construction of Precast Concrete Buildings in New Zealand*, PCI journal vol.47,no.5, September/October,pp60-75.

Pampanin, S., Priestley, N.J., and Sritharan, S. (2001). *Analytical modelling of the Seismic Behaviour of Precast Concrete Frames Designed with Ductile Connections*, Journal of Earthquake Engineering, Vol.5, No.3, pp329-367.

Pampanin, S., Pagani, C., and Zambelli, S.,(2004) *Cable-Stayed and Suspended post-tensioned Solution for Precast Concrete Frames: The Brooklyn System*. Proc of NZ Concrete Industry Conference, Queenstown.

Percassi, S.J.(2002). *Rocking column Structures with Supplementary Damping Device*, M.S.Thesis, State University of New York at Buffalo, New York, USA.

Priestley, M.J.N. and MacRae, G.A., (1996). *Seismic Tests of Precast Beam-to-Column Joint Subassemblages with Unbonded Tendons*, PCI Journal, January/February, 1996, pp. 64-81.

Priestley, M.J.N., Sritharan, S., Conley, J.R., Pampanin, S. (1999). *Preliminary Results and Conclusions from the PRESSS Five-Storey Precast Concrete Test Building*, PCI Journal, Vol. 44, No. 6, pp 43-67.

Priestley, M.J.N. and Tao, J.R.T. (1993). *Seismic Response of Precast Prestressed Concrete Frames with Partially Debonded Tendons*, PCI Journal, vol. 38, no.1, p.58-69.

Rahman, A. and Restrepo, J.I., (2000) *Earthquake Resistant Precast Concrete Buildings: Seismic Performance of Cantilever Walls Prestressed Using Unbonded Tendons*. Research Report 2005-5, Department of Civil Engineering, University of Canterbury, New Zealand.

Surdarno, I., (2003). *Performance of Thin Precast Concrete Wall Panels under Dynamic Loadings*, ME thesis, University of Canterbury, New Zealand.

Spieth, H.A, Arnold, D. Davies, M., Mander, J.B, and Carr, A.J (2004). *Modelling of post-tensioned precast reinforced concrete frame structure with rocking beam-column connections*. Paper 32 2004 NZSEE conference.

Stanton, J.F., Stone, W.C. and Cheok, G.S. (1997). *A Hybrid Reinforced Precast Frame for Seismic Regions*, PCI Journal, vol. 42, pp. 20-32.

Stone, W.C., Cheok, G.S., and Stanton, J.F. (1995), *Performance of hybrid moment-resisting precast beam-column concrete connection subjected to cyclic loading,* ACI Journal, Vol. 91, No, 2 March-April.

Toranzo-Dianderas,L.A.(2002). *The use of rocking walls in Confined Masonry Structures: a Performance Based Approach*, PHD. Thesis, Department of Civil Engineering, University of Canterbury, Christchurch, New Zealand.

Wyllie, L.A., and Filson, J.R., *"Armenia Earthquake Reconnaissance Report"* Earthquake Spectra, Special Supplement, EERI Pub. 89-101, Aug.1989, 175pp.

2 Section Two: Theoretical Behaviour of a Rocking Connection.

Section Summary

Five jointed precast seismic frames with different tendon profiles and connection details are proposed based on a seismic Damage Avoidance Design (DAD) philosophy. The precast beams and columns are designed elastically with the non-linear response of the systems provided by gap opening at the connection between the precast units. A steel-to-steel rocking connection is designed to protect the concrete from crushing. Steel angles are used as armour in the corners of the beam ends. The purpose of armouring is to confine the concrete and mitigate the high point force resulting from the rocking motion of the beam to column connection when the system is under seismic sideway. With only prestressing tendons, these jointed systems have limited energy dissipation capability therefore thread-bars are used to provide some supplementary energy dissipation to the frame. A theoretical model of the connection moment-rotation behaviour and lateral force-displacement response is proposed based on rigid body kinematics. The flag shaped hysteresis of the jointed frame is a combination of the nonlinear elastic behaviour of the tendon due to gap opening and the elasto-plastic behaviour of the supplemental energy dissipators. Also derived is a formulation of the maximum displacement (drift capacity) before re-centring is lost due to yielding of the tendon.

2.1 Introduction

Research reported by Cheok and Lew (1993), Stone et cal (1995), Priestley and MacRae (1996), and Priestley et al (1999) on the unbonded jointed post-tensioned precast concrete system have demonstrated the superior seismic performance potential of these systems. Compared to the traditional reinforced construction and traditional "emulation of cast-in-place approach" of the precast construction, jointed precast construction allows faster construction through minimising site labour and cost. By applying the DAD principles developed by Mander and Chang (1997) it is possible to prevent the precast concrete elements from suffering damage during a large earthquake. This will greatly reduce the post earthquake down-time of the structure and thus have considerable economic advantage over the traditional buildings. Also, the unique re-centring characteristic of these jointed systems provided by the unbonded prestressing tendons allows members to return to their original position. This therefore permits the building to be functional after the earthquake. However as it was demonstrated in the previous section, more research work has to be conducted before this new jointed construction system can be widely used in the construction industry.

Depending on their function, frames in buildings are usually classified into two broad categories: (i) Lateral load-resisting frames; and (ii) Gravity load-resisting frames. To resist lateral loads arising from wind and seismic effects, Lateral load-resisting frames are usually placed around the perimeter of the building or along a particular direction within the building. These frames are detailed according to the capacity design philosophy to ensure that a strong column–weak beam mechanism forms. Therefore collapse of the building in the event of a strong earthquake is prevented. Unlike the lateral load-resisting frames, the primary function of a gravity

load-resisting frame is to support the dead load and live load within the building. Floor slabs and non-structural (partition) walls are supported by these frames. As well as carrying gravity loads, the gravity load-resisting frame must be capable of maintaining the lateral sidesway induced by seismic effects.

In jointed precast frames both the lateral load resisting and gravity load carrying function can be achieved through prestress using unbonded post-tensioned tendons. These may be provided by woven high tensile strand (f_{pu}=1800MPa) or high strength high-alloy threadbars (f_{pu}=1100MPa). Using the above mentioned concept, five different jointed precast frame solutions are proposed for seismic resistant buildings and are evaluated in this section. A theoretical model of the rocking beam-to-column joint is also developed using a rigid body rocking kinematic mechanism.

2.2 Proposed Design solution for armoured jointed frames

2.2.1 Straight Tendon with though joint diagonal fuse connectors

As depicted in Figure2-1 (a), the seismic frame is made up of precast beam segment with straight tendon profile and diagonal fuse connectors. This allows the frame to not only carry lateral load but also balance a portion of gravity load. With adequate design, the ductile diagonal connector fuse-bars will protect the tendon from yielding. Damage is therefore restricted to the yielding of the external energy dissipators which can be easily replaced with minimum amount of labour and cost. Because each beam is connected to a column through a separate connector, each span can be stressed separately and provide extra redundancy in the unlikely case of prestress or anchorage failure. Adjustable beam-ends are cast in-situ at ends of each span allowing any variation on precast beam length to be accommodated. When loaded laterally, a gap at

the beam to column interface next to the column face will open and stretch the unbonded tendons through the entire beam span (Figure 2-2(a) and Figure2-3 (a)). This generates a high rocking force at top of the connection. In order to safely transfer this rocking force through the connection and into the precast beam segment, steel armour plates are cast in the beam ends and column faces respectively.

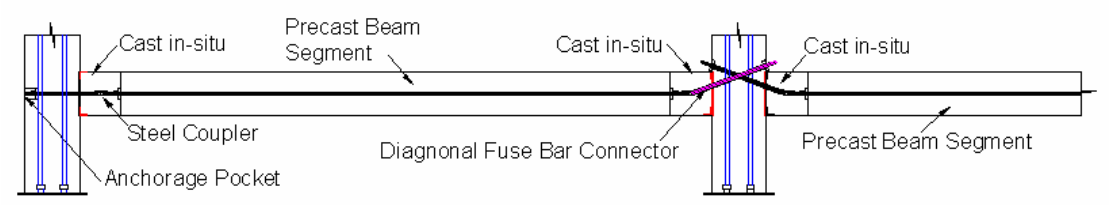

(a) Straight Tendon Solution with through joint diagonal fuse connectors

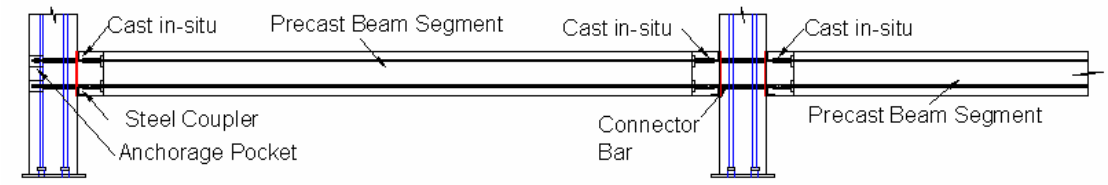

(b) Straight tendons and through-bolt solution

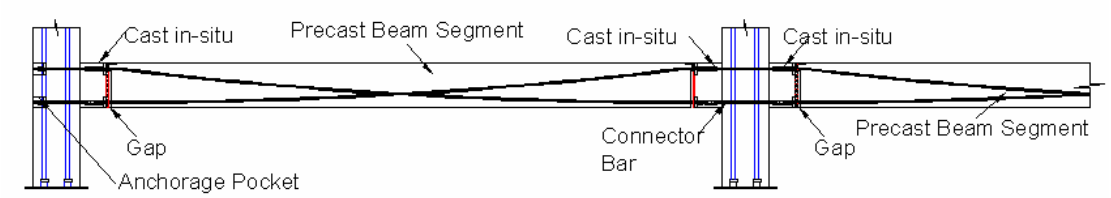

(c)None-tearing solution with draped tendons

(d) Diagonal tendon profile solution with through joint diagonal fuse connector

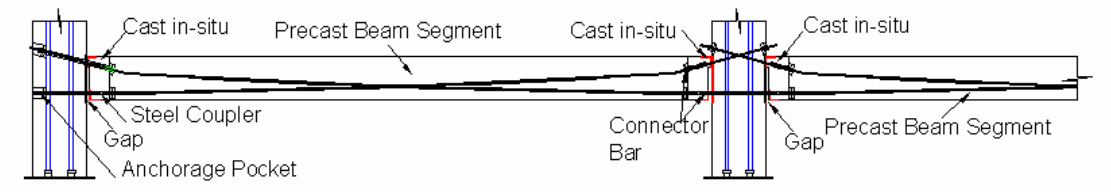

(e) None-tearing solution with diagonal tendon profile.

Figure 2-1: Potential solutions for connection precast prestressed beams to columns.

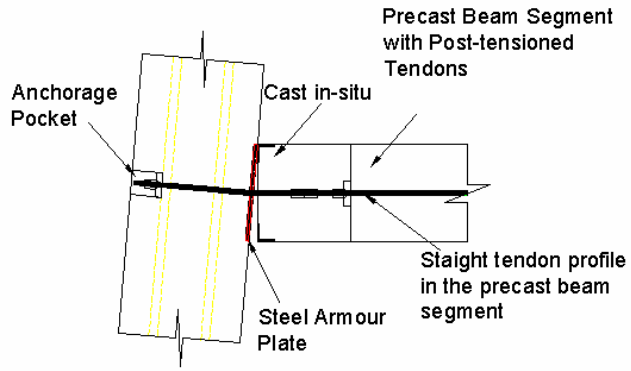

(a) Straight tendon solution with through joint dagonal fuse connetors

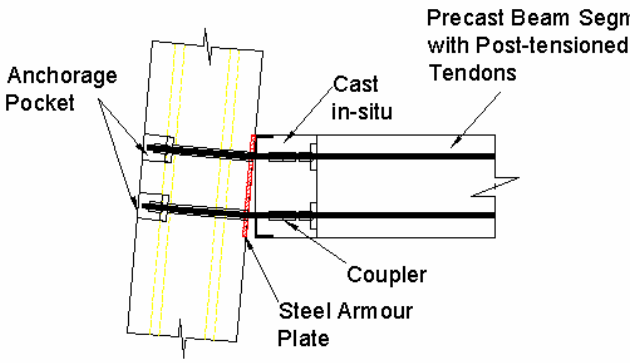

(b) straight tendons and though bolts solution

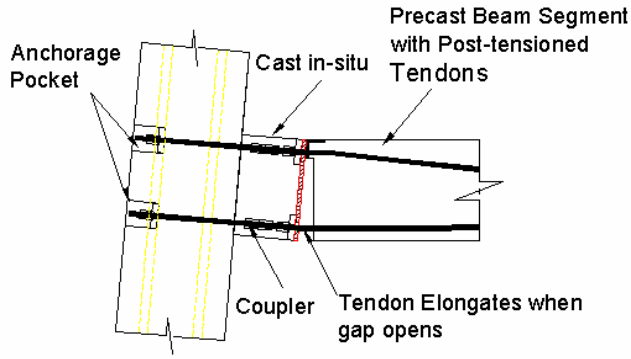

(c) Non-tearing solution with draped tendons

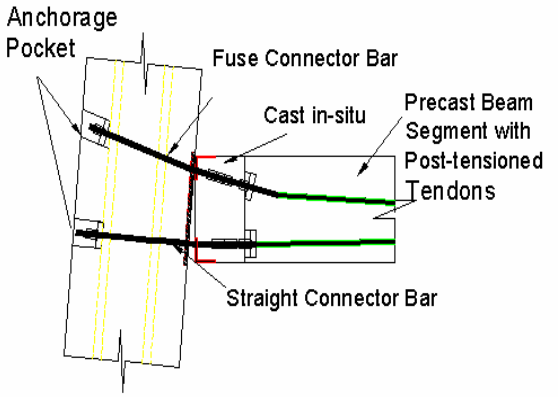

(d) Diagnonal tendon profile solution with through joint diagonal fuse connector

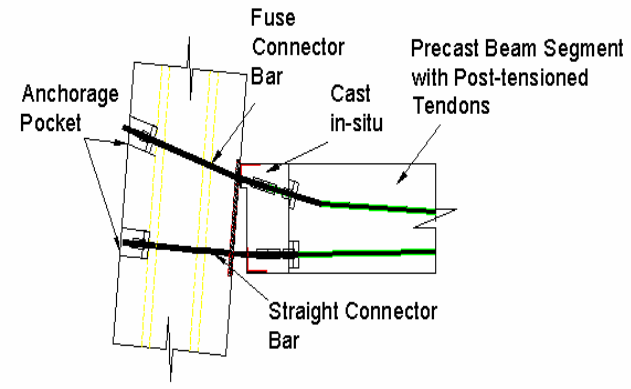

(e) Non-tearing solution with diagonal tendon profile

Figure 2-2: Exterior joint details of the proposed frame solutions.

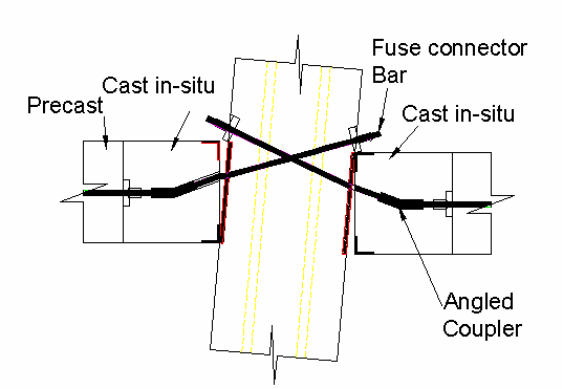

(a) Straight tendon solution with through joint diagonal fuse connectors

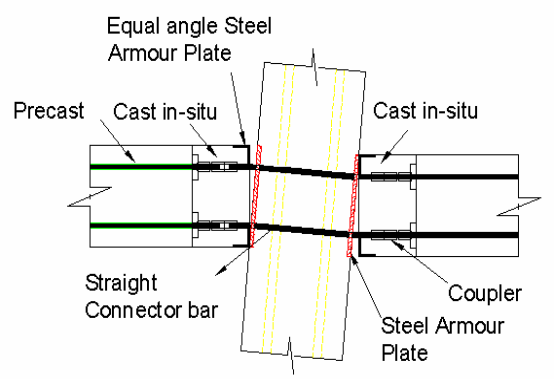

(b) Straight tendons and through bolts solution

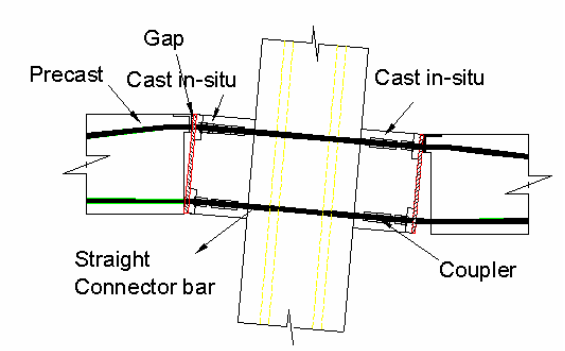

(c) Non-tearing solution with draped tendons

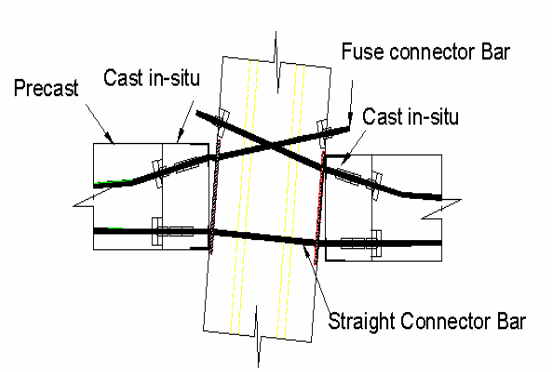

(d) Diagonal tendon profile solution with through joint diagonal fuse connectors

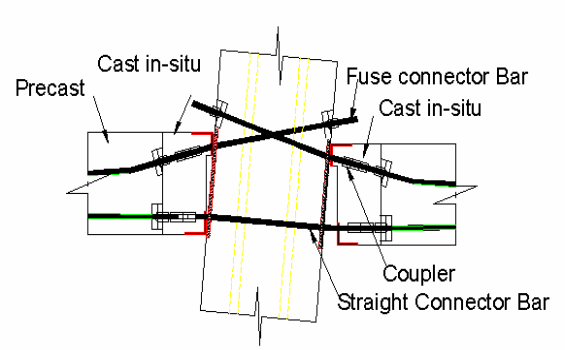

(e) Non-tearing solution with diagonal tendon profile.

Figure 2-3: Interior joint details of proposed frame solutions.

2.2.2 Straight tendons with through-bolt solution

To resist lateral load only, a straight tendon profile can be used as shown in Figure2-1(b). Two unbonded tendons are eccentrically placed about the neutral axis of the beam. The precast beam segments are connected together through the column via two straight connector bolt bars. In the interior joints, the straight unbonded connector bolts connect the unbonded tendons of two adjacent beams via couplers. At the exterior joints, the beam tendons are anchored on the outer face of the column via connector bolts through the column. When under lateral loading, the joint opens at the column face and the tendons elongate as shown Figure2-2(b) and Figure2-3(b) for exterior and interior joints respectively.

If the mid section of each connector bolt is machined down to a smaller diameter, then sacrificial "fuse-bars" are formed. When post-tensioned to near yield, these fuse-bars will maximize the total energy dissipation of the frame system during the first cycle after the lateral force exceeds the yield strength of the frame. Such a design enhances the seismic performance and resistance against the "near-field" earthquakes. Other supplementary energy dissipators could also be installed across the connections in the frame.

Traditional prestressing strands can also be used. The strands can be fed through the entire building span and post-tensioned afterwards. While the energy dissipation of the system is relies solely on the external or internal supplementary energy dissipator installed in the system. The benefit of this system is its simplicity and ease of construction.

2.2.3 Non-tearing solution with draped tendons

By providing a partial gap at the ends of a precast beam segment in the seismic resisting frame as shown in Figure2-1(c), the precast beam segments are able to remain horizontal (no vertical displacements) when the frame is subjected to lateral loading. This minimizes damage to the floor units that are cast on top of the beam segment. However the effective stiffness of the beam segments will be reduced in such frames. This reduction in effective beam stiffness due to the dispersion of concentrated force at the rocking joint will reduce the lateral resistance of the entire frame. Adequate evaluation of the effective stiffness of such beam is therefore necessary.

It is important in such systems that the tendons run diagonally between the two rocking connections, as this ensures all tendons will experience sufficient elongation during gap opening and therefore provide adequate lateral resistance for the frame. Straight connector bars are used to connect the tendons of adjacent beams through columns. To balance some gravity load, tendons may also be draped in this frame system. As shown in Figure2-3(c) when under lateral loading, the jointed connection of an interior beam-to-column joint will open at one side of the column as the beam segment rotates about the top edge while at the other side of the column, the gap will close. In the exterior joint Figure2-2(c), the draped tendons are anchored on the outer face of the column through two connector bars.

2.2.4 Diagonal tendons profile with through joint diagonal fuse connectors

To balance gravity load, straight tendons are placed diagonally inside the precast beam element as shown in Figure2-1(d). Straight fuse connectors are used to connect adjacent precast beams through the column. The advantage of using these fuse connectors are: (1) protection of the main tendons in the beam and (2) can be easily replaced when damaged after an earthquake. If traditional prestressing strands were used, they can be fed through the beam after they have been dropped in place. Less cast-in-situ ends are required therefore reducing the amount of propping and increasing construction speed. Compared to solution 2, the cross over tendon profile increases the overall unbonded tendon length therefore increasing the drift capacity of the frame. However this is harder to construct than solution 2. Details of the exterior joint and interior joints under lateral loads are shown in Figure2-2 (d) and Fgirue2-3 (d) respectively.

2.2.5 Non-tearing solution with diagonal tendon profile

This design solution is a none-tearing solution version of design 4. As shown in Figure2-1(e) the lateral resisting system has exactly the same tendon profile as that in Figure2-1(d). But there are partial gaps introduced at beam ends to reduce the damage to the floor system as was discussed in design solution 3. Compared to the designs 1 and 2, designs 3, 4 and 5 are a little more difficult to construct, since bending of the tendon is required to achieve the desired tendon profile.

2.3 Design solution Evaluation

To evaluate the above proposed design solutions, push over curves of the interior beam to column joint from each different design solution are estimated as shown in Figure2-4 using concept developed by Arnold (2004) and Davies (2004). To allow rational comparison of the test results, all the properties such as tendons types and size, concrete strength, steel plate thickness beam and column cross section sizes of all the interior joints are fixed. A beam size of 400mmx560mm and column size of 700mmx700mm is used in all beams to column joints.

Figure 2-4 showed that, design 3 and 4 have much lower initial stiffness than design 1, 2 and 5 because the partial gap introduced at either end of the precast beam segment. Through a rational analysis, it is found that the effective stiffness of partially gap beam is calculated to be only some 20% of the gross stiffness. Large frame displacement at low lateral force levels will cause damage to non-structure components such as windows and door lintel beams within the building. Despite the low initial stiffness, design 3 and 4 have the same lateral load capacity as of the design 1,2 and 5.

The “yield” drifts of all the interior joints are found to be 3.3%, 2.2%, 2.1%, 2.5%, 2.5% in Designs 1 to 5, respectively. The reason for this is because longer unbonded tendons are able to elongate more than the shorter tendons. In Design 1, diagonal fuse-bars connectors are inserted at an angle to couple together the tendons in the beams to the column. Compared to Designs 2 and 3 in which straight through bolts bars are used to connect adjacent beam to columns, this increases the total tendon length in Design 1. Therefore, a higher yield drift level is expected in design solution 1. Design 4 and 5 have the same yield drift level as they have same tendon profile.

Based on the above observation, Design 1 has some advantages over the other design solutions. The high initial stiffness of the frame limits the frame displacements at low seismic drift level and therefore offers better protection to the non-structural elements from damage. Moreover, due to the larger frame drift capacity tendons are less likely to rupture in an extremely rare seismic event.

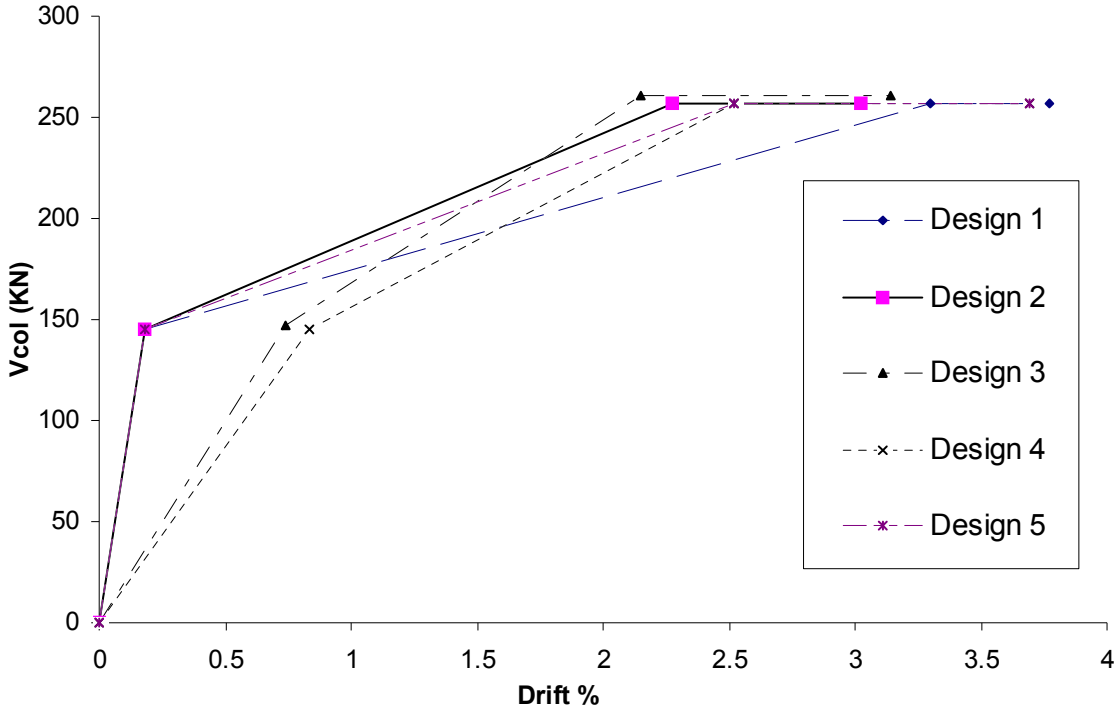

Figure 2-4: Theoretical pushover behaviour of the proposed jointed frame solutions

2.4 Theoretical behaviour of a Jointed Post-tensioned beam-to-column Connection

2.4.1 Moment-rotation response

Unbonded tendons or debonded reinforcement in beams violate strain compatibility of the section, therefore, traditional section analysis can not be used to analyse beam sections with any debonded reinforcing steel, unbonded post-tensioning, or both. Two unknown parameters namely, neutral axis position c and concrete strain ε_c must be solved to find the section strength of the beam. Pampanin et al (1999) proposed an "Equivalent monolithic beam method" to calculate the moment-rotation response of a hybrid beam to column joint. Based on the global member equilibrium requirement, a second relationship between concrete strain and steel strain is found from an iterative procedure they developed. However, if the connection is protected by steel armouring plate on both interfaces, due to the high stiffness and yield strength of steel compared to concrete, it is expected that a very small compression zone (less than 1% of the beam depth) will form at the armoured interface. Therefore, for modelling of the armoured system the connection rotations are assumed to occur about the top and bottom edges of the rocking interface with the compression zone neglected. The assumption permits the use of simple rigid body kinematics to evaluate the connection behaviour.

With only unbonded post-tensioning and supplementary dissipaters passing across the connection interface, the connection moment capacity M_{con} of the unbonded post-tensioned beam column may be expressed by following equation:

$$M_{con}^{\pm} = M_{ps}^{\pm} + M_{diss}^{\pm} \qquad \textbf{(2-1)}$$

in which: $M_{ps}^{\pm} = P_{ps}^{\pm} e_{ps}^{\pm}$; $M_{diss}^{\pm} = P_{diss}^{\pm} e_{diss}^{\pm}$ are moment about rocking edge due to prestress tendons and energy dissipators respectively, where P_{ps} and P_{diss} are prestress

force and dissipator force, and e_{ps} and e_{diss} are the eccentricity of the prestress and energy dissipator about the rocking edges, respectively.

The prestress force of the tendon is dependent on the size of the gap-opening of the connection and the initial prestress level of the tendon itself, this may expressed as:

$$P_{ps}^{\pm} = P_{ps\_inital} + \frac{A_{ps}E_{ps}}{L_t} e_{ps}^{\pm} |\theta_{con}| \qquad \textbf{(2-2)}$$

where A_{ps} = total area of the presterss tendon; E_{ps}= Elastic Modulus of the tendon; L_t = Length of the unbonded tendon; D=beam depth; and θ_{con} = connection rotation with sign convention shown in Figure2-5.

As the gap opens at beam-column interface, tendons will elongate along their unbonded length. This increase in tendon strain will increase the level of tension force in the tendon until the tendon yields. By considering Figure2-5 the connection rotation due to only the rigid body rotation mechanism to cause yield of the prestressing may be expressed as:

$$\left|\theta_{con\ yield}^{\pm}\right|_{RBR} = \left(1 - \frac{f_{ps\ i}}{f_{ps\ yield}}\right) \frac{f_{ps\ yield}}{E_{ps}} \frac{L_t}{e_{ps}^{\pm}} \qquad \textbf{(2-3)}$$

where f_{ps_i}= initial tendon stress; f_{ps_yield}= yield stress of tendon; E_{ps}= Elastic Modulus of the tendon; L_t = total unbonded tendon length; e_{ps} = eccentricity of the tendon from beam central line; and D= beam depth.

Note: when initial prestress force f_{ps_i}= $f_{ps\_yield,}$ $\theta_{con\ yield}^{\pm} = 0$ which means that the structure has no additional deformation capacity under the yielding capacity of the tendon. The gap will not open until the yield capacity of the tendon is reached.

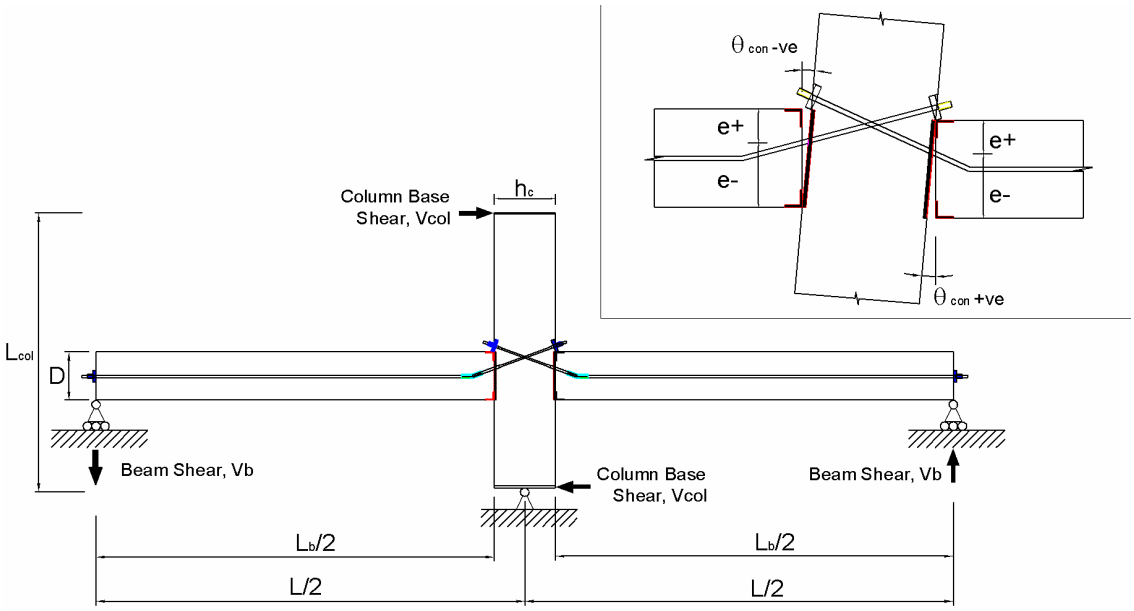

(a) Details of the joint

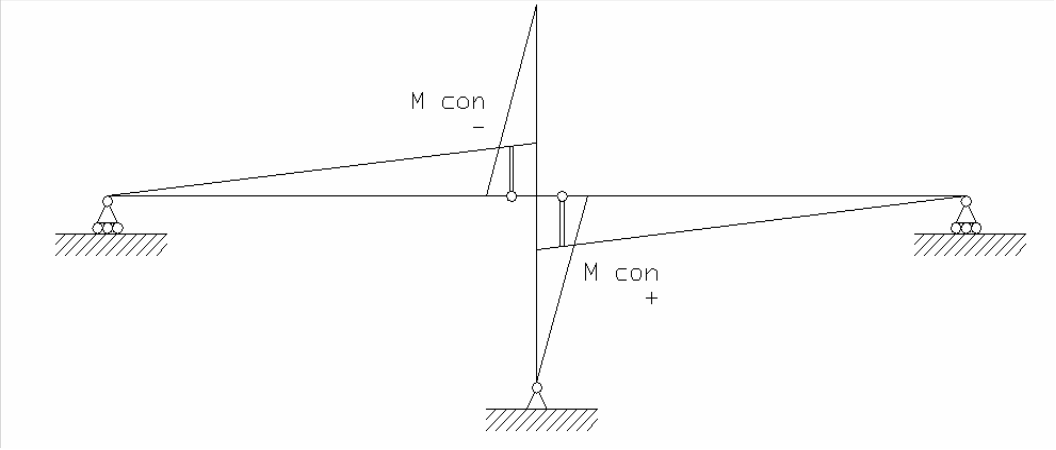

(b) Bending Moment of the joint

Figure 2-5: Details of beam-to-column joint and bending moment diagram of the joint.

Clearly, the yield connection rotation depends on the initial presstress level and the yield strength of tendons, the geometry of the tendon layout and the unbonded tendon length.

Using geometry a relationship between column rotation θ_{col} and beam connection rotation θ_{con}, the column rotation at presstress yielding $|\theta_{col}|_{yield}^{RBR}$ due to rigid body rotation is:

$$|\theta_{col}|_{yield}^{RBR} = \frac{(\varepsilon_{ps\ yield} - \varepsilon_{ps\ initial}) * L_t}{e_{ps}^{\pm}} \frac{L_b}{L} \qquad \textbf{(2-4)}$$

where (ε_{ps_yield} -$\varepsilon_{\ initial}$) = change in strain in tendon due to gap opening; L_t = original unbonded tendon length; and e_{ps} = eccentricity of the tendon from beam central axis.

The column rotation due to elastic deformation of the subassembly can be expressed as:

$$|\theta_{col}|_{yield}^{Elastic} = \frac{\Delta_{yield}^{Elastic}}{L_{col}} \qquad \textbf{(2-5)}$$

where, $\Delta_{yield}^{Elastic}$ = elastic column displacement at prestress yielding and L_{col} = length of the column.

The total yield rotation ($\theta_{col\ yield}$) is therefore sum of both elastic rotation and rigid body rotation components:

$$\theta_{col\ yield} = |\theta_{col}|_{yield}^{Elastic} + |\theta_{col}|_{yield}^{RBR} \qquad \textbf{(2-6)}$$

2.4.2 Force-Displacement response

The lateral deflection of the subassembly at the top of the beam-column subassembly, Δ_{col}, can be resolved into two components as Δ_e and Δ_{RBR} as shown in Figure2-6:

$$\Delta_{col} = \Delta_e + \Delta_{RBR} \quad \textbf{(2-7)}$$

where Δ_e = column deformation due to elastic bending; and Δ_{RBR} = column deformation due to rigid body deformation.

The displacement of the column due to flexure of the column and beam units Δ_e can be evaluated using the moment area method. Assuming a rigid beam-column joint, the elastic displacement (Davies 2004) is given by:

$$\Delta_{Elastic} = \frac{V_{col}}{12}\left[\frac{(L_{col}-D)^3}{EI^*_{col}} + \frac{(L_{col})^2(L_b)^3}{L^2\left(EI^*_b\right)}\right] \quad \textbf{(2-8)}$$

where EI^*_{col} = effective column stiffness; and EI^*_b = effective beam stiffness.

At gap opening, the beam and column is only subjected to elastic flexural, deformation therefore the total displacement at top of the column is:

$$\Delta_{col} = \Delta_{elastic} \quad \textbf{(2-9)}$$

The rigid body displacement of the subassembly due to rigid body rotation of the member is determined by the connection rotation and subassembly geometry:

$$\Delta_{RBR} = 2L_{col}\theta_{col\ RBR} \quad \textbf{(2-10)}$$

The connection rotation caused by rigid body rotation can be evaluated by the changing in strain level of the tendons across the connection and may be calculated from:

$$\left|\theta_{col\ RBD}\right| = \frac{(\varepsilon_{ps} - \varepsilon_{initial}) * L_t}{e^{\pm}_{ps}} \frac{L_b}{L_{bay}} \quad \textbf{(2-11)}$$

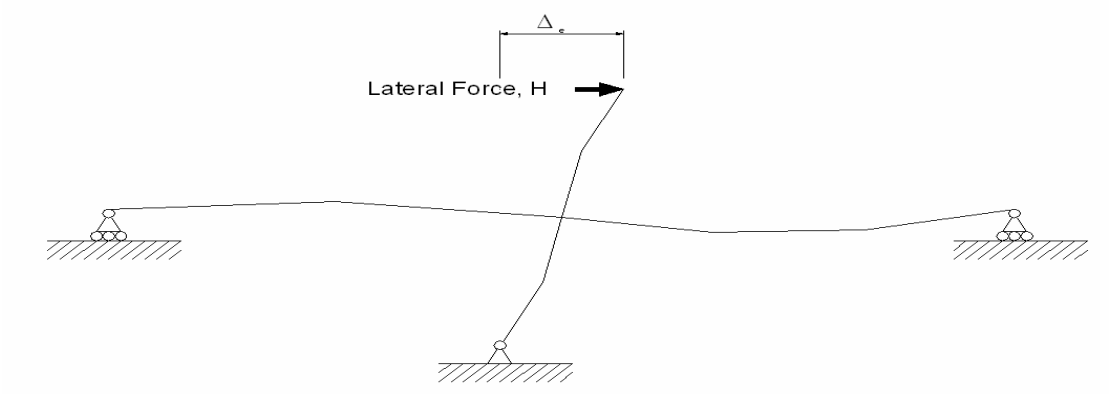

(a) Elastic Deformation of members

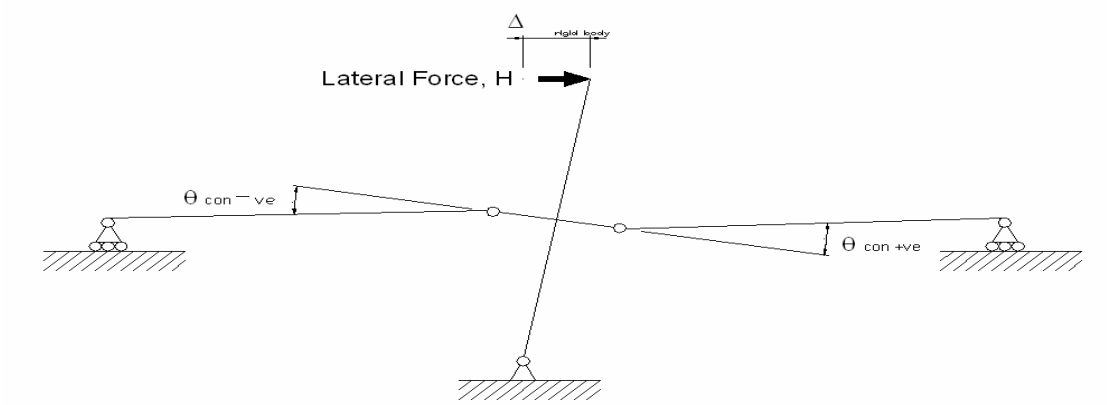

(b) Rigid Body deflection due to connection rotation

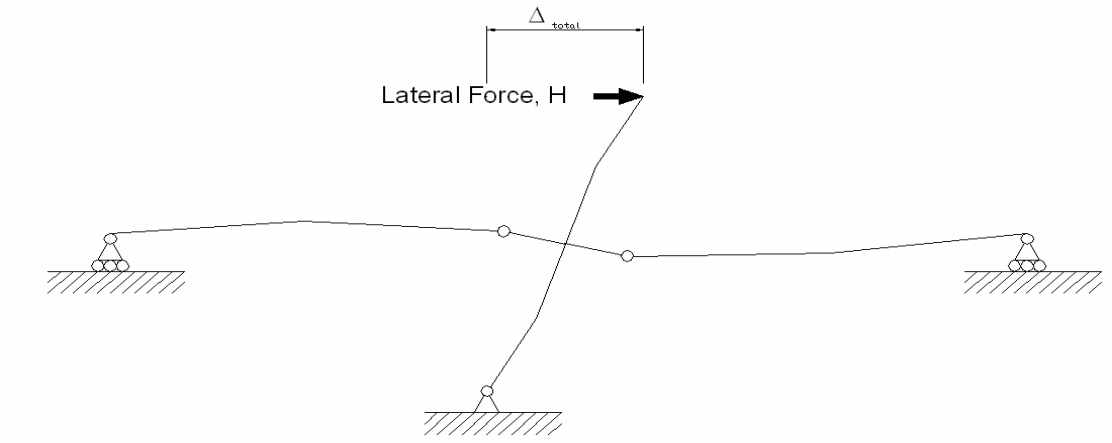

(c) Combined rigid body rotations and elastic deformations

Figure 2-6: Total deflection separated into components of rigid body rotation and elastic deformation.

Substituting **(2-11)** into **(2-10)**, the column displacement due to rigid body rotation can be evaluated from following equation:

$$\Delta_{RBR} = 2L_{col}\frac{(\varepsilon_{ps} - \varepsilon_{initial}) * L_t}{e_{ps}^{\pm}}\frac{L_b}{L} \qquad \textbf{(2-12)}$$

Total displacement at prestress yield can be found by summing displacement of rigid body rotation and elastic displacement:

$$\Delta_{col}^{ps\ yield} = \frac{V_{col}}{12}\left[\frac{(L_{col} - D)^3}{EI_{col}^*} + \frac{(L_{col})^2 (L_b)^3}{L^2\left(EI_b^*\right)}\right] + 2L_{col}\frac{(\varepsilon_{ps} - \varepsilon_{initial}) * L_t}{e_{ps}^{\pm}}\frac{L_b}{L} \qquad \textbf{(2-13)}$$

Moment equilibrium of the beam-column joint as shown in Figure2-5 requires:

$$V_{col} * L_{col} = M_{con}^{+} + M_{con}^{-} \qquad \textbf{(2-14)}$$

Equating **(2-14)** with**(2-1)**, the column base shear can be expressed as:

$$V_{col} = \frac{\left(P_{ps\ \ total} D + P_{diss\ \ total} D\right)}{L_{col}}\frac{L}{L_b} \qquad \textbf{(2-15)}$$

If the supplementary energy dissipators are to yield before gap opening which is commonly the case then the column base shear required to just open the joint may be expressed as:

$$V_{col\ \ gap} = \left(A_{ps\ \ \ total} f_{ps\ initial} + A_{diss\ \ total} f_{y\ \ diss}\right)\frac{D}{L_{col}}\frac{L}{L_b} \qquad \textbf{(2-16)}$$

Similarly the column shear required to yield the prestress in the joint may be written as:

$$V_{col\ \ yield} = \left(A_{ps\ total} f_{y\ ps} + A_{diss\ total} f_{y\ diss}\right)\frac{D}{L_{col}}\frac{L}{L_b} \qquad \textbf{(2-17)}$$

2.4.3 Re-centring limit

Hysteretic behaviour of a rocking beam to column joint with unbonded tendons and supplementary energy dissipators is a combination of the nonlinear elastic hysteretic behaviour of the tendons and elasto-plastic hysteretic behaviour of the energy dissipators Figure2-7 (a). The flag shaped hysteresis of the rocking joint is characterised by 5 parameters as shown in Figure2-7 (b): the initial stiffness before gap opening K_1 and Post stiffness K_2 after the gap opens, the lateral force corresponding to connection opening V_{col}^{Gap} , the lateral force corresponding to prestress yielding point V_{col}^{ps} a and the re-centring point Δ_{rc}.

The re-entering limit defines the maximum drift capacity of the joint before any permanent residual drift in the joint after removal of the lateral load. The re-centring limit depends on characteristics of energy dissipators, prestressing tendons and geometry of the joint. Using simply trigonometry the re-centring point Δ_{rc} may be expressed as:

$$\Delta_{rc} = \frac{V_{col}^{ps} - 2V_{col}^{diss}}{K_2} \qquad \textbf{(2-18)}$$

where V_{col}^{diss} = the yield strength of the beam to column joint with only external energy dissipators; V_{col}^{ps} = the yield strength of the beam to column joint with both prestressing and energy dissipators; K_2 =the post gap-opening stiffness of the joint.

If the external energy dissipators yield immediately after joint opening, the post gap-opening stiffness of the joint is independent of the dissipators and is determined by the prestressing properties and system geometry (Davies, 2004):

$$K_{p2} = \left(\frac{L}{L_b}\right)^2 \left(\frac{D}{L_c}\right)^2 \frac{A_{ps\,total} E_{ps}}{L_t} \qquad \textbf{(2-19)}$$

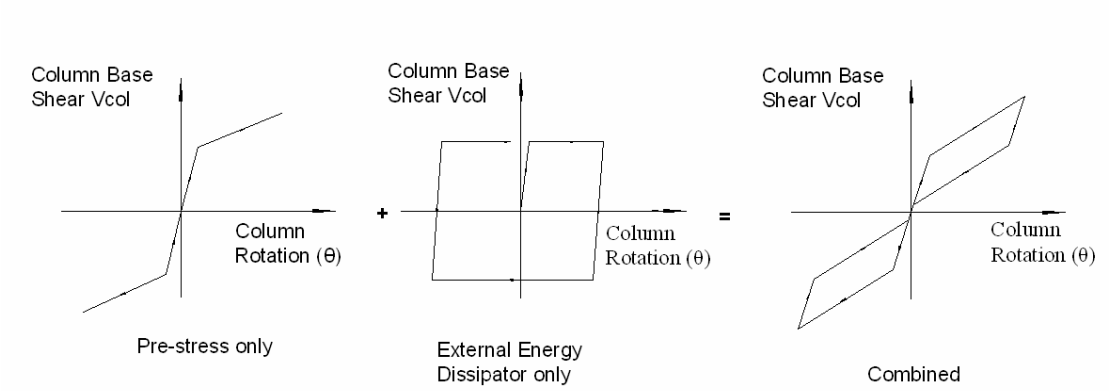

(a) Idealized Flag-shaped hysteretic rule for Unbonded Post-tensioned Precastbeam to column Joint

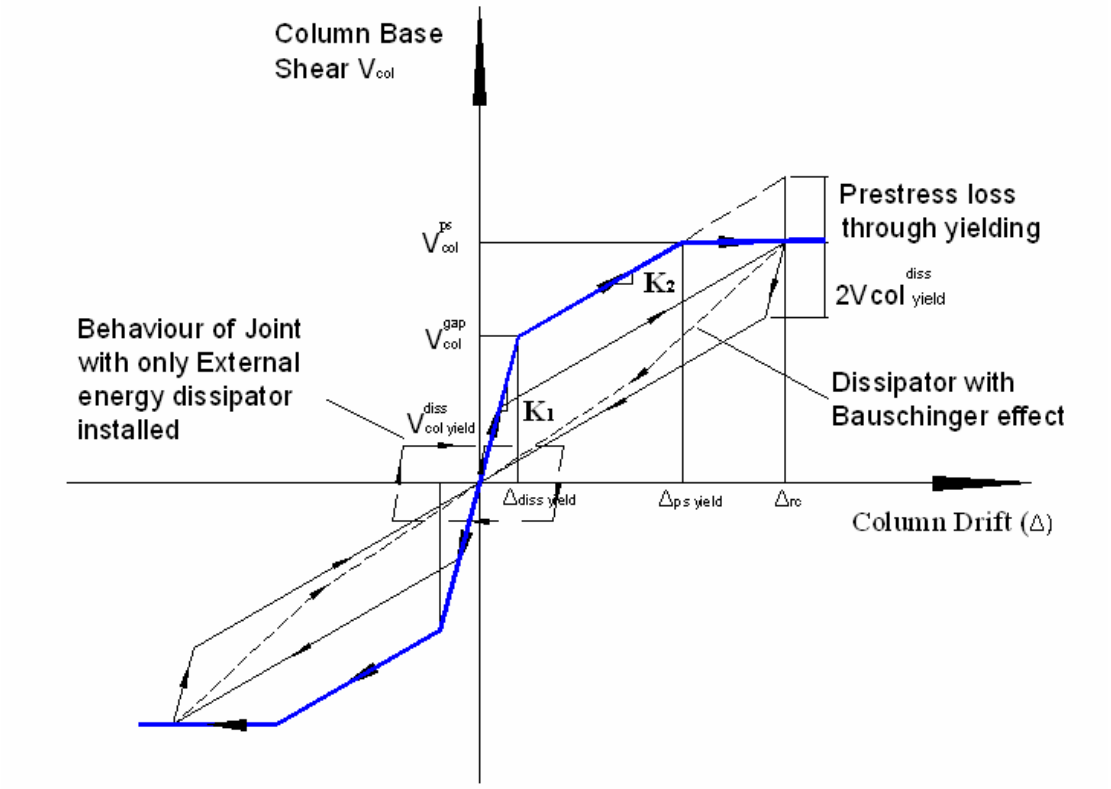

(b) Theoretical cyclic load-displacement relationship of an unbonded post-tensioned beam to column-joint with Re-centring limit

Figure 2-7: Theoretical load-displacement relationship of an unbonded post-tensioned beam-to-column joint.

The yield strength of the joint with only fuse rods installed is:

$$V_{col}^{fuse} = \frac{P_{diss} D}{L_{col}} \frac{L}{L_b} \quad \textbf{(2-20)}$$

And the strength of the joint with energy dissipator attached to it can be expressed as:

$$V_{col}^{ps} = \frac{P_{ps\ yield} D + P_{diss} D}{L_{col}} \frac{L}{L_b} \quad \textbf{(2-21)}$$

Substituting **(2-19)**, **(2-20)**, and **(2-21)** into **(2-18)**and rearranging give the displacement beyond which re-centring is lost:

$$\Delta_{rc} = \frac{\left(A_{ps\ total} f_{y\ ps} - A_{diss} f_{y\ diss}\right) * L_{col}}{A_{ps\ total} E_{ps}} \frac{L_t}{D} \frac{L}{L_b} \quad \textbf{(2-22)}$$

This can be expressed in terms of column drift θ_{rc}:

$$\theta_{rc} = \left(\frac{f_{y\ ps}}{E_{ps}} - \frac{A_{diss}}{A_{ps\ total}} \frac{f_{y\ diss}}{E_s} \right) \frac{L_t}{D} \frac{L}{L_b} \quad \textbf{(2-23)}$$

2.4.4 Supplementary energy dissipator

To aim at maximum energy dissipation while still ensuring the full re-centring capability of the joint, the connection moment provided by the prestressing must be sufficient to overcome the resisting moment generated in the supplementary energy dissipators, in mathematic form:

$$\lambda_{diss} M_{diss} < \phi M_{ps} \quad \textbf{(2-24)}$$

where λ_{diss} = the dissipator material overstrength factor and Φ = a prestress understrength factor; M_{diss} = connection moment generated by dissipators; and M_{ps} = connection moment generated by the prestressing.

It is desired to keep the fuse length to be a minimum value to avoid buckling during gap closing. However, sufficient length should be provided to avoid low fatigue fracture of the dissipator when connection undergoes large rotation. Based on

kinematics of the connection and applying the low-cycle fatigue recommendation of Mander et al (1994) the minimum safe dissipator length (L_d) can be calculated from following equation:

$$L_d > \theta_{con} \frac{kD}{2\left(\frac{0.08}{\sqrt{2N_f}} + \varepsilon_y\right)} \qquad \textbf{(2-25)}$$

where ε_y = the yield strain of the dissipator; θ_{con} = design connection rotation; N_f = number of cycle to fatigue cracking; kD= position of the energy dissipator.

2.4.5 Detailing of disturbed Region

Large contact forces generated form the rocking motion must be safely transferred to the precast elements. According to the St.Venant principle it might expected that high stress region will extend into the beam over a length of approximately one member depth away from the rocking interface. Steel plates can be cast into the ends of the beam to prevent concrete from crushing at the rocking edges. Additional stirrups can be used to increase the compressive strength of the concrete behind the steel armour by increasing confinement. Also additional layers of longitudinal reinforcement should be placed at end of the beam to help spread the high compression force.

2.4.6 Hysteretic Energy dissipation

The effective equivalent viscous damping ζ_{eff} of the jointed frame system can be found by adding: the intrinsic natural damping $\zeta_{intrinsic}$, radiation damping $\zeta_{rocking}$ and hysteretic energy dissipation ζ_{hy}

$$\xi_{eff} = \xi_{\text{int}rinsic} + \xi_{rocking} + \xi_{hy} \qquad \textbf{(2-26)}$$

For a concrete frame building the intrinsic natural damping $\zeta_{intrinsic}$ is typically in a range of 2-5%. It is expected that for building frames where the members are prestressed and quite slender, the effective viscous damping arising from rocking impacts of the beam-column connection will be quite small and is assumed here to be zero in the present research. For column to foundation connections the radiation damping can be evaluated from the slenderness ratio of the column based on recommendation of Mander and Cheng (1997).

According to Chopra (2001), the equivalent viscous damping due to hysteretic energy dissipation can be evaluated from (Figure2-8):

$$\xi_{hy} = \frac{1}{4\pi}\frac{E_D}{E_{so}} \qquad \textbf{(2-27)}$$

Where E_d = area enclosed by the hysteretic loop, E_{so} = maximum strain energy (Chopra 2001)

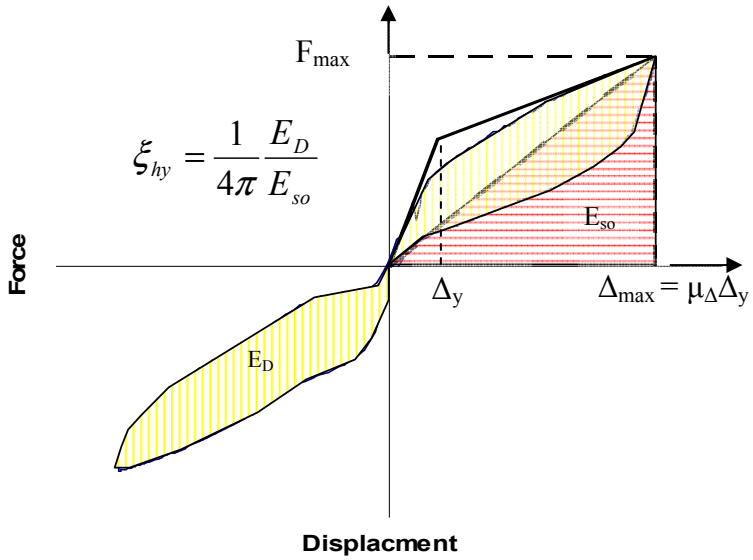

Figure 2-8: Equivalent viscous damping.

According to Pekcan, et al (1999), the nonlinear hysteresis damping of the energy dissipator in the joint can be expressed as equivalent viscous damping using following equation:

$$\xi_{hy} = \frac{1}{4}\pi\frac{E_D}{E_{so}} = \frac{2}{\pi}\eta\frac{(1-\alpha)\left(1-\frac{1}{\mu_\Delta}\right)}{(1-\alpha+\mu_\Delta\alpha)} \qquad \textbf{(2-28)}$$

where, the μ_Δ = displacement ductility and; α= ratio of finial to initial stiffness; η = energy absorption efficiency factor defined as the absorbed energy (E_D) in Figure 2-8 with respect to an elasto-perfectly plastic system (E_{so}). (i.e. $E_D^{EPP} = 4F_{max}(\mu-1)\Delta_y$). Typical values of η for well designed ductile reinforced concrete is 0.35-0.4.

2.5 Concluding Remarks

Modelling concepts for a jointed beam to column connection designed from a Damage Avoidance Design point-of-view are presented. This involves the complete design and modelling of the beam joint details as well as supplemental energy dissipators. Damage in the joint is limited to the replaceable supplementary energy dissipators and fuse connector bars. The theoretical moment-rotation and lateral force behaviour of the jointed connection is also presented.

Based on these design concepts developed in this section on the jointed connections, five different jointed frame systems are proposed and theoretically evaluated. The theoretical force-displacement relationship of each of the five interior joint of the proposed frame systems is calculated, plotted and compared. In conclusion of this section the design solution with straight tendon and diagonal fuse connector bars (design solution 1) displays both higher initial stiffness and yield drift capacity among all five proposed frames.

2.6 References

Arnold, D.M (2004). *Development and Experimental Testing Of a Seismic Damage Avoidance Designed Beam to Column Connection Utilising Draped Unbonded Post-Tensioning* Masters, Thesis, Department of civil Engineering, University of Canterbury, Christchurch, New Zealand.

Cheok, G.S. and Lew, H.S. (1991), *Performance of precast concrete beam to column connections subject to cyclic loading.* PCI journal, Vol. 36, No.3, pp56-67.

Chopra A.K., (2001) *Dynamics of Structures: Theory and Applications to Earthquake Engineering*, Prentice Hall, New Jersey.

Mander, J.B., Panthaki, F.D., and Kasalanati, A. (1994), *Low-Cycle Fatigue Behaviour Of Reinforcing Steel*, Journal of Material in Civil Engineering, Vol. 6, No.4, pp453-468.

Mander, J.B., and Cheng, C.T. (1997). *Seismic Resistance of Bridge Piers Based on Damage Avoidance Design*, Technical Report NCEER-97-0014, Department of Civil, Structural and Environmental Engineering, State University of New York at Buffalo, New York, USA.

Pekcan, G., Mander,.J.B., and Chen,.S.S., (1999), *Fundamental Considerations for The Design of Non-linear Viscous Dampers*. Department of Civil, Structural and Environmental Engineering, State University of New York at Buffalo, USA.

Priestley, M.J.N. and MacRae, G.A., (1996). *Seismic Tests of Precast Beam-to-Column Joint Subassemblages With Unbonded Tendons*, PCI Journal, January/February, 1996, pp. 64-81.

Priestley, M.J.N., Sritharan, S., Conley, J.R., Pampanin, S. (1999).*Preliminary Result and Conclusions from the PRESSS Five-Storey Precast Concrete Test Building*, PCI Journal, Vol. 44, No. 6, pp 43-67.

Stone, W.C., Cheok, G.S., and Stanton, J.F. (1995), *Performance of hybrid moment-resisting precast beam-column concrete connection subjected to cyclic loading,* ACI Journal, Vol. 91, No, 2 March-April.

3 Section Three: Experiments On The Seismic Resistance Of An Armoured Rocking Beam-To-Column Connection.

Section Summary

A near full scaled jointed prestressed concrete beam-to-column joint constructed in accordance with the Damage Avoidance Design (DAD) philosophy is tested under displacement controlled quasi-static reverse cyclic loading. The performance of the joint is assessed under unidirectional loading along both orthogonal directions as well as concurrent under bidirectional loading. The specimen performed well up to 4% column drift. Only some minor superficial cracks are observed in precast beams. The precast column remains uncracked and damage-free. Good performance is attributed to steel angles which are used to armour the beam ends to mitigate the potential for concrete crushing. Under bi-directional a loading proposed tapered shear-key layout is used to protect the beams against torsional movements. No torsional cracks are observed during bi-lateral loading. Good agreement between a theoretical model and experimental tests is demonstrated. A theoretical energy absorption efficiency factor (η) of the subassembly is found to be 8.75% when test with only prestressing and is increased to 19% when supplementary energy dissipators are installed. Both of the energy absorption efficiency factors fit well with the measured experimental values.

3.1 Introduction

Jointed precast frame systems have been studied by several researchers (MacRae 1994, Stone et. al. 1995, Priestley et. al. 1999). It has been reported that in the jointed precast frame, large nonlinear deformations are accommodated via gap opening and closing at the interface between the precast elements. Due to the action of unbonded prestress, a significant reduction in damage over conventional reinforced concrete systems is achievable with design focused on damage control. Furthermore, the re-centring effect in the unbonded prestress allows the jointed precast frame systems to return to its undeformed shape with negligible residual displacement upon removal of the lateral loads.

Mander and Cheng (1997) proposed a Damage Avoidance Design (DAD) philosophy whereby armouring of member ends is introduced to further mitigate any damage potential. Davies (2004) and Arnold (2004) applied the DAD principles and demonstrated that with a steel-to-steel armoured connection, precast concrete beam-to-column connection elements can be effectively protected from damage. However detailing of steel-to-steel armours required an extensive amount of welding in order to fabricated the steel caps of the precast elements. The experimental study presented herein progresses from that previous work, but aims to simplify the steel-to-steel connection details and to investigate the behaviour of such jointed precast frame system under bidirectional lateral loading.

A near-full (80%) scaled two-way beam-to-column joint subassembly consists of two seismic beams and one gravity beam designed according to DAD principles. The connection development is based on a typical 10 storey office building to be constructed in New Zealand. An adjustable precast beam is also developed to reduce construction difficulties and to accommodate any length variation tolerance in the

precast beams. The subassembly is tested under displacement controlled reversed quasi-static lateral unidirectional and bidirectional loadings. The experiment results and findings are presented, and conclusions are drawn that are relevant to design and implementation.

3.2 Specimen Design

3.2.1 Subassembly dimensions

An 80% scaled beam-to-column joint subassembly was constructed. The test subassembly represents a jointed precast beam-to-column joint abstracted from one of the lower storeys of a typical New Zealand office building depicted in Figure 3-1. The 3-dimentional subassembly consists of two seismic half-beams and one gravity half-beams in the orthogonal direction (Figure 3-1 (e)). The specimen dimensions were: 700mm square column, 400mm wide by 560mm deep beam segments in both orthogonal and transverse directions. The length of beams and column segment in the subassembly were 4m and 3.2m respectively (this assumes the point of inflection is at mid-span of beam and mid-height of column).

The rocking joint moment capacity is based on a typical prototype structure hinge region with a nominal moment strength of 500kN-m. The main resistance is provided by two 26.5mm diameter high alloy high strength (f_y=1100MPa) prestressing thread-bars (Dywidag^{TM}) in the test subassembly.

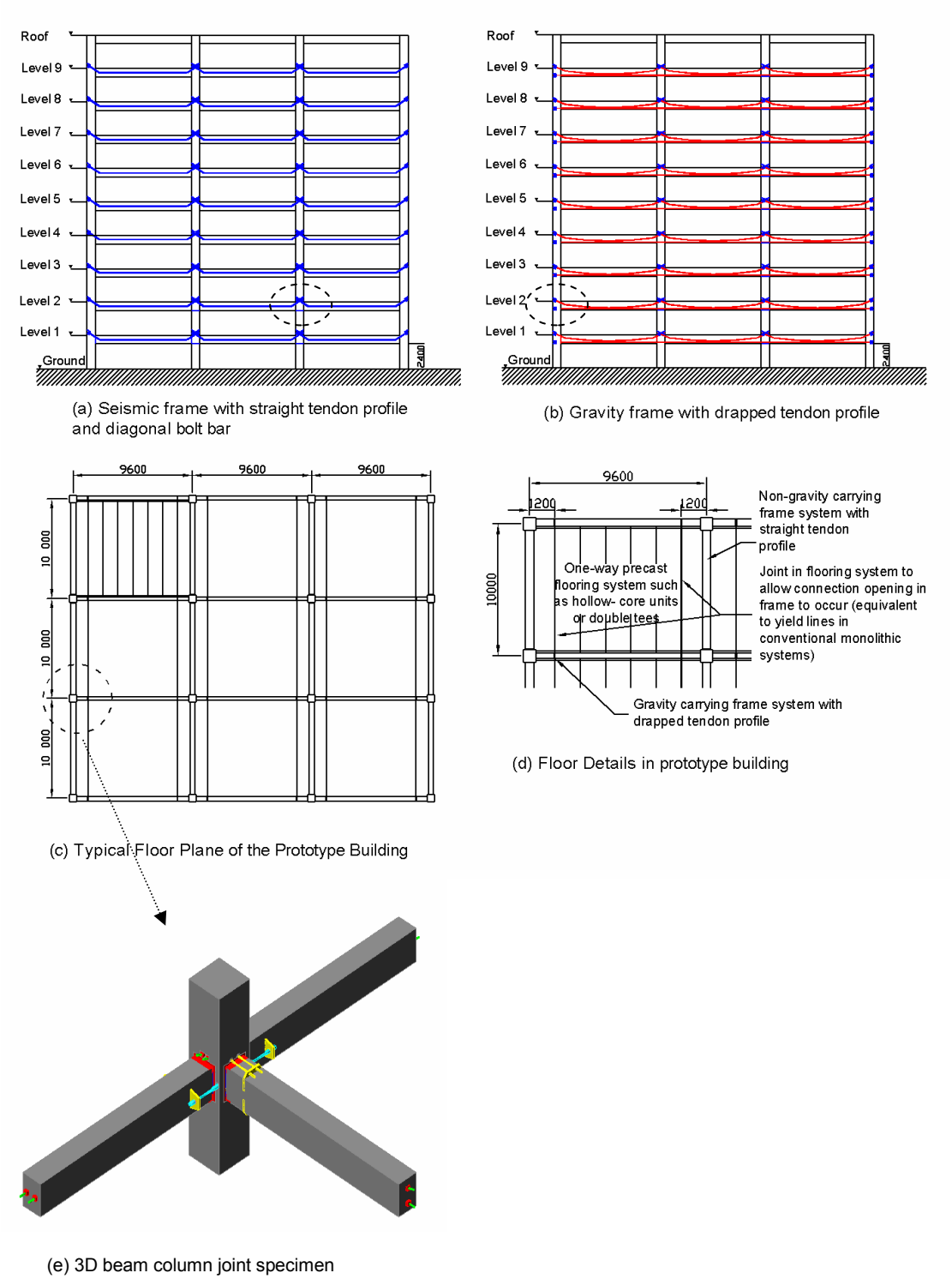

Figure 3-1: Proposed prototype building layout with jointed precast frames and a typical 3D beam to column joint within the building.

3.2.2 Subassembly drift capacity assessment

In the subassembly, the precast beams were joined to the precast column via high strength threadbars. As the central 700mm was machined down they are referred to herein as "fuse bolt-bar". Bolt-bars with a fuse area of only 75% of the original area were provided to ensure the main prestressing bars within the span of the beam or any of the couplers did not yield. Such fuse bolt-bars can be restressed or replaced if excessively yielded. When the gap between beam and column opens, due to the difference in the cross sectional areas of the fuse bolt-bars and main beam tendons, the stress developed in the full beam tendon will be less than the stress developed in the fuse bolt-bars. The total amount of gap opening is therefore contributed by two components: (1) the elongation of the fuse bolt-bars and (2) the elongation of the main beam prestressing tendons.

The drift capacity of the subassembly has two components, the drift due to elastic flexure of the beam and column elements and the drift due to rigid body rotation of the beam and column elements. For the present experimental study, the small drift component due elastic flexure is neglected. The yield drift capacity of the subassembly can therefore be calculated by:

$$\theta_{col\ yeild} = (\varepsilon_{ps\ yield} - \varepsilon_{initial}) \frac{L_t}{e_{ps}} \frac{L_b}{L} \qquad \textbf{(3-1)}$$

where $\varepsilon_{ps\ yield} - \varepsilon_{initial}$ = total change in prestress strain at prestress yielding; L_t= unbonded tendon length, L_b = beam length (i.e. between adjacent column face); L= bay length (i.e. between adjacent column centreline); e_{ps} = prestress eccentricity at the connection.

Modifying equation (3-1) to account for the difference in areas of fuse bolt-bars and the main beam prestress gives the yield drift of the subassembly as follows:

$$\theta_{col\ yield} = \frac{\left(\varepsilon_{ps\ yield} - \varepsilon_{ps\ initial}\right) * \left(l_{bolt} + \frac{A_{bolt}}{A_{ps}} * l_{ps\ beam}\right)}{e_{ps}} * \frac{L_b}{L} \qquad \textbf{(3-2)}$$

where: l_{bolt} = length of the fuse bolt-bar; l_{ps} = prestress length in the precast beam; A_{bolt} = total area of the bolt bar; A_{ps} = total area of the beam prestress.

Applying equation (3-2) to the specimen geometry, the column drifts at first yield of the 80% scaled test subassembly are 2.6% and 3.0% for east-west and north-south loading, respectively. Detailed calculations are given in Appendix B.

3.2.3 Precast beams

Details of the reinforcement layout for the precast beams are given in Figure 3-2. Two 26.5mm diameter high-strength high-alloy prestressing threadbars (Dywidag^{TM}) were used for the post-tensioning of the beam. A straight-tendon profile with diagonal-fuse "bolt-bar" layout was designed for the two seismic beams, while a draped-tendon profile was designed for the gravity beam to balance the dead loads. Loads assumed were for a typical office building: 3.5kPa floor load, 0.75 kPa superimposed dead load and probable live load of 0.65 kPa. To protect the concrete from damage during rocking, the ends of the precast beams that join at the column face were armoured. Steel angles, 100mmx100mmx12mm thick, were placed at the top and bottom corners of the beam. At one beam end, an adjustable beam-end was implemented by allowing a small portion of the beam ends to be cast on site. Providing such an adjustable beam-end at several span intervals along the frame allows tolerances in precast beam length to be accommodated during construction.

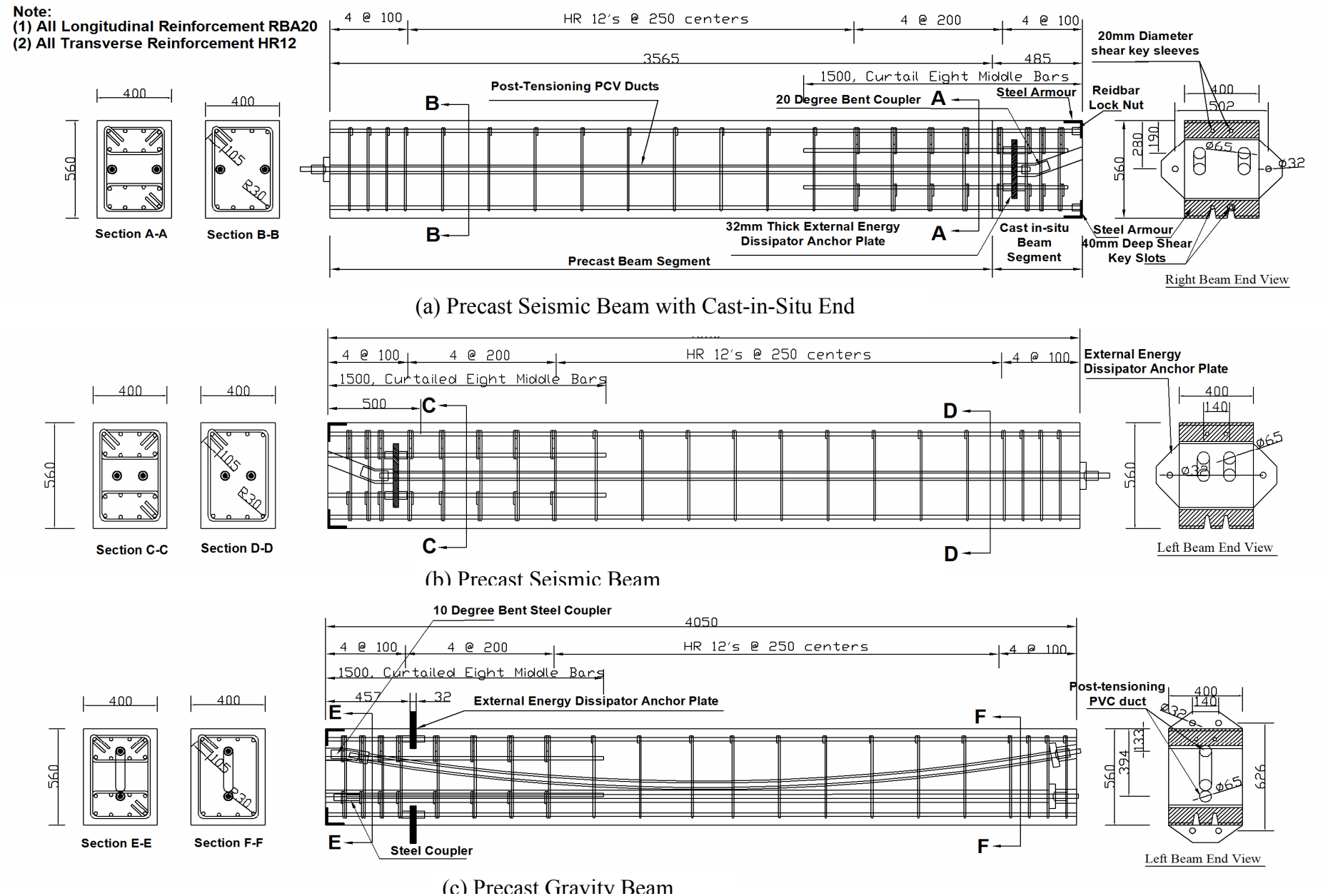

Figure 3-2: Reinforcing details of precast concrete beams.

A cracked elastic design was employed to detail the longitudinal reinforcement in the precast beam segments. The approach followed that proposed by Arnold (2004) was followed for designing the longitudinal rebars. Detailed design calculations are given in Appendix B. In this design approach, sufficient quantity of mild steel was provided to ensure that yield of the longitudinal reinforcing is prevented, while the concrete compressive stresses are kept below 70 percent of the 28 day strength (f'_c). This ensures the precast elements remain essentially elastic even when the connection reaches its calculated over-strength capacity.

Shear Design of the precast element follows the New Zealand Concrete Standard NZS3101:1995. With a total initial axial load of 398kN provided by the two prestressing threadbars, the required transverse reinforcement was less than for a conventional system. A maximum allowable stirrup spacing of 250mm was used at the middle section of beam. Closely spaced (100mm centre to centre) stirrups were placed at beam ends to help transfer the large rocking and post-tensioning forces.

3.2.4 Column Details

Figure 3-3 presents the reinforcing details of the precast concrete column. The 700mm square precast concrete column was post-tensioned by four unbonded 32mm diameter (Macalloy^{TM}) high strength threaded rods to simulate the level of axial load ($0.1f'_c\ A_g$) that would be expected on the lower storey of the office building. Three 400mm wide by 560mm long by 20mm thick mild steel plates were cast at column faces where the precast beams met with the column face.

Only minimum longitudinal reinforcement ratio was provided (ρ_t =0.008) using 12 HD 20 threaded rebars (Reidbar^{TM}). This low reinforcement ratio prevents congestion of reinforcement in the joint region and therefore minimizes construction difficulties.

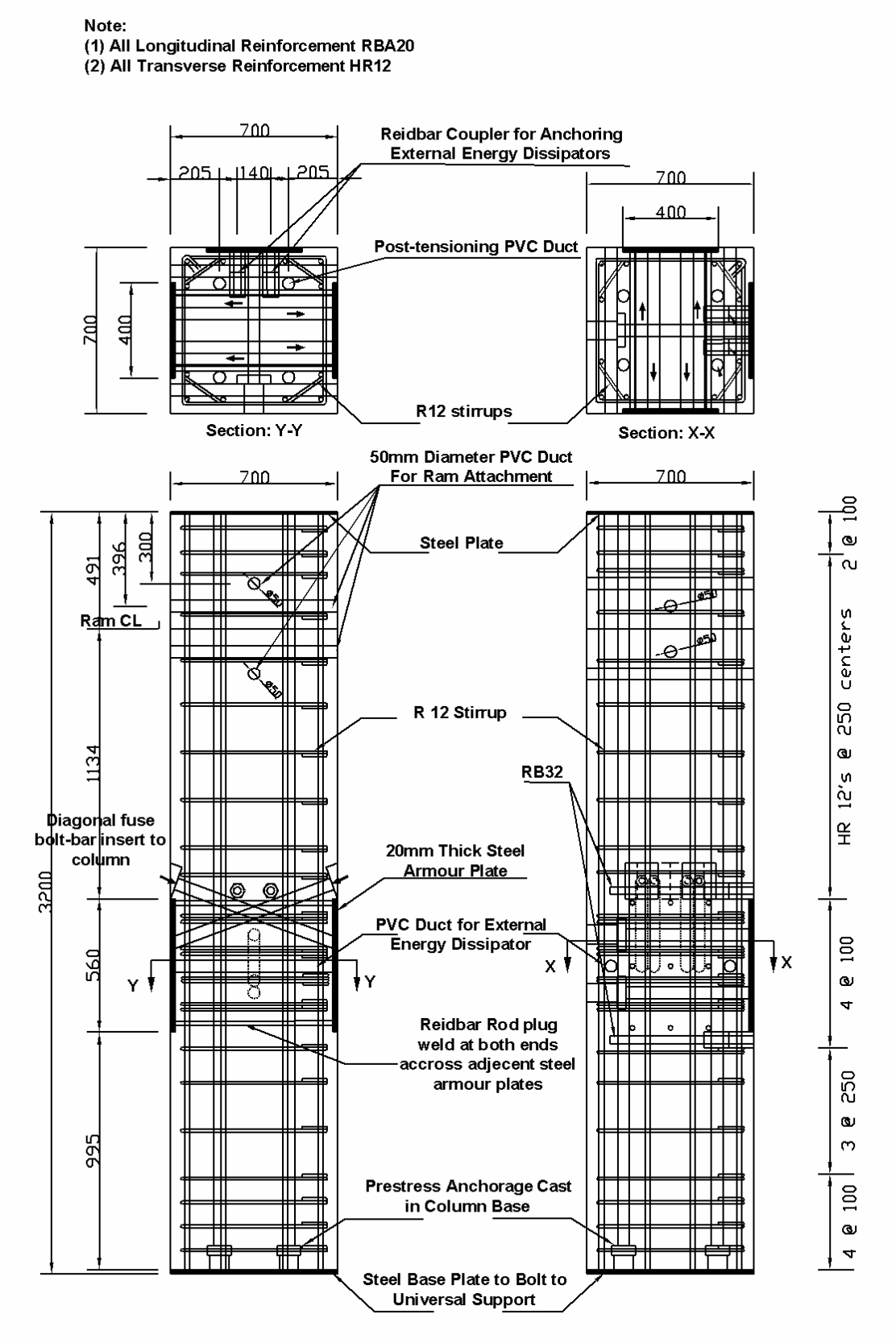

Figure 3-3: Reinforcing details of the precast concrete column.

Due to the high axial load (2000 kN) provided by the tendons, only a minimum amount of shear reinforcement with a R12-200mm centres was found to be necessary to resist the most adverse shear force generated into the column.

Five double HR12 hoop sets spaced at a centre-to-centre spacing of 100mm were placed in the joint region to assist the transfer of the large design shear forces through the joint. At both ends of the column, 4 hoop sets at 100mm centres were used to resist the prestress bursting forces into column. To prevent concrete from crushing the concrete stress behind steel plate was designed to be limited to 0.7f'c. By assuming the force is spread at an angle of 45 degree through the plate, the thickness of the steel plate adopted was calculated to be 20mm.

3.2.5 Capacity protection and energy dissipation

Supplementary energy dissipators in the form of fuse bars were introduced to the specimen. These were mounted externally to facilitate rapid replacement between tests. The diameter/length of the fuse regions used were 15/10mm and 13/212mm for the two seismic beams and gravity beam respectively (see Appendix B for detailed calculation)

3.3 Expected stiffness and force-deformation behaviour

Given that the beams had armoured ends, deformations can be decomposed into two components: elastic (pre-gap opening) behaviour; and rigid body (post-gap opening) behaviour. The expected force-deformation response in each of the two directions is given in the following:

3.3.1 East-West Loading

Pre-gap-opening stiffness:

Before gap opens at the beam-to-column connection, the subassembly deforms elastically. The initial pre-gap-opeing stiffness may be expressed as:

$$K_e = \frac{12(EI^*_{beam})/L_b^3}{\left(\frac{L_{col}}{L}\right)^2 + \left(\frac{L_{col}-D}{L_b}\right)^3\left(\frac{EI^*_{beam}}{EI^*_{col}}\right)} \qquad \textbf{(3-3)}$$

where EI^*_{beam} and EI^*_{col} are effective beam and column rigidity; L_b =precast beam length; L=clear span between column centre lines; L_{col}= column height; and D= beam depth.

Gap-opening force:

Since usually the supplementary energy dissipators will yield soon after the connection opens, the lateral force at gap-opening may be approximated by:

$$V_{col}^{gap} = \left(\frac{P_{ps\ initial}D + F_{diss\ yield} * e_{diss}}{L_{col}}\right)\frac{L}{L_b} \qquad \textbf{(3-4)}$$

where $P_{ps\ initial}$= total initial prestressing force in tendon; $F_{diss\ yield}$ = total yield force of the supplementary energy dissipators; D= beam depth; e_{diss}= eccentricity of the supplementary energy dissipator from the rocking edge; L=bay length; and L_b= precast beam length.

Post-gap opening stiffness:

Soon after the supplementary energy dissipator yields, the stiffness of the rigid body force-displacement response is independent of the dissipators and is given by Davies (2004):

$$K_{p2} = \left(\frac{L}{L_b}\right)^2 \left(\frac{D}{L_{col}}\right)^2 \frac{A_{ps\ total} E_{ps}}{L_t} \quad \textbf{(3-5)}$$

However, in this particular subassembly, to prevent the prestress inside the precast beam from yielding, the diagonal fuse bolt-bars are machined down to 75% of their original area, hence the stiffness of the bolt-bar is:

$$K_{bolt} = \frac{A_{bolt}\, E_{ps}}{l_{bolt}} \quad \textbf{(3-6)}$$

where A_{bolt} = the total fuse area of the fuse bolt-bar; E_{ps} = Young's Modulus of the Elasticity of the bolt-bar; l_{bolt}= the fuse length of the fuse bolt-bar.

Therefore the combined stiffness of the prestress within the subassembly is:

$$K_{comb} = \frac{K_{bolt} * K_{ps}}{K_{bolt} + K_{ps}} \quad \textbf{(3-7)}$$

where K_{bolt} = stiffness of the fuse bolt-bar, K_{ps} =stiffness of the prestress in the precast beam: $K_{ps} = \frac{A_{ps} E_{ps}}{l_{ps}}$.

Therefore the post-gap opening stiffness is:

$$K_{p2} = \left(\frac{L}{L_b}\right)^2 \left(\frac{D}{L_{col}}\right)^2 K_{comb} \quad \textbf{(3-8)}$$

Force and displacement limits (yield force and displacement):

The lateral force to cause yield of the prestress in subassembly is:

$$V_{col}^{yield} = \frac{P_{ps\ yield} D + F_{diss\ yield} e_{diss}}{L_{col}} \frac{L}{L_b} \quad \textbf{(3-9)}$$

where D=beam depth; $F_{diss\ yield}$ =total yield force of the external energy dissipator;

L= length between column centrelines; L_b= precast beam length; L_{col}= column height.

The yield drift of the column is:

$$\Delta_{yield}^{Total} = \Delta_{yield}^{Elastic} + \Delta_{yield}^{RBR} \quad \textbf{(3-10)}$$

where: $\Delta_{yield}^{Elastic}$ = column drift at yield of prestress due to elastic deformation and can be evaluated using equation (2-8) developed in previous section; Δ_{yield}^{RBR} = column drift at yield of prestress due to rigid body rotation and is given by:

$$\Delta_{yield}^{RBR} = \frac{\left(\varepsilon_{ps\ yeild} - \varepsilon_{ps\ initial}\right)\left(l_{bolt} + \frac{A_{bolt}}{A_{ps}} l_{ps}\right)}{\left|e_{ps}\right|_{\max}} \frac{L}{L_b} L_{col} \quad \textbf{(3-11)}$$

where l_{bolt}= fuse bolt-bar length; l_{ps}= length of the main prestressing in the precast beam; L=bay length (between column centre lines); L_b= length of the precast beam, L_{col}= column height.

3.3.2 North-South Loading

Pre-gap-opening stiffness:

Pre-gap-opening stiffness of the subassembly in North-South direction can also be predicted using the formula proposed by Davies (2004):

$$K_e = \frac{12(EI_{beam}^*)/L_b^3}{\left(\frac{L_{col}}{L}\right)^2 + \left(\frac{L_{col} - D}{L_b}\right)^3 \left(\frac{EI_{beam}^*}{EI_{col}^*}\right)} \quad \textbf{(3-12)}$$

where EI_{beam}^* and EI_{col}^* are effective beam and column rigidity;

Gap-opening force:

To balance the gravity load, the top tendon in the gravity beam of the subassembly was draped. Although tendons are eccentrically placed with respect to neutral axis of the beam, but at beam-to-column joint interface, the top draped tendon and bottom straight tendon are approximately symmetrical about neutral axis of the beam. Therefore, an average tendon eccentricity of $e_{ps} = \frac{D}{2}$ can be used in calculating the connection rotation. Thus the lateral force corresponding the gap-opening may be approximated by:

$$V_{col}^{gap} = \left(\frac{P_{ps\ initial} \frac{D}{2} + F_{diss\ yield} e_{diss}}{L_{col}} \right) \frac{L}{L_b} \qquad \textbf{(3-13)}$$

Post-gap opening stiffness

Like the post-gap opening stiffness in East-West loading direction, the post-gap opening stiffness in North-South direction is given by the same formula:

$$K_{p2} = \left(\frac{L}{L_b} \right)^2 \left(\frac{D}{L_{col}} \right)^2 K_{comb} \qquad \textbf{(3-14)}$$

where:

$$K_{comb} = \frac{K_{bolt} * K_{ps}}{K_{bolt} + K_{ps}};\ K_{bolt} = \frac{A_{bolt} E_{ps}}{l_{bolt}};\ \text{and}\ K_{ps} = \frac{A_{ps} E_{ps}}{l_{ps}}.$$

Force and displacement limits (yield force and drift)

The shorter straight bottom tendon in the precast gravity beam has slightly higher stiffness than the draped top tendons, simply because it has a shorter length. This means that the subassembly will have a smaller yield drift when connection opens at bottom than when connection opens at top. The uniformly applied gravity

load on top of the gravity beam, applies a downward shear force on the shear keys at the column face. When the subassembly is pushed in a direction such that connection opens at the bottom, the downward shear force present at the top shear keys will produce a negative moment about the columns neutral axis which will tend to reduce the yield drift of the subassembly. When pushing to the right, the shear key present at the bottom of the beam which will tend to increase the yield drift of the subassembly. The effects on the yield drift of subassembly in the North-South direction, due to tendon stiffness differential and gravity loads counteract and thus balance each other. Therefore the yield force of the subassembly along the north-south direction may be expressed as:

$$V_{col}^{yield} = \frac{P_{ps\,yield}\frac{D}{2} + F_{diss\,yield}e_{diss}}{L_{col}} \qquad \textbf{(3-15)}$$

where the yield drift of the column is:

$$\Delta_{yield}^{Total} = \Delta_{yield}^{Elastic} + \Delta_{yield}^{RBR} \qquad \textbf{(3-16)}$$

where: $\Delta_{yield}^{Elastic}$ = column drift at yield of prestress due to elastic deformation in the north-south direction can be evaluated form the bending moment diagram assuming the beam-to-column joint is rigid and may be evaluated from:

$$\Delta_{Elastic}^{N-S} = \frac{V_{col}}{12}\left[\frac{(L_{col}-D)^3}{EI_{col}^*} + \frac{2*(L_{col})^2(L_b)^3}{L^2\left(EI_b^*\right)}\right] \qquad \textbf{(3-17)}$$

where Δ_{yield}^{RBR} = column drift at yield of prestress due to rigid body rotation and is given by:

$$\Delta_{yield}^{RBR} = \frac{2*\left(\varepsilon_{ps\ yeild} - \varepsilon_{ps\ initial}\right)*\left(l_{bolt} + \frac{A_{bolt}}{A_{ps}} l_{ps}\right)}{D} \frac{L}{L_b} L_{col} \qquad \textbf{(3-18)}$$

Using the formulas developed above, the theoretical force-displacement of the subassembly along both East-West and North-South loading directions are calculated in Appendix B.

3.4 Effective stiffness of the precast concrete member

It is noted that using the gross section (uncracked) stiffness in seismic analysis is considered to be inappropriate, because cracking in the concrete member occurs early and stiffness reduces rapidly as member response becomes inelastic. In order to account for this reduction in member stiffness, New Zealand concrete design code specified a reduction factor of 0.35 to the gross-section stiffness of beams, while a value between 0.4-0.7 is specified for a column.

In a jointed precast frame, the large inelastic rotation is accommodated via gap opening and closing at the unbonded post-tensioned connections. At the ends of the member, large concentrated forces are expected. According to St. Venants' principle, the high stress region behind the force will spread to approximately one section depth. Using the well-known Moment-Area theorems, the effective rigidity of the precast member can be approximated from:

$$\psi = \frac{EI_{eff}}{EI_g} = \frac{1}{6*\left(\frac{1}{\alpha^3\beta} - 1\right)\frac{D}{L_b}\left(1 - \frac{D}{L_b}\right) + 1} \qquad \textbf{(3-19)}$$

where L_b=precast beam length, α=effective section depth ratio, β=effective section width ratio D=beam depth. The complete derivation of above effective stiffness ratio is reported in Appendix C.

If values of α=0.5 and β=1 and 0.5 are assumed for uni-and bi-directional loading, then the value of ψ= 26%and ψ=14% for uni-and bi-directional loading are obtained respectively.

3.5 Sequence of Subassembly fabrication and assembly

Construction of subassembly was initiated with the fabrication of the reinforcing cages for all four precast elements (three precast beams and a precast column) Beam and column armour plates were then match fabricated to ensure proper alignment of the post-tensioning bars, shear keys and external energy dissipators across the rocking connections. Fuse-bar anchor plates were placed in the correct alignment within the beam cages before the steel armour plates were plug welded on the beam-end.

PVC ducts were used as the post-tensioning conduit in the precast beams and column. Bent PVC knee-connections were used to achieve the desired bend in the PVC ducts around the bent coupler. Steel cage templates with the exact geometry of the column joint was constructed, and this template was locked onto the end of the precast seismic beam via two fuse bolt-bars during casting to ensure proper alignment of the shear keys and prestress between column and beam. Polystyrene and wood block-out were placed at the top of the precast beams to form a shear key pocket that allowed the top shear keys to be installed later during assembly.

Seven days after casting, the formwork was stripped. The precast column was then lifted onto the universal support, bolted and braced. Bottom shear keys were installed onto the steel armour plates, and the precast beams were lifted and dropped into position. The top shear keys were then installed. For full span beams (in the prototype building), no propping is required as the beam will rest on the bottom shear keys along. However, for the test subassembly with one column and half span precast beams, temporary propping system were used to support all the beams. The fuse bolt-bars were installed and sung-tightened to secure all beams. Stirrups and PVC ducts were placed within the cast-in-situ ends of the beam, temporary formwork constructed and concrete was poured (Figure 3-4). The temporary formwork was stripped one day after casting and the specimen was left in position for another 28 days before any prestress was applied.

(a) Gravity Beam

(b) Seismic Beams

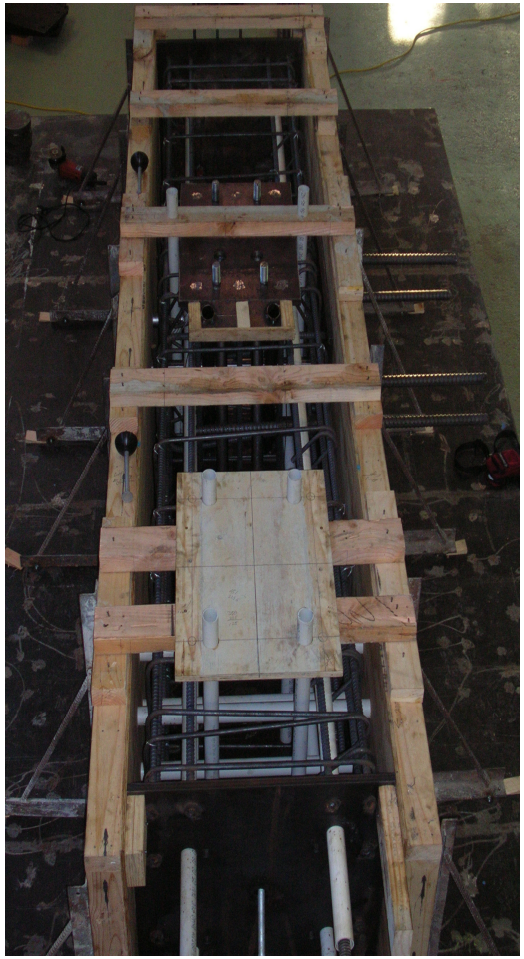

(c) Column

(d) Casting of the cast-in-situ beam end.

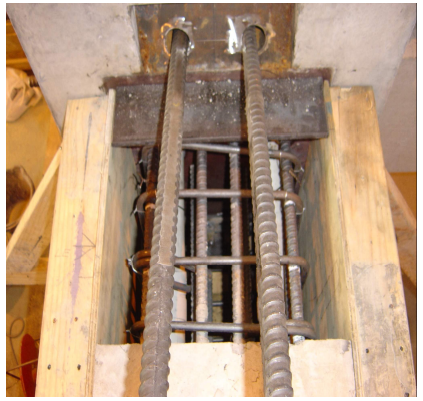

(e) Reinforcement details of the adjustable beam ends.

Figure 3-4: Photos of the precast beams, columns and cast-in-situ end.

3.6 Experimental Set-up and Instrumentation

After the specimen was assembled, reaction frames were placed around the specimen. Two large hydraulic actuators (see Figure 3-5 (a)), one along the East-West direction (Ram A) and the other along the North-South direction (Ram B) were installed across the reaction frames on top of the column. A third hydraulic actuator (Ram C) was also been installed along the East-West direction at end of the gravity-carrying beam to keep specimen movement in-plane when performing unidirectional tests. Ram C also provided a means of measuring the amount of torsion in the specimen (if any) during bidirectional testing. Movement of Ram C was synchronised to move in the same direction as Ram A but with only half of the travel of the Ram A.

Additional vertical load was applied on top of the gravity beam (i.e South beam to simulate gravity effects through a 300kN capacity hydraulic jack on top of the gravity beam (Figure 3-5 (c)). A steel plate with a ball bearing joint on top of the hydraulic jack is bolted down to a universal support fixed on the strong floor through four threaded rods. A 1.5 meter long by 200mm deep by 400mm wide timber beam was used to uniformly spread the “gravity” load along the beam.

A total of 12 load cells were used to measure strut forces at beam ends, force in the hydraulic rams, and prestress force in the Dywidag tendons. Three linear potentiometers with 50mm stroke were installed along each face of the three rocking connections to monitoring the connection opening and closing. Two linear potentiometers with 100mm travel were installed beneath each precast beam near their rocking connection to capture the vertical movements. Eight string pots were placed in various locations around specimen to capture any out-of-plane movement.

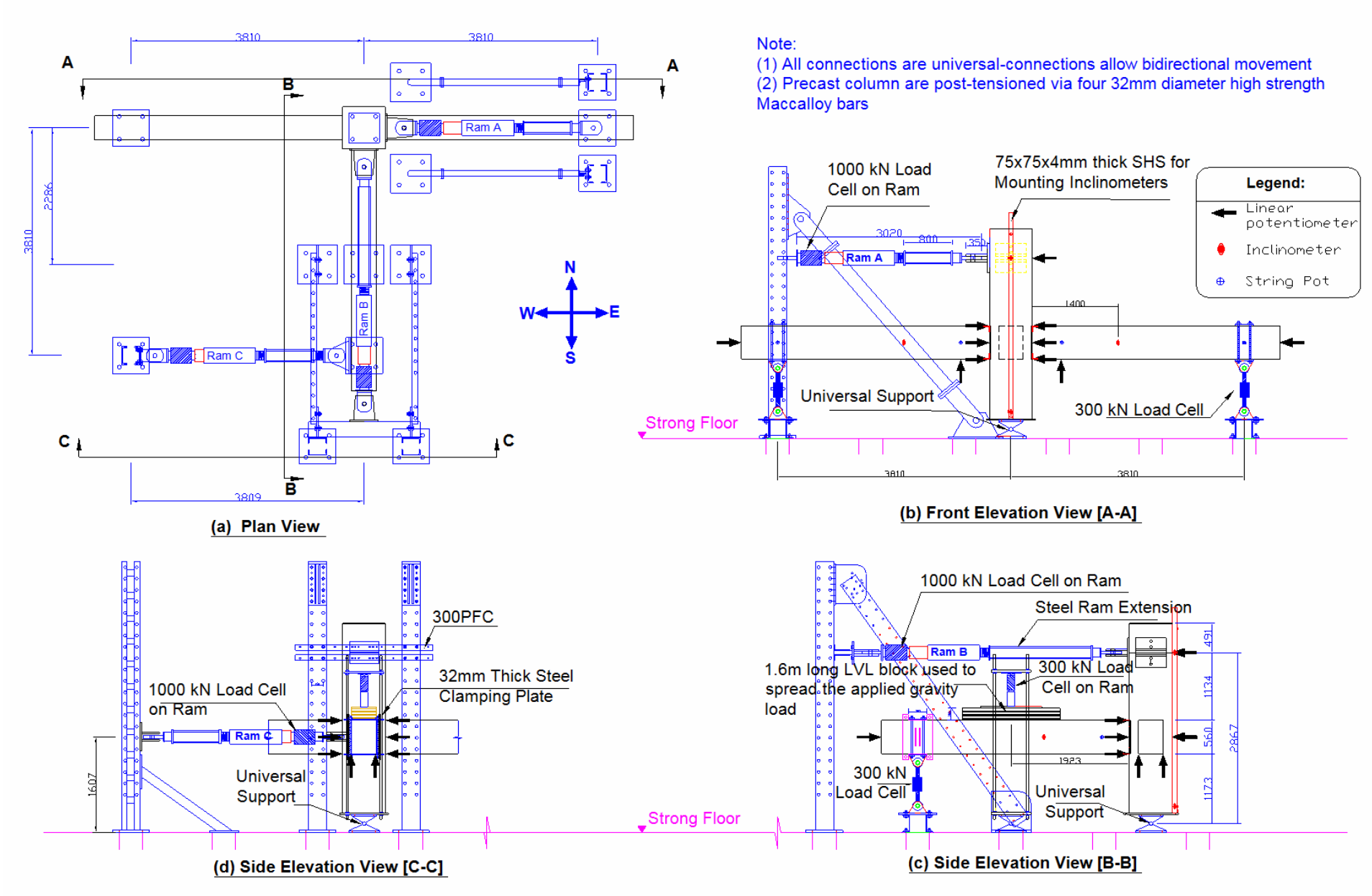

Figure 3-5: Details of the experiment set-up.

Strain gauges, (Tokyo Sokki type FLA-5-11-3L), with 5mm gauge length, were used to monitor longitudinal strains in the fuse Bolt-bars. Two 5mm gauges were attached on surface of each threaded fuse rod energy dissipators.

3.7 Data Acquisition system

Figure 3-6 presents a schematic of the test control and data acquisition system used in this experiment. The system is composed of two parallel subsystems: (1) the controller subsystem and (2) the data logging subsystem.

In the Data Logging subsystem, all measurements of displacements and strains were recorded through purpose-built Data Logging Boxes. These serial boxes convert the output from the instrumentation to digital signal which was then converted and recorded by a special-purpose software programme. During the experiment, this software was configured to display in real time the lateral load versus displacement hysteretic response.

In the Controller subsystem, a computer controller interface programme is coded using LabView 7.1 software. This controller interface program reads from the input file and activates the hydraulic rams through a user-defined trigger condition. At the end of each time interval, the specimen movement is recorded through a controller box and compared to the target movement read from the input file. When the measured movement approaches the target movement within the acceptable tolerance limit, the programme triggers the next target movement along the input file. Typical trigger values used for lateral displacement are ±0.5mm and those for lateral force are ±1kN.

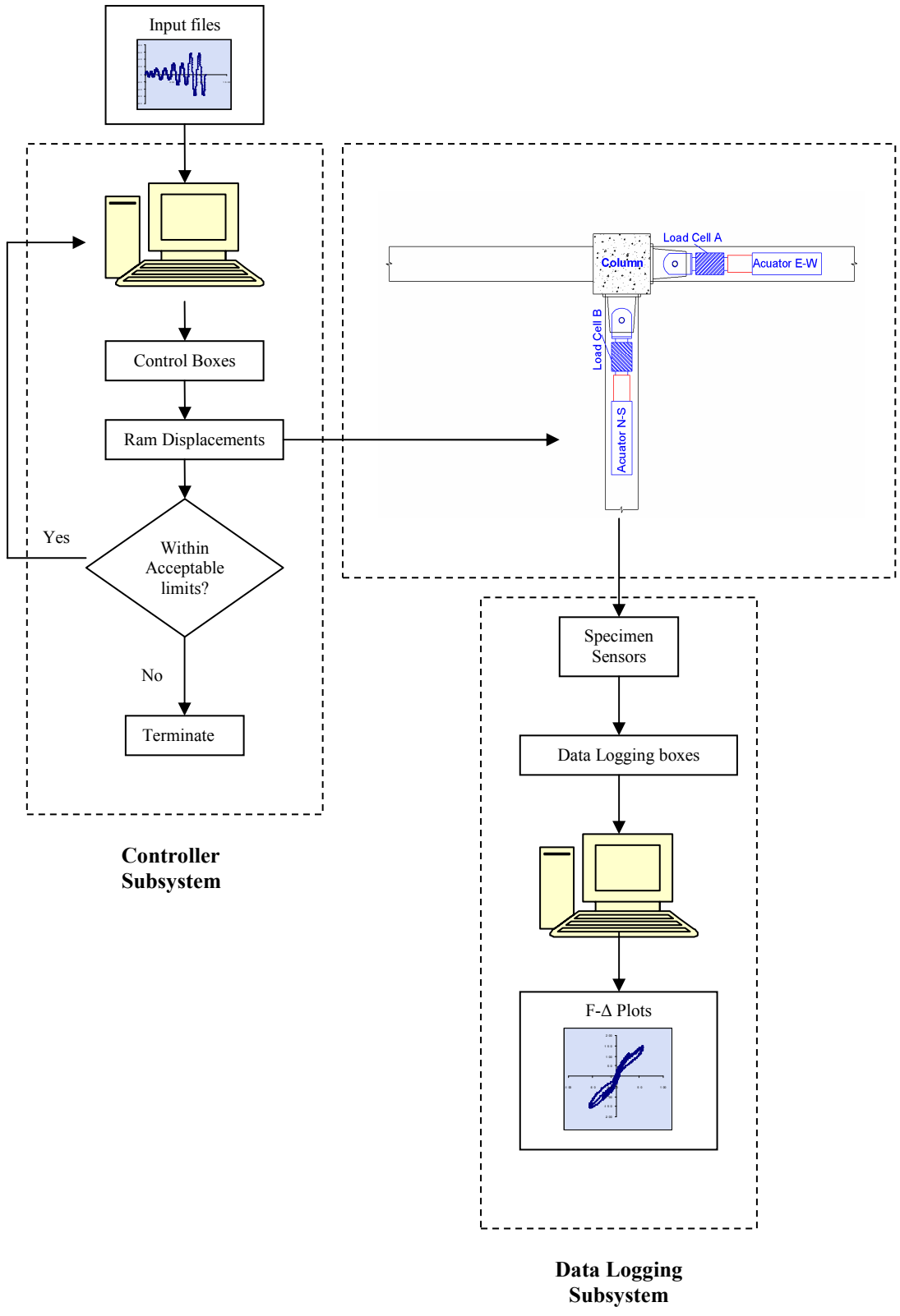

Figure 3-6: Data acquisition system.

3.8 Testing Procedures and Loading Protocol

3.8.1 Testing procedures

Experimentation was initiated with unidirectional tests to the design drift level of 2%. In these unidirectional tests, the effect of post-tensioning and energy dissipators on the subassembly response was evaluated. Following the unidirectional test, bidirectional tests were performed up to the design drift level of 2%.

To investigate the performance of the subassembly beyond the design drift level, the specimen was subjected to unidirectional loading up to 3% drift in each principal direction. Finally, bidirectional tests with 4% drift in the radial direction were performed.

3.8.2 Unidirectional loading

Separate unidirectional displacement controlled quasi-static tests were performed along both E-W and N-S directions of the specimen. During these tests, the specimen was subjected to a sequence of quasi-static loading cycles in displacement control. The applied displacement protocol consists of two drift cycles at each drift amplitude of 0.25%, 0.5%, 1%, 1.5%, 2%, 3% and 4%.

3.8.3 Bidirectional loading

To study the behaviour of the subassembly under concurrent bi-directional loading, two different types of biaxial loading paths were used namely: (1) Cosine-based four-leaf clover pattern given by the $x = \alpha Cos(2\theta)Cos(\theta)$, and $y = \alpha Cos(2\theta)Sin(\theta)$; and (2) Sine-based four-leaf clover pattern given by $x = \alpha Sin(2\theta)Cos(\theta)$, and $y = \alpha Sin(2\theta)Sin(\theta)$. As in case of the unidirectional test,

the bidirectional test started with a drift level at 0.25% and gradually increased to 4% column drift in radial direction.

3.9 Experimental results and observation

The experimental results are presented in three parts: (i) a series of unidirectional tests up to 3% column drift in which the performance of the subassembly with only prestress is compared with the performance of the subassembly with both prestress and threaded rod energy dissipators. (ii) a series of biaxial tests up to design level drift of 2% in which the performance of the subassembly with and without threaded rod were investigated. (iii) A series of biaxial tests to 4% column drift to investigate subassembly behaviour beyond the design drift level.

3.9.1 Unidirectional loading tests

Before subjecting the specimen to bidirectional tests, unidirectional tests in both the seismic frame (East-West) and gravity frame (North-South) direction were conducted separately. The subassembly performed as expected with rotation concentrated at the rocking interface between precast beams and column in both directions.

Figure 3-7 shows that in both E-W and N-S loading directions: a bilinear elastic force-drift response was achieved when the subassembly was tested with only the prestress present. Figure 3-8 shows that when threaded rods were added across the connections in the subassembly, a flag shaped force-drift response was achieved. All the tests showed promising re-centring characteristics as expected. The subassembly suffered minor superficial cracking on precast beams after 3% drift. The precast

column remained uncracked and damage free. The well-spaced cracks along the precast beam closed up on removal of the lateral load. Due to the partially prestressed nature of the beams, these minor cracks were expected.

Good agreement between theoretically predicted and experimentally observed results (Figure 3-7and Figure 3-8) verified the adequacy of the design theory developed in the previous section and validates the adequacy of the rigid body kinematic modelling of the mechanism. The effective stiffness formula developed based on St.Venant's principle in the previous section realistically models the subassembly. It may be noted that slightly higher initial stiffness value of 5% are due to the high sensitivity of the α and β values assumed.

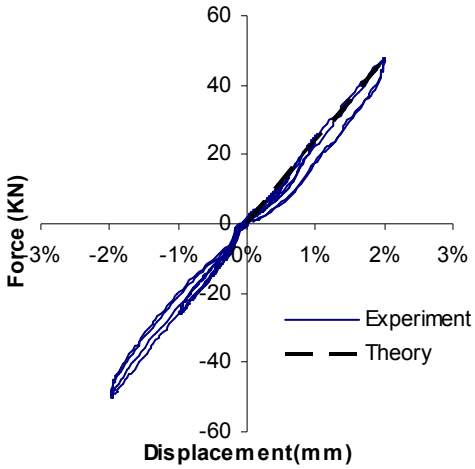

(a) E-W Loading with minimum initial prestressing force.

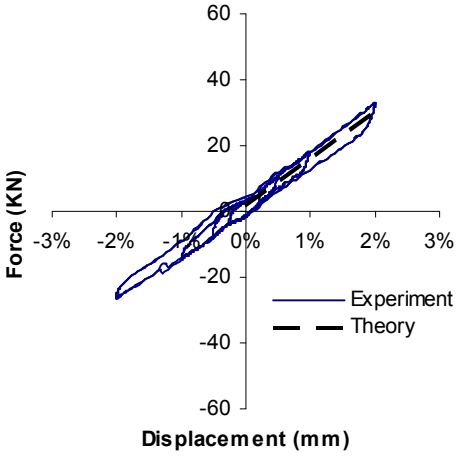

(b) N-S Loading with minimum initial prestressing force.

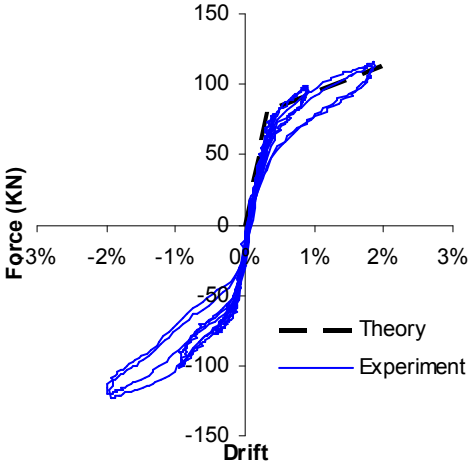

(c) E-W Loading up to 2% lateral drift with initial prestressing force level of 50% of bar yield.

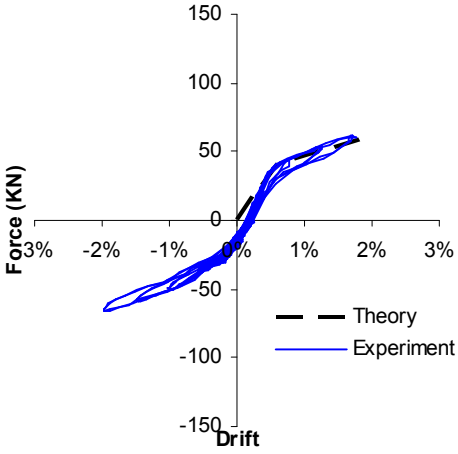

(d) N-S Loading up to 2% drift with initial prestressing force level of 50% of bar yield.

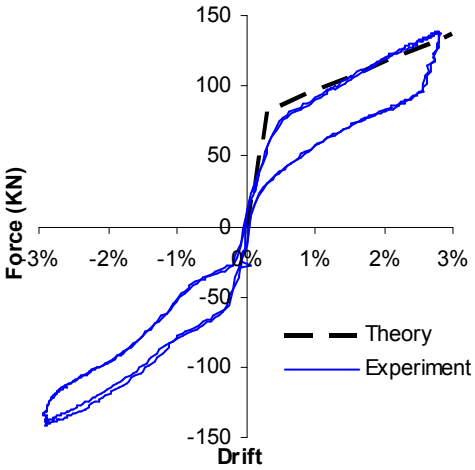

(e) E-W loading 3% lateral drift with initial prestressing force level of 50% of bar yield

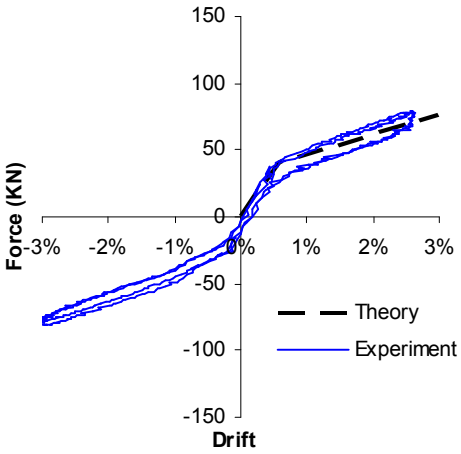

(f) N-S loading 3% lateral drift with initial prestressing force level of 50% of bar yield.

Figure 3-7: Force-Displacement response of subassembly with prestressing only, tested under unidirectional loading to 3% lateral drift.

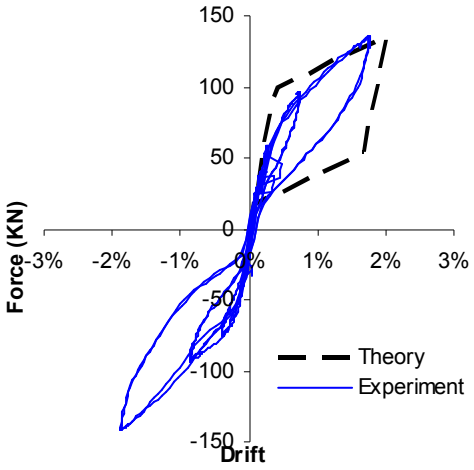

(a) E-W Loading up to 2% lateral drift with threaded fuse dissipators.

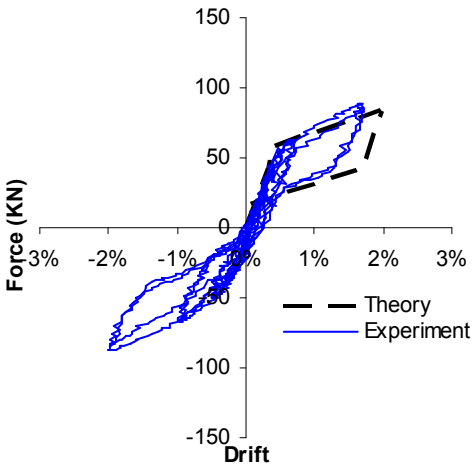

(b) N-S Loading up to 2% with threaded fuse dissipators.

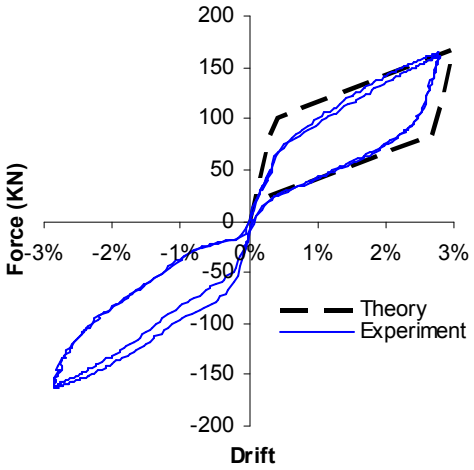

(c) E-W Loading 3% lateral drift with threaded fuse rod dissipators

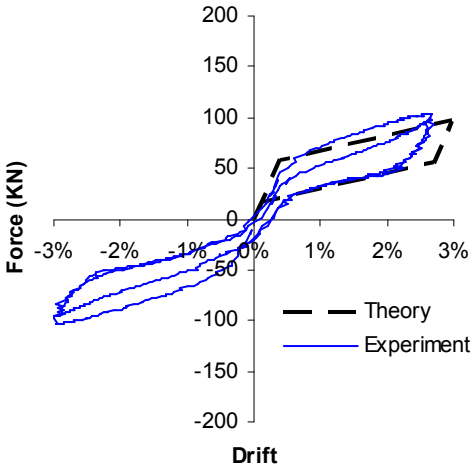

(d) N-S Loading 3% drift with threaded fuse rod dissipators

Figure 3-8: Force-Displacement response of subassembly with threaded fuse-rods tested under unidirectional loading to 3% lateral drift.

3.9.2 Bidirectional loading up to design drift of 2%

Figure 3-9 summarises the experimental results of the subassembly tested under bidirectional loading. The displacement control was governed by a 4-leaf clover pattern of the cosine type. The results show: (a) plane view of the bidirectional drift orbit (Cosine 4-leaf Clove), (b) force-displacement hysteresis plots, (c) displacement inputs along East-West and North-South direction and (d to g) some photographs of the subassembly. When tested first without any external energy dissipators, the subassembly exhibited bilinear elastic behaviour in both East-West and North-South direction. It is pointed out that the subassembly was tested to 2% drift in a radial (diagonal) direction. No torsional cracks were observed because the designed shear keys at the connection provided good resistance against torsional moments during the tests. The maximum (in-plane) lateral forces were found to be 100kN in the EW direction and 51kN in NS direction at the maximum drifts.

The supplementary energy dissipators were then installed across all the connections and the subassembly retested under same bidirectional loading pattern. The results are summarised in Figure 3-10. The maximum lateral force was found to be: 124kN in E-W direction and 80kN in N-S direction. Some minor tension and compression cracking was observed immediately behind the steel amour plate. Nevertheless, the subassembly returned to its original centred position upon removal of the lateral loads with negligible residual drift.

(d) Damage behind steel armour plate on the seimic beam

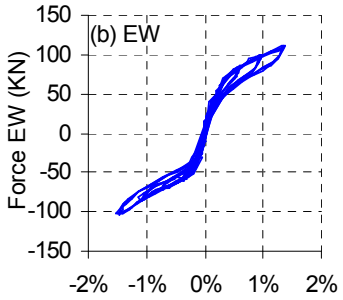

(e) Spalling of concrete

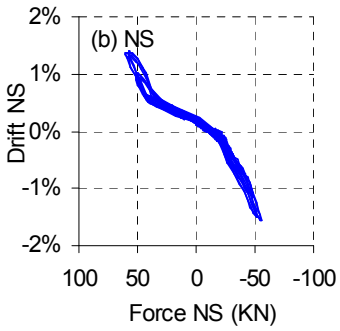

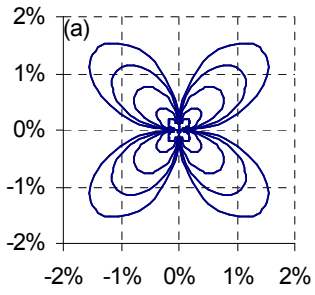

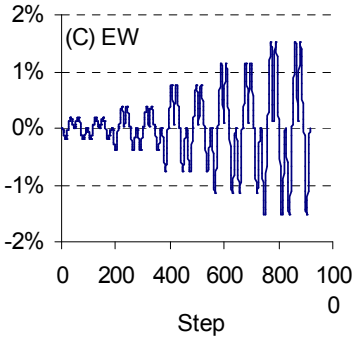

(f) Gravity beam to column Connection opening at 2% drift

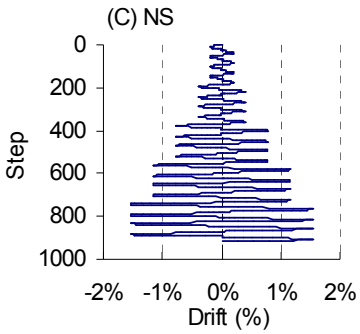

(g) Damage behind top steel armour Plate on the Gravity beam

Figure 3-9: Experimental results of subassembly tested under bidirectional cosine cloves loading with prestressing only showing: (a) Plan view of the bidirectional drift orbit (cosine 4-leaf clove), (b) Force-displacement plots, (c) Displacement inputs and photographs showing: (d) Damage behind the angled armour plate on seismic beam, (e) Spalling of concrete on seismic beam, (f) Typical connection at 2% drift and (g) Damage on top of the gravity beam.

During bidirectional loading, the precast beams were observed to rock on only one corner at the connection. The large force generated from bidirectional loading caused some minor cracks behind the steel amour plate, but all these cracks closed when the load was removed. The supplementary energy dissipators were found to be effective however buckling did occur during testing Figure 3-10 (d) and (f)).

The effective stiffness of the beam was found to be only some 16% of the gross stiffness. This is attributed to the reduction of the contact area at the rocking interfaces during bidirectional loading. The subassembly has a lower lateral load resistance when precast beams rocks on one corner under bidirectional loading. The effective stiffness formula developed on the basis of the St Venants' principle is evidently an adequate explanation of the reduced stiffness. An additional experimental observation is that the armoured rocking beam ends deform flexibly along depth of the beam when the gap opens up at the connection. This flexibility of the beam ends cause more deformation in comparison to the theoretical prediction of the model which assumes a rigid body rotation mechanism and therefore predicts a lower effective beam stiffness.

The results from bidirectional loading tests with sine based 4-leaf-clover input are presented in Appendix E. The force-displacement relationships in both principal directions from these tests were found to be similar to the behaviour of the unidirectional loading in the sense that major displacement cycles were imposed on the specimen along both principal axes.

(d) Buckling of Energy Dissipator at 2% drift (Seismic Beam)

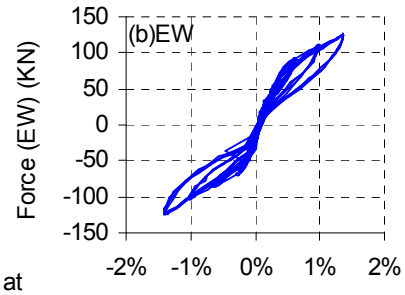

(e) Damage under beam

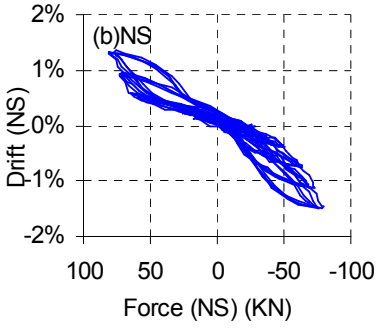

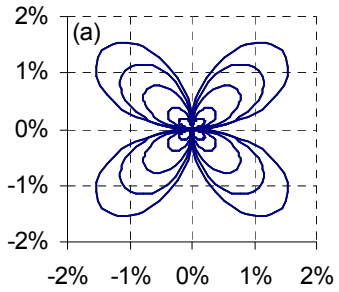

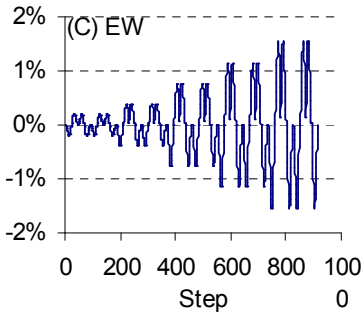

(f) Bucking of Energy Dissipator at 2% drift (Gravity Beam)

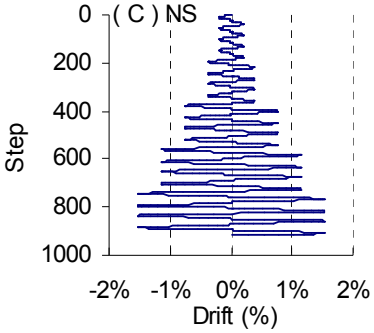

(g) Opening of Connections at 2% drift

Figure 3-10: Experimental results of subassembly tested under bidirectional Cosine cloves loading with threaded rod energy dissipators showing: (a) Plan view of the bidirectional drift orbit (Cosine 4-leaf clove), (b) Force-displacement plots, (c) Displacement inputs and photographs showing (d): Bucking of energy dissipator on seismic beam, (e) Damage under beam, (f) Threaded rod dissipator on top of Gravity beam at 2% drift and (g) Opening of joint connections at 2% Drift.

3.9.3 Bidirectional loading to 4% column drift

To study the behaviour of the subassembly after the design basis earthquake (DBE) which has 10% probability of occurrence in 50years, tests were performed under bidirectional Cosine based 4-leaf clover up to 4% radial column drift. This level of displacement can be considered to be in excess of the seismic demands imposed by a maximum considered earthquake (MCE) which has 2% probability of occurrence in 50years.

The performance of subassembly with prestress only, is compared with the performance of the subassembly with both prestress and threaded energy dissipators in Figure 3-11. As expected more cracks were observed when the subassembly was tested up to 4% drift when compared to the design drift level (2%). Nevertheless, the subassembly maintained a good strength at 4% drift level.

The fuse bolt-bars in the precast beam were found to just exceed their yield strength at the 4% column drift. This provided some supplementary extra energy dissipation to the subassembly. As a result, a slight reduction of peak strength was observed during the second loading cycles. The fuse bolt-bars were re-stressed after each test to maintain the initial prestress level in the subassembly.

It is realized that large fiction generated around the bent coupler results slightly stepped force-displacement curves at low drift level, which has been observed in all previous tests. A smoother transition in the prestressing conduit around the bent region should mitigate this behaviour.

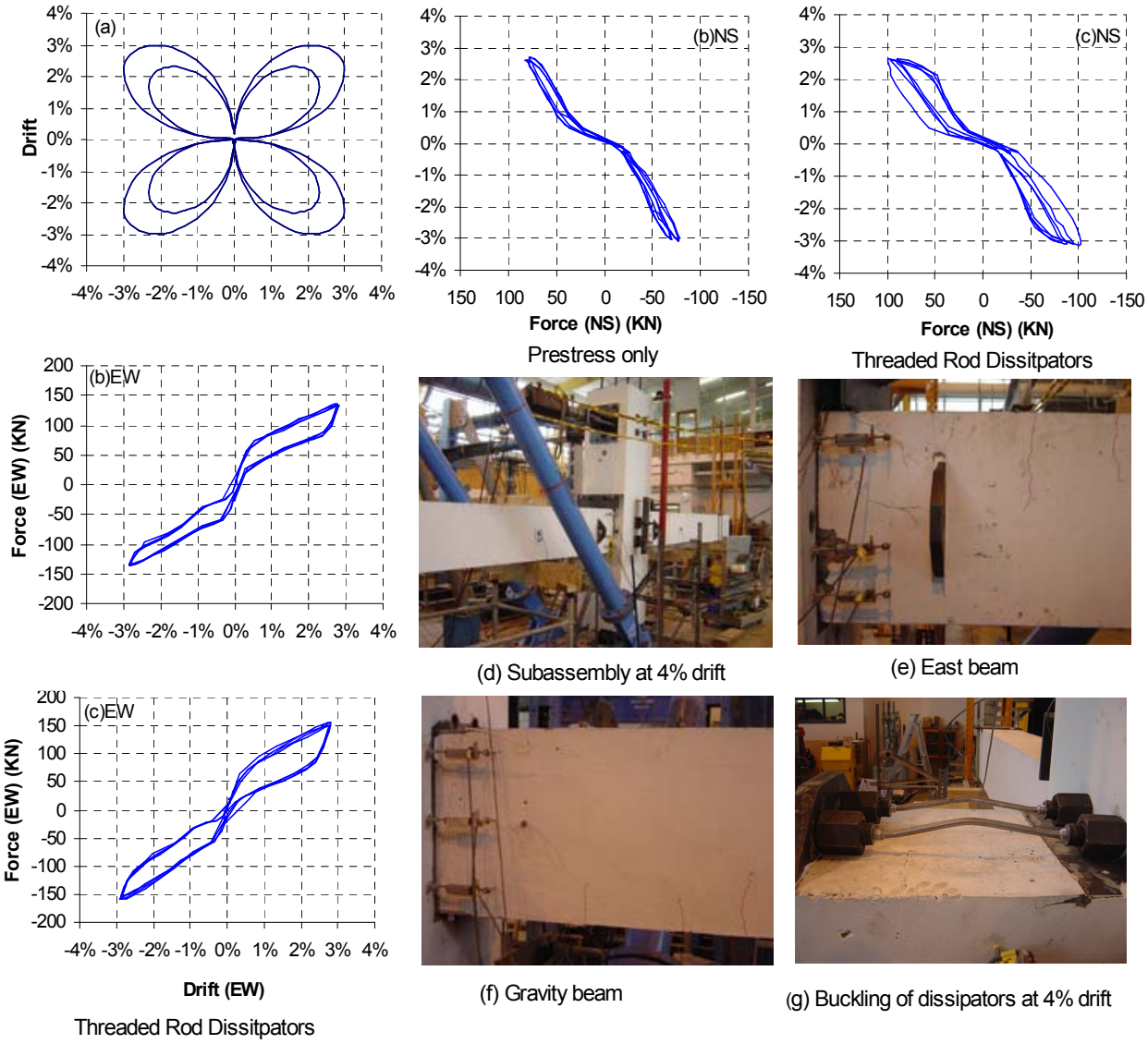

Figure 3-11: Experimental results of subassembly tested under bidirectional Cosine 4-leaf cloves to 4% drift showing: (a) Plan view of the bidirectional drift Orbit, (b) Force-displacement plots of subassembly without dissipators, (c) Force-displacement plots of subassembly with prestress and threaded rod dissipators installed and photographs showing: (d) Subassembly at 4% drift., (e) Damage in east beam, (f) Damage in gravity beam(g) Buckling of fuse rods at 4% drift

3.9.4 Hysteretic energy dissipation

Hysteretic energy dissipation of the subassembly can be considered in terms of equivalent viscous damping. According to Pekcan et al (1999), the equivalent hysteretic damping of a bi-linear structural system is given by equation (2-28) in Section 2.

For the rocking precast concrete frame system with flag shaped loops, the prestress force within the tendon at both ends can be expressed via well-known prestressing loss formula as:

$$\frac{F_2}{F_1} = e^{(-\mu\alpha - \kappa l)} \qquad \textbf{(3-20)}$$

where F_1= force at jack end and F_2= force at the anchor end, μ= angular coefficient of friction, α=angle change of the tendon in radian unit, κ= wobble loss coefficient, and l= length of the tendon where prestress loss are considered.

Assuming κl the wobble loss is small and can be neglected, and the friction loss $\mu\alpha$ values are also small so that the higher order term in the series expansion can be neglected, the prestress losses in the tendon after opening or closing of the gap δF is:

$$\delta F = \mu\alpha F_1 \qquad \textbf{(3-21)}$$

Combining the equivalent viscous damping developed by Clough below:

$$\xi_{hy} = \frac{1}{4\pi}\frac{E_D}{E_{so}} \qquad \textbf{(3-22)}$$

where E_D= area enclosed in the actual hysteresis loop and E_{so}= area under the equivalent linear elastic hysteresis curve. The energy efficiency factor (η) defined in Equation (2-8) by Pekcan et al (1999) can be modified for the present subassembly with only prestress to be: $\eta_{ps} = \mu\alpha$.

When supplementary energy dissipators are added, the equivalent viscous damping of the subassembly can be found by further modifying the energy absorption efficiency factor to take consideration the effect of both prestressing losses and the yielding of the energy dissipators:

$$\eta_{diss+ps} = \frac{\mu\alpha + \left(\frac{F_{y\,diss}}{F_{\max}}\right)}{1 + \left(\frac{F_{y\,diss}}{F_{\max}}\right)} \qquad \textbf{(3-23)}$$

According to Pekcan et al (1999) typical values of η for well designed ductile reinforced concrete is 0.35-0.4. For the subassembly with an coefficient of friction μ= 0.25 for threaded bar, and a 20 degree α= 0.35rad bent coupler, the energy absorption efficiency factors of the subassembly with prestressing alone is $\eta_{ps} = 8.75\%$.

When energy dissipator with a yield strength of $F_{y\,diss}$ = 53kN added and F_{max}= 398kN (i.e. yield strength of the "bolt-bar") the energy absorption efficiency factor is increased to $\eta_{ps+diss} = 19\%$.

Using these results along with Equation (2-8) with α= 0 the theoretical equivalent viscous damping is plotted for the prestress only and prestress plus supplemental energy dissipators in Figure 3-12, respectively. Also plotted is the graph in the observed equivalent viscous damping factors, as determined form the area enclosed by the hysteresis loops in the experiments. Although the levels of damping are small, particularly of the prestress only case, the approach seems to adequately model the effects of hysteretic energy absorption. It is believed that the high energy dissipation values observed at lower drift level resulted from the temporary high lateral force required to overcome of friction and mobilize the bent couplers in the connection.

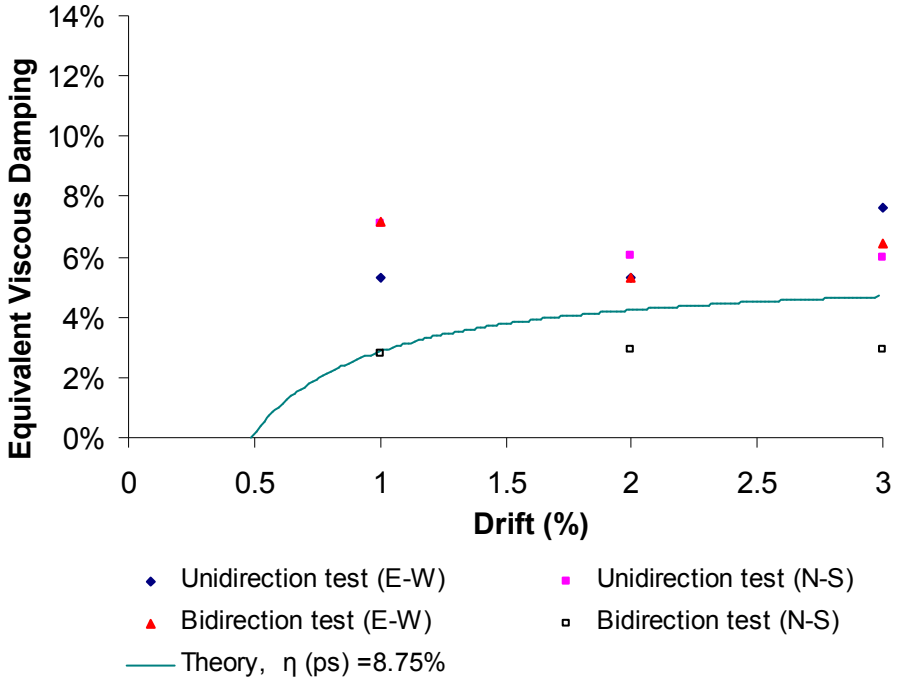

(a) Minimum prestress and prestress only

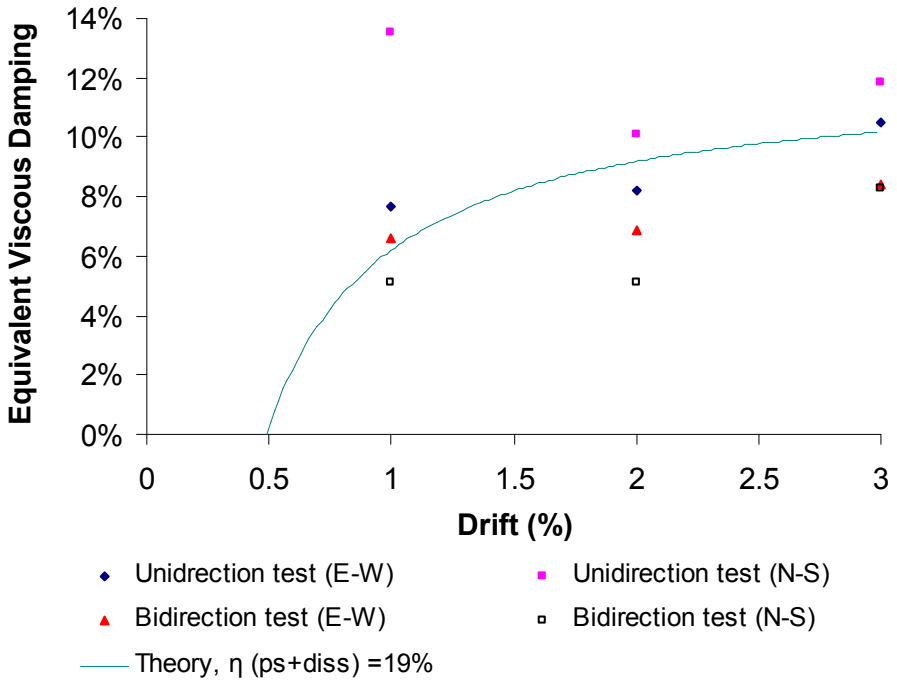

(b) Prestress with supplementary energy dissipators

Figure 3-12: Equivalent viscous damping of the subassembly.

3.10 Concluding Remarks

Based on the experimental investigation described herein, the following conclusions are drawn:

1. Simple steel armoured rocking connection designed without welding is feasible in protecting precast concrete elements against seismic damage.
2. The proposed displacement based design and detailing procedures are shown to be adequate. The subassembly performed well up to biaxial column drifts of 4%. Minor superficial service cracking was observed in the precast beams, while the precast column remained damage free.
3. The tapered shear key details provided between the beam ends and the column face offered satisfactory resistance against imposed tensional moments that tended to twist the beam under bidirectional moments up to the 4% (radial) column drift limit.
4. Although the supplementary mechanical energy dissipators provided adequate energy absorption especially when in tension, due to compression buckling in compression reduced their effectiveness during cycles following the previous peak displacement.
5. From the test results, the apparent stiffness of the beam member is in the order of $EI_{eff} = 0.16\ EI_g$. The reduction can be explained by the effect of the high point forces at the beam ends during rocking using St Venants' principle. Based on a rational analysis approach, a formula has been derived to determine this reduction in stiffness.
6. Certain detailing improvements have been identified from the results of the present experiments. Particularly noteworthy is the need for a smooth transition in the vicinity of the cable duct deviation. Eliminating the bent

coupler would be helpful in mitigating stepped hysteresis behaviour at low drift levels.

7. Although the rocking behaviour at the beam ends was effective in creating a bilinear elastic response, some rolling type resistance was evident due to the reduced stiffness observed in the experiments. This minor adverse effect could be easily mitigated by recessing the concrete back from the armouring some 3 to 5 mm during the beam casting process.

3.11 Reference

Arnold, D.M (2004). *Development and Experimental Testing Of a Seismic Damage Avoidance Designed Beam to Column Connection Utilising Draped Unbonded Post-Tensioning* Masters, Thesis, Department of civil Engineering, University of Canterbury, Christchurch, New Zealand.

Davies, M.N (2004) Seismic Damage *Avoidance Design of Beam-Column Joints using Unbonded Post-Tensioning: Theory, Experiments and Design Example.* Masters, Thesis, Department of civil Engineering, University of Canterbury, Christchurch, New Zealand.

MacRae, G.A., and Priestley, M.J.N. (1994), *Precast Post-Tensioned Ungrouted Concrete Beam-Column Subassemblage* Tests, Report No. SSRP-94/10, Department of Applied Mechanics and Engineering Sciences, University of California San Diego, California, USA.

Mander, J.B., and Cheng, C.T. (1997). *Seismic Resistance of Bridge Piers Based on Damage Avoidance Design*, Technical Report NCEER-97-0014, Department of Civil, Structural and Environmental Engineering, State University of New York at Buffalo, New York, USA.

Pekcan, G.,Mander,.J.B.,and Chen,.S.S., (1999), *Fundamental Considerations for The Design of Non-linear Viscous Dampers.* EESD Journal, Vol 28, P1405-1425.

Standards New Zealand, (1992), NZS 4203: 1992. *Code of practice for general structural design, and design loadings for building*. Standards New Zealand, Wellington.

Standards New Zealand, (1995), NZS 3101: Part 1:1995: *Concrete Structures Standard*, Standards New Zealand, Wellington.

Stone, W.C., Cheok, G.S., and Stanton, J.F. (1995), *Performance of hybrid moment-resisting precast beam-column concrete connection subjected to cyclic loading,* ACI Journal, Vol. 91, No, 2 March-April.

4 Section Four: Design Improvements and Future Work

Section Summary

Potential improvements in the seismic design of a large 3-dimensional jointed beam to column joint subassembly are proposed based on results of physical tests from previous section. Two new precast seismic beams with an improved connection details are proposed. Two 26.5mm diameter high strength high alloy threadbars (Macalloy^{TM}) are used in prestressing the new seismic beams to provide a total connection moment of 256kN-m. In the new connection the 100mmx100mmx12mm thick steel angle-armour plates are installed in a reverse fashion with the flange pointing outwards towards the beam end. Concrete at the beam-end at the connection is recessed back 3mm to ensure that the beam rocks only on the edge of the steel amour plate and no concrete makes contact with the column. Bent couplers in the previous design are replaced with a new draped tendon profile. Diagonal fuse "bolt-bars" are joined by a straight (instead of the previously bent) coupler. The threaded rod energy dissipator layout used is retained in the improved design as they are easy to install and replace. Further improvements for a possible future research works are also suggested.

4.1 Introduction

Significant damage to structures during recent earthquakes such as Loma Prieta 1989, Northridge 1994, and Kobe 1995, has highlighted the need of not only seismically safe structures that ensures life-safety for occupants, but also damage-free. Thus following an earthquake the structure can be re-instated to service and re-occupied immediately with minimum downtime and minimal repairs. The proposed armoured and jointed precast concrete structure provides good basis to achieve such "damage-avoidance" seismic performance.

Precast-prestressed concrete beam-column joints that use unbonded tendons have been extensively tested for reliable seismic resistance and performance. The present research on the seismic performance of the jointed precast beam to column connection has demonstrated that separating columns and beams will reduce the amount of damage inflicted on both column and beams in the event of an earthquake. All of the inelastic rotation is accommodated through a single gap opening at the beam to column connection. This gives the jointed structure some significant advantages over the traditional monolithic construction, particularly form the point of view of damage avoidance.

The efficiency of a fully welded armoured steel-steel jointed beam-column connection in protecting precast frame elements against seismically induced damage was demonstrated by Davies (2004) and Arnold (2004). But the extensive welding used in constructing their connections markedly increases the manufacturing cost of such armoured precast beams. To simplify the steel-steel armouring detail in the jointed frames, steel angles are used to amour the precast beam ends at the rocking connections. As part of the present study, the proposed simplified connection details were tested under both uni-directional loading and bi-directional loading as part of

this study and described previously in Section three. Test results showed that precast beams with steel angle armour end gives sound protection against seismic damage. However, as a result of these most recent experiments further improvements to the connection details have been identified.

4.2 Connection Detail Improvements

The experimental testing programme presented in Section Three has enabled the identification of several potential improvements in seismic design of the rocking connection which are summarised below:

4.2.1 Steel Armour Plates:

During previous testing, steel armouring on the ends of beams in the beam to column connection performed well in protecting concrete from crushing in all the precast beams. A connection detail that uses angles and required no welding is demonstrated to be feasible. However, due to the large difference in the stiffness of concrete and steel, cracks initiated at the tip of the amour plate causes the beam rotate about tip of the armour plate rather than around the edge of the steel amour plate. This behaviour reduces the initial stiffness of the subassembly.

It was also observed that some rolling resistance resulted when beam rocks against the column, which was caused by the uneven surfaces between the concrete and steel amour plate at the beam-end. An improvement to the rocking mechanism should result by recessing the concrete back from the steel armour plate during casting.

In comparison to the armoured details provided by Davies (2004) and Arnold (2004), the less heavily armoured ends in the subassembly tested in this research are lighter and more flexible. The flexible beam ends increase the deformation and lower

the initial stiffness of the subassembly. As a future research direction, a finite element model could be used to accurately capture this flexible-rocking behaviour at the rocking connections in the subassembly to provide a means to estimate the effective stiffness of such rocking beams.

4.2.2 Prestress Profile

A bent coupler was used in the subassembly tested in this research at the joint of fuse "bolt-bar" with the main longitudinal prestress thread bar in the precast beam. This diagonal bolt bar prestress profile not only gives the structure some load-balancing capability but also increases the redundancy level of the building. The fuse region along the "bolt-bar", provides some extra energy dissipation in the event of a strong earthquake as well as strengthening the building against near-field earthquakes. However, the test results indicate that a smoother transition in the vicinity of the cable duct would be preferable. A practical solution is to improve this prestress by draping the tendon within the precast beam and use a straight coupler to join the fuse "bolt-bar" with the draped tendon.

4.2.3 Energy Dissipators

The threaded rod energy dissipators used in the subassembly contribute approximately 12% of equivalent viscous energy at 3% column drift. Limited buckling of the threaded rod dissipator was observed during testing that have lowered the amount of energy dissipated in the subsequent cycles. A potential alternative way to improve the hysteretic performance and prevent the bucking of the threaded rod is to sleeve the fuse area and grout the sleeve. However, this may not be a feasible solution as the beam will end up sitting outwards on the elongated dissipators which results in and additional source of overall flexibility. Nevertheless, external energy

dissipator layout used in the subassembly has the advantage of easy replacement which shortens the preparation time between individual tests in the experiment. However, casting the energy dissipators within the connection could be advantageous for the prototype structure as it is less obtrusive.

It is proposed that new types of energy dissipators should be explored. In particular, dissipators that have either re-centring capability, or can creep to maintain zero force or tension when the joint is closed. Viscous or visco-elastomeric dampers may be suitable for this purpose.

4.3 A Proposed Solution

To further simplify the connection details in the jointed precast beam-to-column connection and to provide a practical solution that will utilise the full potential of the precast prestressed jointed construction, two new precast beams with improved end armoured details design based on the design philosophy incorporated in present research are proposed.

Figure 4-1 shows the new connection details of the proposed improved beam-to-column connection. The steel angle armour plate used in the proposed new design is placed at a reverse position compared to the present design solution developed in Section 3, with the horizontal flange of the steel angle pointing toward the column face. The concrete surface at the end of the new armoured precast beams is recessed back 3mm form the edge of the horizontal flange of the steel angle. This improves the rocking mechanism of the beams on column faces by reducing the connect area in the connection. No welding is required during construction the new armoured connection as the steel angles are secured on the ends of the longitudinal beam reinforcements through several (Reidbar^{TM}) nuts. Two steel stiffener plates need to be locked behind

the steel angle armour plate at the beam end to help confine the concrete and stiffen up the beam end.

A new prestress scheme with diagonal high strength (Maccalloy^{TM}) fuse "bolt-bar" jointed onto the beam prestress via a straight coupler is proposed. With such a layout, some gravity load may be balanced if desired. For the sake of convenience in experimental testing, external threaded energy dissipators may continue to be used in both gravity and seismic precast beams. The shear key layout used in the beams may also be retained the same as before, since they have been demonstrated to be very effective in resisting torsional movements and moments.

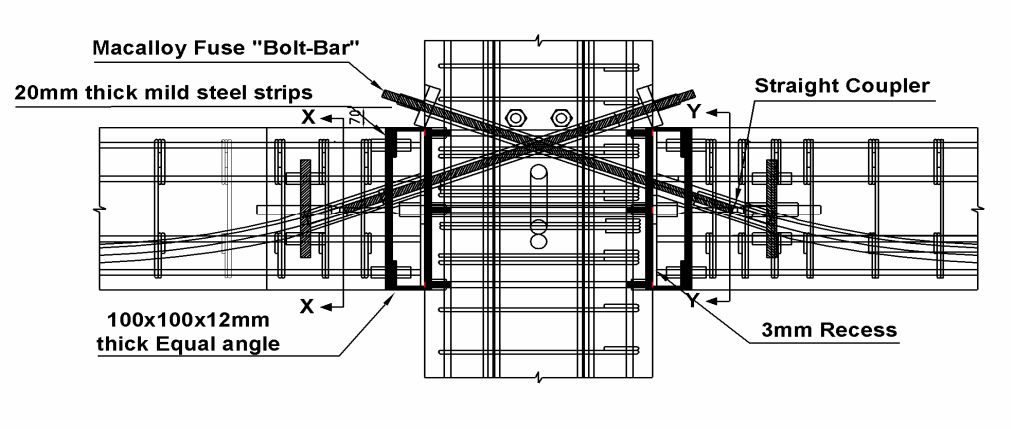

(a) Elevation View

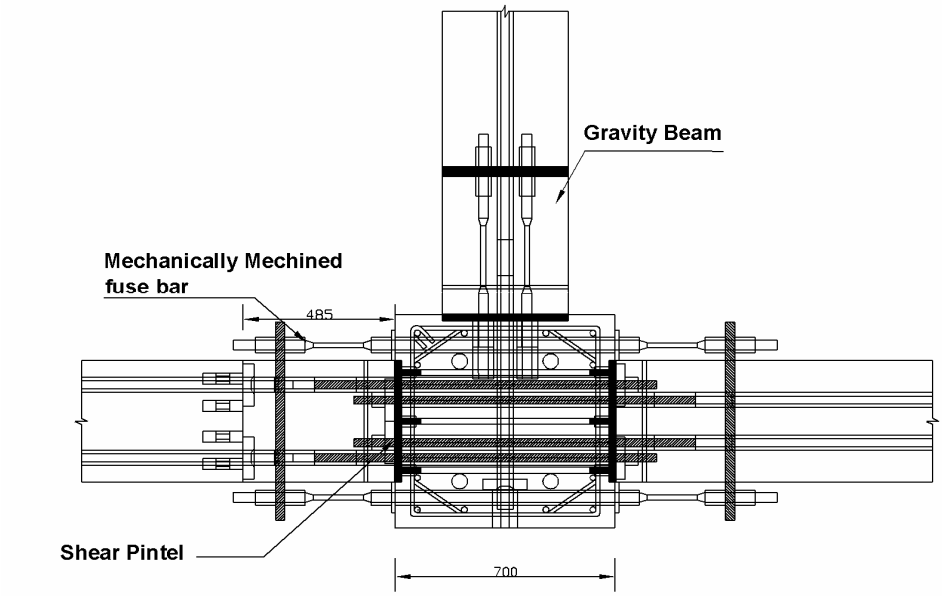

(b) Plan View

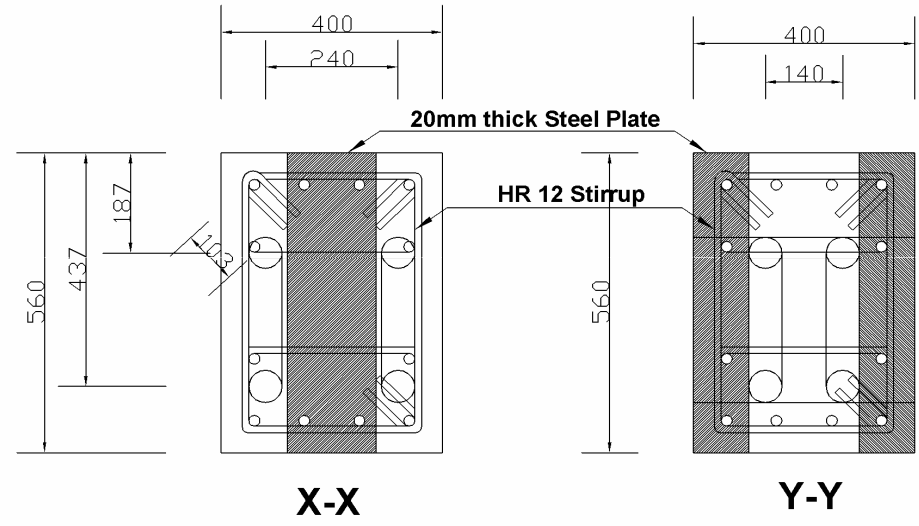

(c) Section Details

Figure 4-1: Proposed Improved Connection Details of the subassembly

4.4 Recommendations for Future Work

Based on the research presented in this thesis, the following topics are considered to be promising directions for future research:

1. To develop a full 3-dimensional computational model of jointed precast buildings and compute their expected seismic performance under near-field and far-field earthquakes and compare these results with conventional ductile cast-in place reinforced concrete buildings.
2. To conduct research on suitable types of energy dissipators for the jointed frames that may not need replacing and also possess re-centring characteristics.
3. To further study the effective beam stiffness using FEM computer models.
4. To further experiment research on the system by means of shake table tests on the large scaled 3-dimensional beam-column joint subassembly considering the performance of the new connection detail developed in the present research and different types of floor slabs.
5. To analytically investigate the dynamic response of the proposed system and verify the seismic design approach through dynamic time-history analysis.
6. To conduct DAD methodology conformation experiments on a large scaled concrete frame superassembly with jointed connections using the pseudo-dynamic test method.

4.5 Reference:

Arnold, D.M (2004). *Development and Experimental Testing Of a Seismic Damage Avoidance Designed Beam to Column Connection Utilising Draped Unbonded Post-Tensioning* Masters, Thesis, Department of civil Engineering, University of Canterbury, Christchurch, New Zealand.

Davies, M.N (2004) Seismic Damage *Avoidance Design of Beam-Column Joints using Unbonded Post-Tensioning: Theory, Experiments and Design Example.* Masters, Thesis, Department of civil Engineering, University of Canterbury, Christchurch, New Zealand.

Appendix A: Material Properties

Table A-1: Concrete Cylinder Tests:

	Concrete Compressive Strength (Mpa)		
	At 7 Days	**At 28 Days**	**At testing**
Beam Cylinders	38	44	46
Column Cylinders	40	46	50
Cast in-situ Cylinders	53	59	63

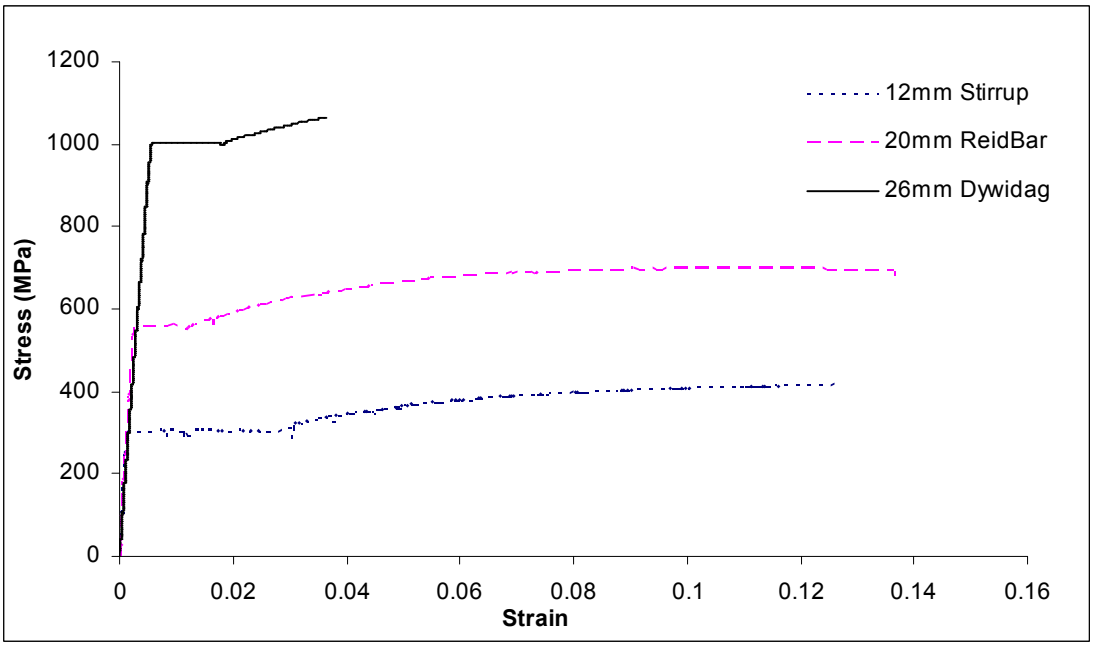

Figure A-1: Material Tensile tests: Reinforcing HR 12 Stirrup, Grade 500 Reidbars and the high strength high alloy (Dywidag^{TM}) thread bar (950/1050 grade) with 26.5mm diameter.

Appendix B: Subassembly Design:

B.1 Subassembly Drift Capacity Assessment:

East-West Loading (Seismic Beams):

l_{bolt} = 1200mm, l_{ps} = 4050mm Lb=8000mm and L=8700mm e_{ps}^{-} =370mm, e_{ps}^{+} =190mm, A_{bolt}/A_{ps} =0.75,

$$\theta_{col\ yeild}^{+} = \frac{0.0025*(1200+0.75*4050)}{190}*\frac{8000}{8700} \approx 0.051 rad \qquad \textbf{B-1}$$

$$\theta_{col\ yeild}^{-} = \frac{0.0025*(1200+0.75*4050)}{370}*\frac{8000}{8700} \approx 0.026 rad \qquad \textbf{B-2}$$

The negative yield drift capacity governs so the design drift for East-West loading is 0.026 rad.

North-South Loading (Gravity beam):

l_{bolt} = 700mm, l_{ps} =4050, Lb=8000mm and L=8700mm, $e_{ps}^{-} = e_{ps}^{+}$ = =D/2=280mm

$$\theta_{col\ yeild} = \frac{0.0025*(700+0.75*4050)}{280}*\frac{8000}{8700} \approx 0.03 rad \qquad \textbf{B-3}$$

B.2 Precast Element Design:

Precast beams and columns are designed to remain in an essentially elastic condition even whilst subjected to the over-strength conditions of the beam to column connections.

For a high axial load level, a fully elastic design can be performed using an elastic stress block analysis. The resultant stress block formed by combing the axial load and bending stress blocks should be kept within elastic stress limits. If the maximum concrete tension stress before cracking is set to $\alpha\sqrt{f_c^{'}}$ and the maximum elastic compressive concrete stress set to $\beta f_c^{'}$ the elastic section moment will be the lesser of :

Tension Limit:

$$M_{elastic} = \left(\alpha\sqrt{f_c^{'}} + \frac{P}{A_g} \right) S_x \qquad \textbf{B-4}$$

Compression limit:

$$M_{elastic} = \left(\beta f_c^{'} + \frac{P}{A_g} \right) S_x \qquad \textbf{B-5}$$

in which P= the level of axial load A_g = the gross cross-section area and S_x= the elastic section modulus. It is suggested that α=1.0 for partially prestress section (where $f_c^{'}$ is in MPa units), and β=0.7. It is expected that for cases of highly loaded columns, the tension stress limit will normally govern.

For the proposed subassembly with: 400mm wide by 560mm deep beams with an initial prestress of P= 398kN and 700mm square column with a total axial load of 2000kN,

For precast beams:

Tension Limit

$$S_x = \frac{bd^2}{6} = \frac{400*560^2}{6} \approx 20.9e6mm^2 \quad \textbf{B-6}$$

$$M_{elastic} = \left(1.0*\sqrt{45} + \frac{398000}{400*560}\right)*20.9e6 = 177\,\text{kN-m} \quad \textbf{B-7}$$

Compression limit:

$$M_{elastic} = \left(0.7*45 + \frac{398000}{400*560}\right)*20.9e6 = 695\,\text{kN-m} \quad \textbf{B-8}$$

Therefore the tension limit governs and $M_{elastic} = 177\,\text{kN-m}$

For precast column

Tension limit

$$S_x = \frac{bd^2}{6} = \frac{700*700^2}{6} \approx 57.1e6mm^2 \quad \textbf{B-9}$$

$$M_{elastic} = \left(1.0*\sqrt{45} + \frac{2000000}{700*700}\right)*57.1e6 = 616\,\text{kN-m} \quad \textbf{B-10}$$

Compression limit:

$$M_{elastic} = \left(0.7*45 + \frac{2000000}{700*700}\right)*57.1e6 = 2031\,\text{kN-m} \quad \textbf{B-11}$$

Connection moment M_{con} is given

$$M_{con} = M_{ps} + M_{diss} \quad \textbf{B-12}$$

where M_{ps} =prestress connection moment, M_{diss} =dissipator connection moment

At connection overstrength, the Prestress connection moment is :

Seismic Beams:

$$M_{ps}^{+} = P_{ps\ yeild} * e_{ps}^{+} = \left(0.75 * 2 * \frac{\pi * 26^2}{4}\right) * 190 = 151\,\text{kN-m} \quad \textbf{B-13}$$

$$M_{ps}^{-} = P_{ps\ yeild} * e_{ps}^{-} = \left(0.75 * 2 * \frac{\pi * 26^2}{4}\right) * 370 = 295\,\text{kN-m} \quad \textbf{B-14}$$

Gravity Beams:

$$M_{ps} = P_{ps\ yeild} * e_{ps} = \left(0.75 * 2 * \frac{\pi * 26^2}{4}\right) * 280 = 223\,\text{kN-m} \quad \textbf{B-15}$$

The dissipator connection moment:

Seismic beams:

$$M_{diss} = F_{diss\ yield} * e_{diss} = \left(2 * 350 * \frac{\pi * 15^2}{4}\right) * 280 = 35\,\text{kN-m} \quad \textbf{B-16}$$

Gravity Beams:

$$M_{diss} = F_{diss\ yield} * e_{diss} = \left(2 * 350 * \frac{\pi * 13^2}{4}\right) * 590 = 55\,\text{kN-mcon} \quad \textbf{B-17}$$

Therefore the total connection moment at overstrength is:

Seismic beam:

$$M_{con}^{+} = M_{ps}^{+} + M_{diss} = 151 + 35 = 186\,\text{kN-m} \quad \textbf{B-18}$$

$$M_{con}^{-} = M_{ps}^{-} + M_{diss} = 295 + 35 = 330\,\text{kN-m} \quad \textbf{B-19}$$

Gravity beam;

$$M_{con}^{-} = M_{con}^{+} = M_{ps} + M_{diss} = 223 + 55 = 278\ \text{kN-m} \quad \textbf{B-20}$$

By setting the connection moment in the subassembly to the above calculated overstrength renders the subassembly statically determinate and therefore the shear force and moment demand on beams and column can be evaluated from a free body analysis of the subassembly. Results are summarised in the following table:

TableB-1: Subassembly maximum moment and design shear forces

Design Force	Unit	Column	Seismic Beams	Gravity Beam
M^{+}_{con}	kN-m	397	186	278
M^{-}_{con}	kN-m	397	330	278
V	kN	204	135	73

It can be seen from the above summary table that the column elastic moment capacity is large enough to provide the required design moment. Therefore, theoretically prestressing alone will be sufficient. However, due to the need of confinement of concrete in the joint region, traditional reinforcing design was carried out according to the current Concrete Design standard NZS 3101:1995

Since the elastic moment capacity of the precast beams are less than the design moment capacity, a cracked elastic approach (Davies and Arnold 2004) is adopted in sizing the longitudinal reinforcement as shown below.

The rebars in the precast beams are design to remain in elastic condition, this controls the crack size and also ensure that the cracks close at the cessation of seismic shaking. For a doubly reinforced concrete section with a triangular compression stress block the negative and positive section moment capacities can be calculated form:

$$\phi M_b = \left(C_c \frac{kd}{3} \right) + \left(C_s \, d' \right) - \left(T_s \, d \right) - \left(P_{PS} \, d_{PS} \right) \qquad \textbf{B-21}$$

where C_c = the concrete compressive force; C_s = the steel compressive force; T_s = the tensile steel stress; d = the effective beam depth to the tension mild steel; d' = depth to the compression mild steel reinforcing bars; and d_{PS} and kd are the depth of the post-

tensioning and neutral axis from the extreme concrete fibre in compression. Since the steel stresses will be linearly distributed over the design member's cross section, the maximum concrete compression stress, section forces and neutral axis depth can then be written in terms of a tensile stress, f_s, in the extreme tensile steel.

$$f_c = \frac{f_s}{n}\left(\frac{kd}{d-kd}\right) \qquad \textbf{B-22}$$

$$C_c = \frac{f_s}{2n}\frac{(kd)^2}{(d-kd)}b \qquad \textbf{B-23}$$

$$C_s = f_s A_s^{'}\left(\frac{kd-d^{'}}{d-kd}\right) \qquad \textbf{B-24}$$

$$T_s = f_s A_s \qquad \textbf{B-25}$$

The neutral axial position is given by (Arnold 2004):

$$k = \sqrt{\left(\rho_t + \frac{P}{f_c^{'} bd}\cdot\frac{f_c^{'}}{f_s}\right)^2 n^2 + 2\left(\rho_t \cdot \frac{\bar{y}}{d} + \frac{P}{f_c^{'} bd}\cdot\frac{f_c^{'}}{f_s}\right)n} \; - \; \left(\rho_t + \frac{P}{f_c^{'} bd}\cdot\frac{f_c^{'}}{f_s}\right)n \qquad \textbf{B-26}$$

in which $\rho_t = \frac{A_{s\,total}}{bd}$; b = the section width; $f^{'}_c$ = the concrete compressive strength; n = E_s/E_c the modular ratio; and $\bar{y}$ = the distance to the centroid of the longitudinal steel from the extreme concrete compression fibre.

To evaluate the flexural capacity of a trial cross section, a value of fs is estimated and a solution is found. Iteration continues until the desired moments are achieved and the resulting section stresses compared to the acceptable limits. For beams with draped prestress, it is necessary to plot a capacity vs. demand envelope as moment capacity may vary along the length of the beam depending on the depth to the centroid of the prestress.

A spreadsheet has been set up following above described procedure with the results is summarised in following table:

Table B-2: Cracked Elastic Design of Precast Beams.

Design Parameter		Gravity Beam	Seismic Beam	Column	Unit	Remarks
section width	b	400	400	700	mm	
Section Depth	D	560	560	700	mm	
Reinforcing Cover	d'	55	55	55	mm	
28 Day Concrete Strength	f'c	45	45	45	mm	
Steel yield Strength	fy	500	500	500	MPa	
Yong's Modulus of Concrete	Ec	29171	29171	29171	MPa	
Yong's Modulus of Steel	Es	200000	200000	200000	MPa	
Modulus Ratio	n=Es/Ec	6.9	6.9	6.9		
Reinforcing ratio	ρ_t	0.012	0.012	0.008		
Axial Load/Prestressing Force	P	796394	796394	2251894	N	
Axial Load Ratio	P/f' bd	0.09	0.09	0.11		
Nuetral Axis factor	k	0.40	0.37	0.41		
Concrete Compression Force	Cc	964327	1035111	2479542	N	
Steel Compression Force	Cs	150807	168478	274848	N	
Steel tension force	T	318740	407195	502496	N	
Force Equilibrium	+Cs-Ts-Pps	0	0	0		**OK**
SectionMoment Capacity	M+	312	283	879	KNm	
	M-	312	427	879	KNm	
Steel stress ratio	fs/fy =	0.51	0.65	0.53		
Concrete stress ratio	fc/f'c =	0.65	0.6	0.6		**OK**

Shear design of the precast elements follows standard code procedures (see for example NZS 3101:1995) for sections located outside of plastic hinge zones. This permits the concrete to contribute to the shear strength of the section since concrete degradation due to plastic hinging in the beam and columns sections is prevented by design.

B.3 External Supplementary Energy Dissipator Design:

Seismic beams:

$n_d = 2,\ P_{ps\_ini}$=397kN, $\left|e_{ps}\right|_{\min} = 190$mm, $\left|e_{diss}\right|_{\max}$=280mm, $\phi = 0.8,\ \lambda_o = 1.5$ (for mild steel)

$$F_{d\ yield} = \frac{0.8}{1.5} * \frac{397e3 * 190}{2 * 280} = 72000 \quad N \qquad \textbf{B-27}$$

Therefore require the fuse area for a single dissipator is:

$$A_{diss}^{required} = \frac{F_{d\ yield}}{f_{y\ diss}} = \frac{72000}{350} = 200mm^2 \qquad \textbf{B-28}$$

Try using 15mm diameter rod:

$$A_{diss}^{\Pr ovide} = \frac{\pi * 15^2}{4} = 178mm^2 < A_{diss}^{required} = 200mm^2 \quad OK \qquad \textbf{B-29}$$

G*ravity beam:*

n_d=2, P_{ps_ini}=397kN, $\left|e_{ps}\right|_{\min} = 280$mm, $\left|e_{diss}\right|_{\max}$=590 mm, $\phi = 0.8,\ \lambda_o = 1.5$ (for mild steel)

$$F_{d\ yield} = \frac{0.8}{1.5} * \frac{397e3 * 280}{2 * 590} = 50241 \quad N \qquad \textbf{B-30}$$

$$A_{diss}^{required} = \frac{F_{d\ yield}}{f_{y\ diss}} = \frac{50241}{350} = 143mm^2 \qquad \textbf{B-31}$$

Try using13mm diameter fuse rod:

$$A_{diss}^{\Pr ovide} = \frac{\pi * 13^2}{4} = 132mm^2 < A_{diss}^{required} = 143mm^2 \quad OK \qquad \textbf{B-32}$$

To prevent low cycle fatigue failure of the fuse rod, the required minimum fuse length is calculated form equation2-25:

For seismic beam:

$$L_{d\,\min} = 0.03 * \frac{0.5 * 280}{2 * \left(\frac{0.08}{\sqrt{2 * 2}} + 0.00175 \right)} \approx 100mm \qquad \textbf{B-33}$$

For gravity beam

$$L_{d\,\min} = 0.03 * \frac{1.05 * 280}{2 * \left(\frac{0.08}{\sqrt{2 * 2}} + 0.00175 \right)} \approx 212mm \qquad \textbf{B-34}$$

B.4 Subassembly Response Prediction:

Using the theory developed at section 3, the theoretical later force-displacement response of the test subassembly is calculated and summarised below:

TableB-3: Theoretical behaviour of subassembly with only prestressing.

	E-W Loading		N-S Loading	
	Force (KN)	Displacement (mm)	Force (KN)	Displacement (mm)
Before Loading	0	0	0	0
At Gap Opening	82	15.4	41	8
At Ps Yielding	136	94.6	74	78
Re-centring Limit	136	164	74	124

TableB-4: Theoretical behaviour of the subassembly with prestress and supplementary energy dissipators.

	E-W Loading		N-S Loading	
	Force (KN)	Displacement (mm)	Force (KN)	Displacement (mm)
Before Loading	0	0	0	0
At Gap Opening	82	15.4	41	8
At fuse bar Yielding	116	20.8	58	12
At Ps Yielding	166	100	90	82
Re-centring Limit	166	164	90	124

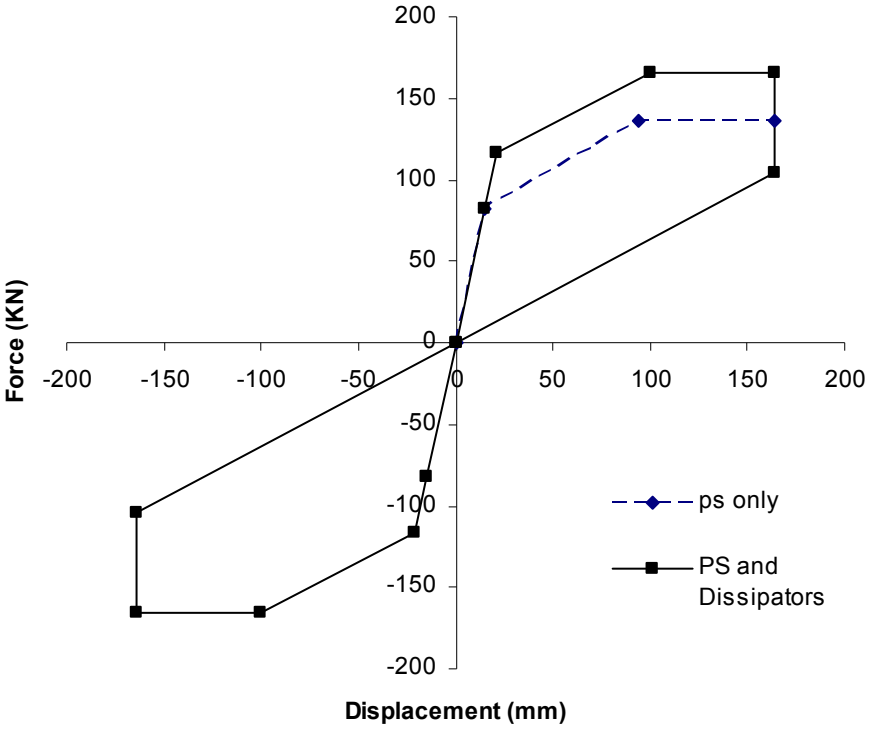

(a) Subassembly Responses in the East-West direction.

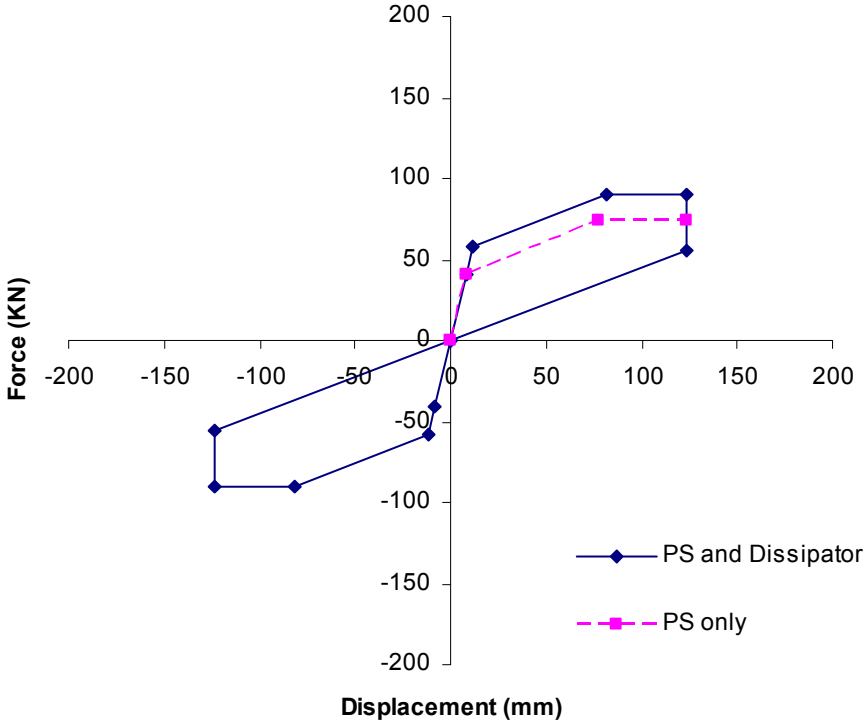

(b) Subassembly Response in the North-South Direction.

Figure B-1: Theoretical Force-Displacement Reponses of the subassembly.

Appendix C: Effective Beam stiffness:

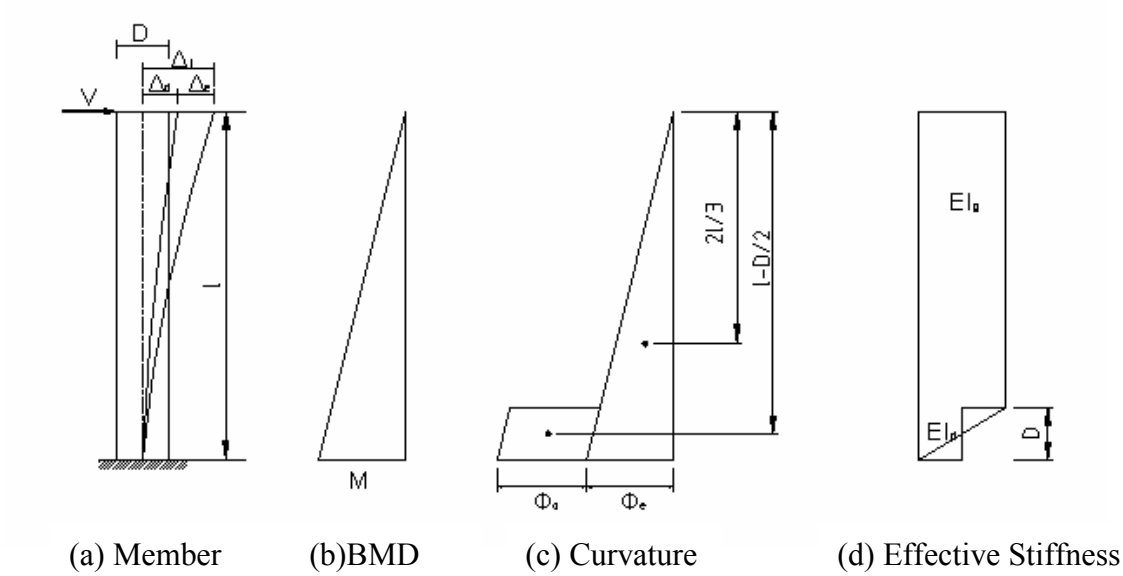

(a) Member (b)BMD (c) Curvature (d) Effective Stiffness

Figure C-1: Effective Beam Stiffness in a Jointed Precast Frame System.

Total deflection (Δ_t) at top of the cantilever is

$$\Delta_t = \Delta_d + \Delta_e \qquad \textbf{C-1}$$

The ratio of the gross stiffness to effective stiffness:

$$\frac{EI_g}{EI_{eff}} = \frac{\Delta_t}{\Delta_e} = \frac{\Delta_d}{\Delta_e} + 1 \qquad \textbf{C-2}$$

The elastic deflection at end of the cantilever is give by:

$$\Delta_e = \frac{Ml^2}{3EI_g} \qquad \textbf{C-3}$$

$$\Delta_d = \phi_d D\left(l - \frac{D}{2}\right) \qquad \textbf{C-4}$$

When loaded under unidirectional loading, the precast beams are expected to rock on the top/bottom edge. According to the St. Venant principle, the large concentrated force will spread at approximate 45 degree angle into the precast beam. Assume an average Beam rigidity of EI_d in the disturb region at bottom of the cantilever. The curvature ϕ_d can be expressed as:

$$\phi_d = \phi_t - \phi_e = \frac{M}{EI_d} - \frac{M}{EI_g} \qquad \textbf{C-5}$$

Substitute C-4 and C-5 into C-3:

$$\frac{EI_g}{EI_e} = \frac{M\left(\frac{1}{EI_d} - \frac{1}{EI_g}\right)D\left(l - \frac{D}{2}\right)}{\left(\frac{Ml^2}{3EI_g}\right)} + 1 \qquad \textbf{C-6}$$

Assume the effect section depth and width along the disturbed region at end of the beam is αD and βB, C-6 can be expressed as:

$$\frac{EI_{eff}}{EI_g} = \frac{l^2}{3\left(\frac{1}{\alpha^3\beta} - 1\right)D\left(l - \frac{D}{2}\right) + l^2} \qquad \textbf{C-7}$$

Substitute $l = \frac{L_b}{2}$ into C-7 and rearrange:

$$\frac{EI_{eff}}{EI_g} = \left[\frac{1}{6 * \left(\frac{1}{\alpha^3\beta} - 1\right)\frac{D}{L_b}\left(1 - \frac{D}{L_b}\right) + 1}\right] \qquad \textbf{C-8}$$

Appendix D: Safety Assessment of Bent Coupler Design

Standard Dywidag^{TM} coupler were heat and bent to desired angle to joint the diagonal fuse "bolt-bar" and the prestressing in the precast beams (Figure D1). Bending of coupler reduced the threadable length form 6 threads (in straight coupler) to 4 threads (in bent coupler). This reduces the strength of the bar-coupler connection therefore a series of tensile tests were carried out to asses the tensile strength of : a plain 26.5mm Dywidag^{TM} bar, tensile strength of the fuse "Bolt-bar" with 21mm and 24mm fuse diameter and tensile strength of the "bolt-bar"-coupler-Dywidag bar connection. The tensile force-displacement is plotted in Figure D-2 and the tensile strength is summarised in Table D-1.

Table D-1: Tensile strength of the post-tension system of the subassembly.

Specimen	Yield Tensile Strength (KN)	Ultimate Tensile Strength (KN)
26mm Dywidag^{TM} Bar	550	583
Bended coupler-Dywidag^{TM} Connection	540	567
Bolt-bar with 21mm fuse diameter	330	375
Bolt- bar with 24mm fuse diameter	520	537

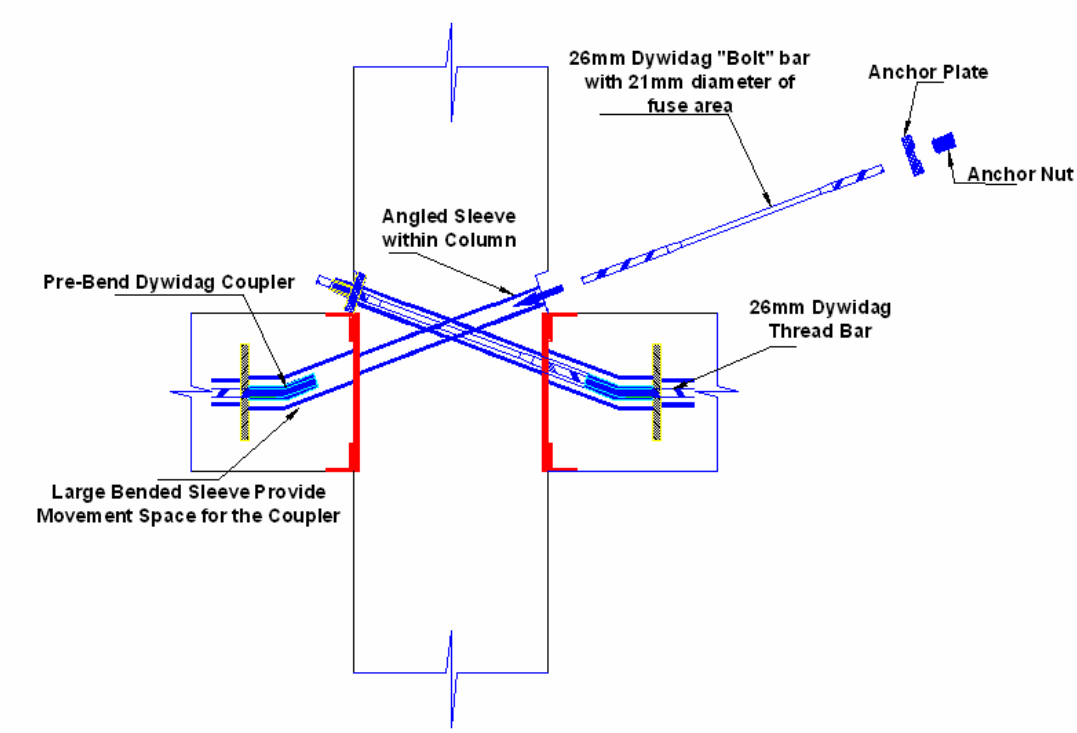

(a) Post-tensioning Connection Details in Seismic Beam

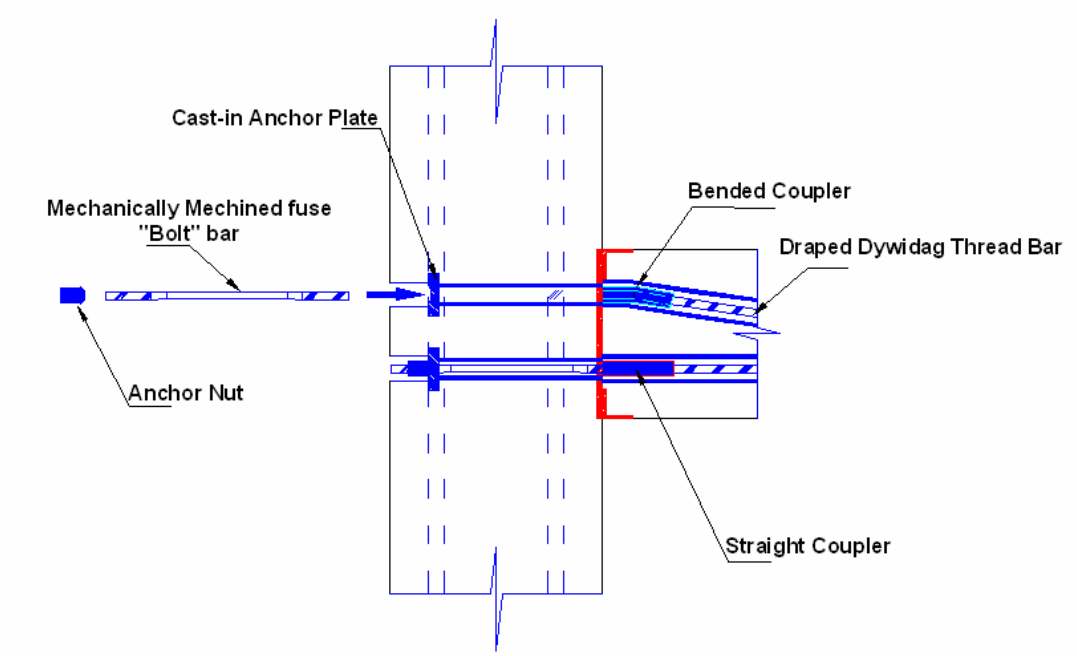

(b) Post-tensioning Connection Details in Gravity Beam

Figure D-1: Connection Details of the Dywidag™-Bended Coupler-"Bolt-Bar" in the Subassembly.

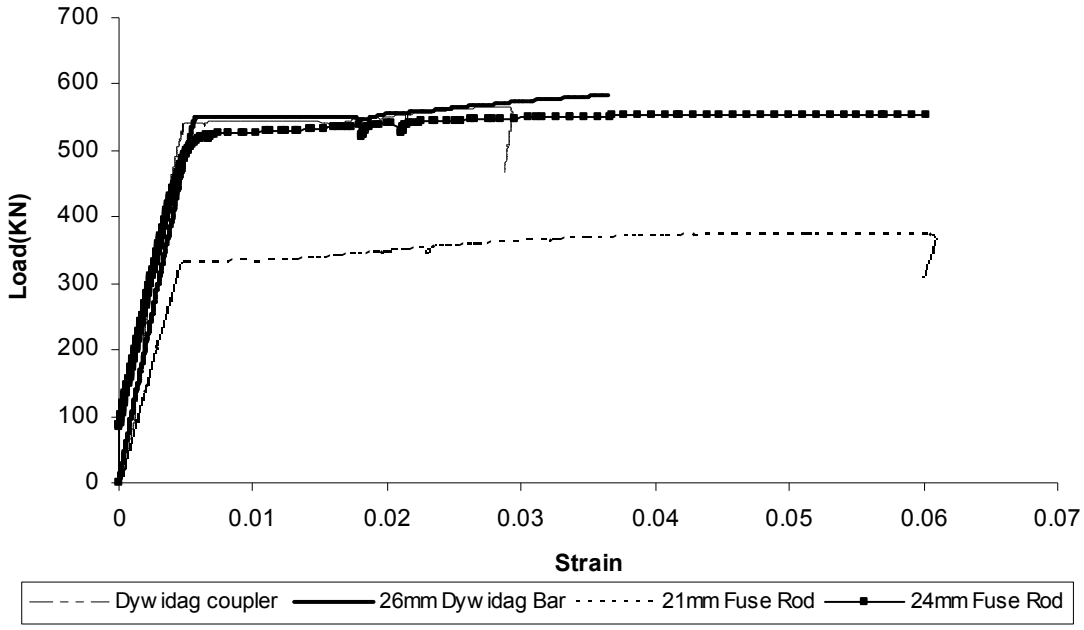

Figure D-2: Tensile Testing of A 26.5mm diameter Dywidag^{TM} bar, Dywidag^{TM} Fuse "Bolt-bar" with fuse diameter of 24mm and 21mm and Bolt-bar-bent coupler connection.

In fear of the premature failure of the Dywidag^{TM} prestressing jointed by the bent coupler in the subassembly; A safety yoke system is designed to convert stored strain energy in the Dywidag^{TM} bar (that would otherwise be converted into kinetic energy) into energy stored in the yoke plate.

Total strain energy at breaking of prestressing is:

$$U_{\varepsilon} = 0.5 * F_{break}^{2} \frac{L_t}{E_{ps} A_{ps}} \qquad \textbf{D-1}$$

where: F_{break}^{2} =breaking force of the fuse "bolt-bar"; L_t = length of the unbonded prestressing; E_{ps}=Yong's modulus of the prestressing; A_{ps} = area of the prestressing.

The plastic strain energy absorption capacity, U_P of the anchor bolt on the yoke plate:

$$U_p = F_{by} * \Delta_b \qquad \textbf{D-2}$$

where F_{by} = yield force of the anchor bolt, Δ_b =elongation of the anchor bolt.

To safely convert the energy stored in the post-tensioning bars into the plastic strain energy in the anchor bolts of the safety yoke, following equation must be satisfied:

$$n_b F_{by} \Delta_b \geq 0.5 * F_{break}^2 \frac{L_t}{E_{ps} A_{ps}} \quad \textbf{D-3}$$

The required yoke bolt length is:

$$l_{yb}^{required} \geq \frac{1}{2\varepsilon_{pb}} \frac{F_{break}^2}{n_b F_{by}} \frac{L_t}{E_{ps} A_{ps}} \quad \textbf{D-4}$$

Try two M16 bolts:

Use plastic strain of ε_p=10%

For a 26.5mm diameter Dywidag^{TM} fuse bolt-bar with a fuse area equal to 75% of its original cross section area, U_ε:

$$F_{break} = A_{bolt} * F_{u\,bolt} = \left(0.75 * \frac{\pi * 26.5^2}{2} \right) * 1100 = 455\,\text{kN} \quad \textbf{D-5}$$

$$l_{yb}^{required} \geq \frac{1}{2 * 0.1} * \frac{(455e3)^2}{2 * 141e3} \frac{4700}{200e3 * 531} \approx 162\,\text{mm} \quad \textbf{D-6}$$

Provide: l_{yb} =200mm> $l_{yb}^{required}$ =162mm OK

Appendix E: Force-Drift Response of the Subassembly:

Unidirectional tests:

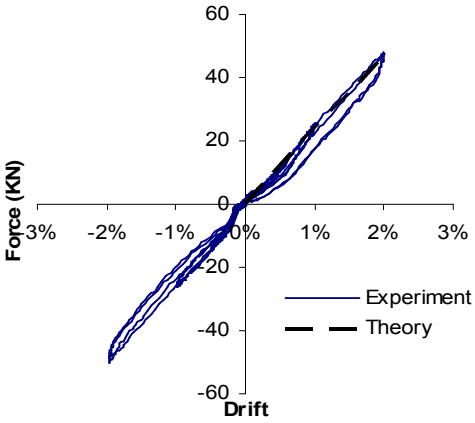

(a) E-W Loading with minimum initial prestressing force.

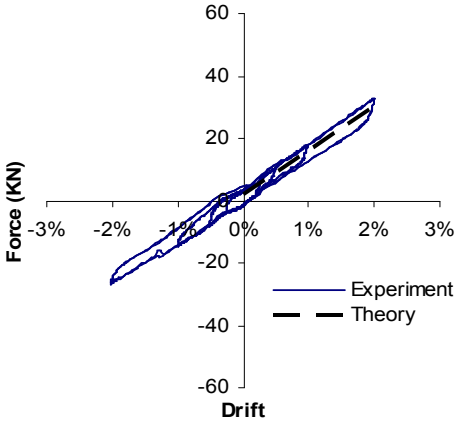

(b) N-S Loading with minimum initial prestressing force.

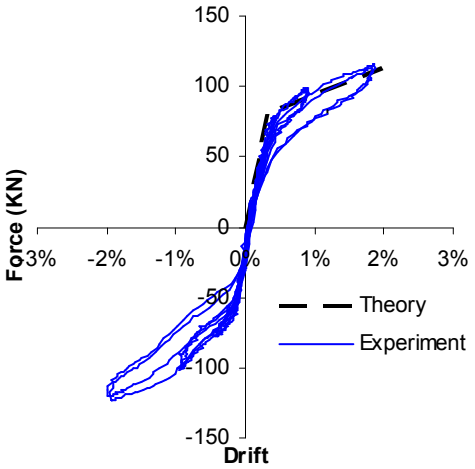

(c) E-W Loading up to 2% lateral drift with initial prestressing force level of 50% of bar yield.

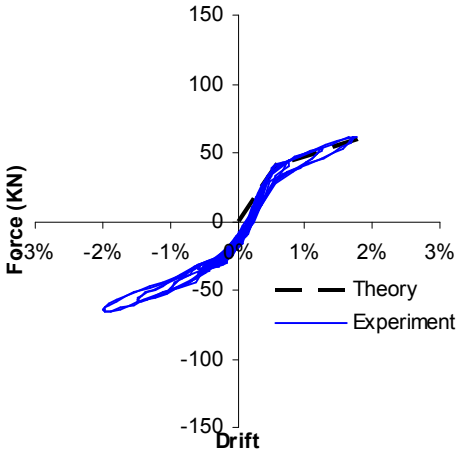

(d) N-S Loading up to 2% drift with initial prestressing force level of 50% of bar yield.

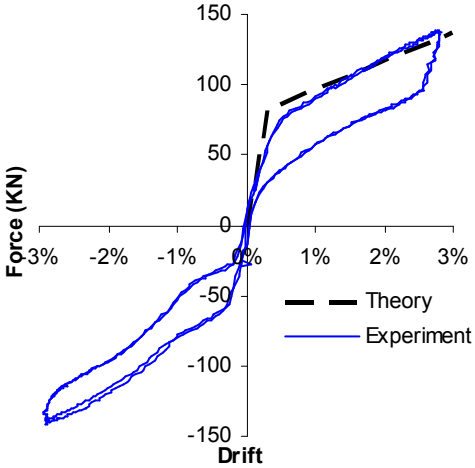

(e) E-W loading 3% lateral drift with initial prestressing force level of 50% of bar yield

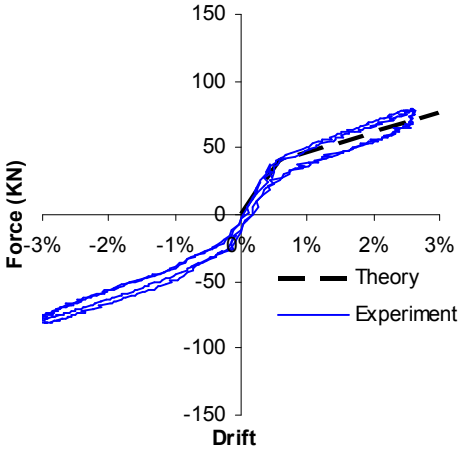

(f) N-S loading 3% lateral drift with initial prestressing force level of 50% of bar yield.

Figure E-1: Force-Drift Response of subassembly with only prestressing tested under unidirectional Loading up to 3% lateral drift.

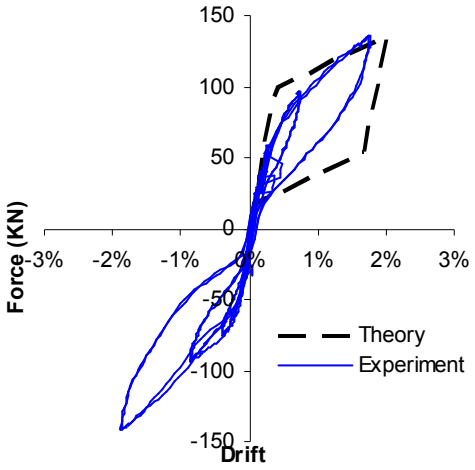

(a) E-W Loading up to 2% lateral drift with threaded fuse dissipators.

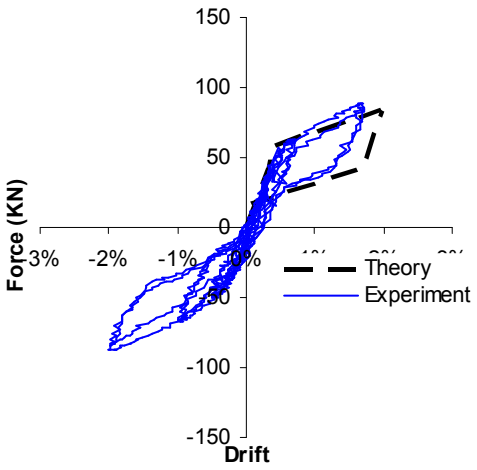

(b) N-S Loading up to 2% with threaded fuse dissipators.

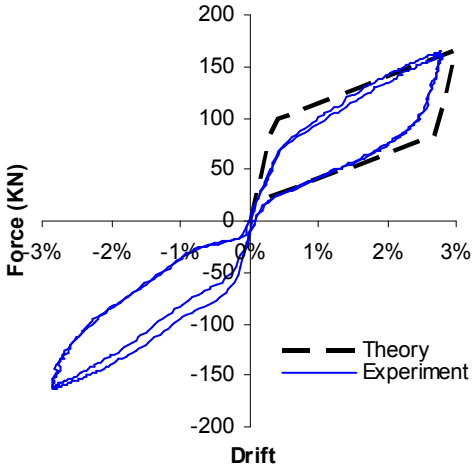

(c) E-W Loading 3% lateral drift with threaded fuse rod dissipators

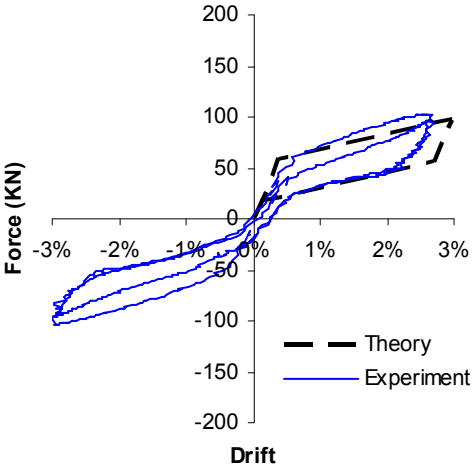

(d) N-S Loading 3% drift with threaded fuse rod dissipators

Figure E-2: Force-Drift response of subassembly with threaded fuse-rods tested under unidirectional at 3% lateral drift.

Bidirectional tests:

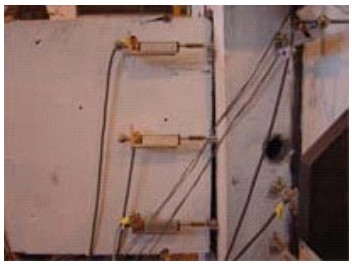

(d) West Beam at 2% drift

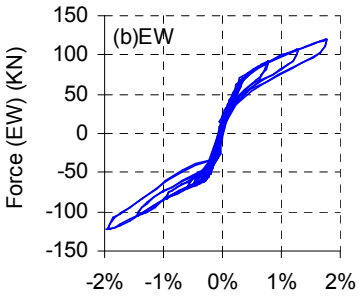

(e) East Beam at 2% drift

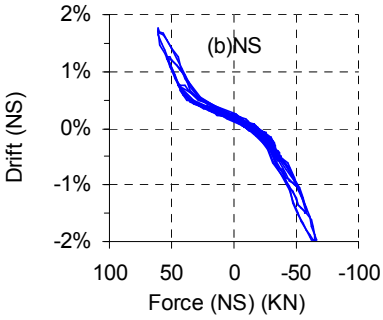

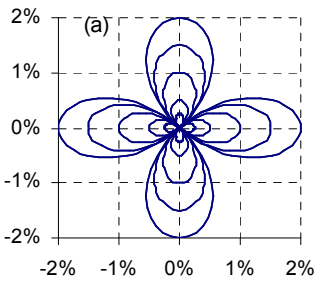

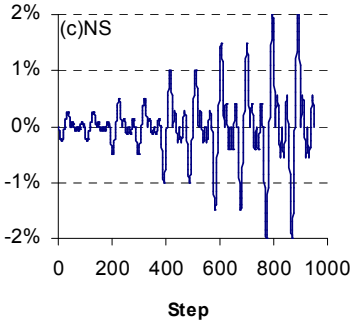

(f) Gravity Beam at 2% drift

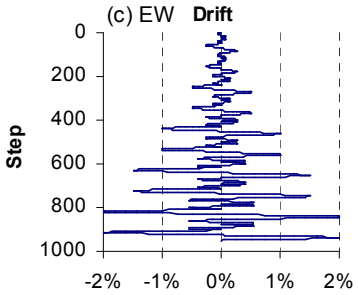

(g) Sepcimen at 2% drift

Figure E-3: Experimental Results of Subassembly Tested under Bidirectional Sine Cloves Loading with prestressing only showing: (a) Plane View of the Bidirectional Drift Orbit (Sine 4-leaf Clove), (b) Force-Displacement plots, (c) Displacement inputs and photographs showing (d) west beam at 2% drift, (e) East beam at 2% drift, (f) gravity beam at 2% drift, (g) and specimen at 2% drift.

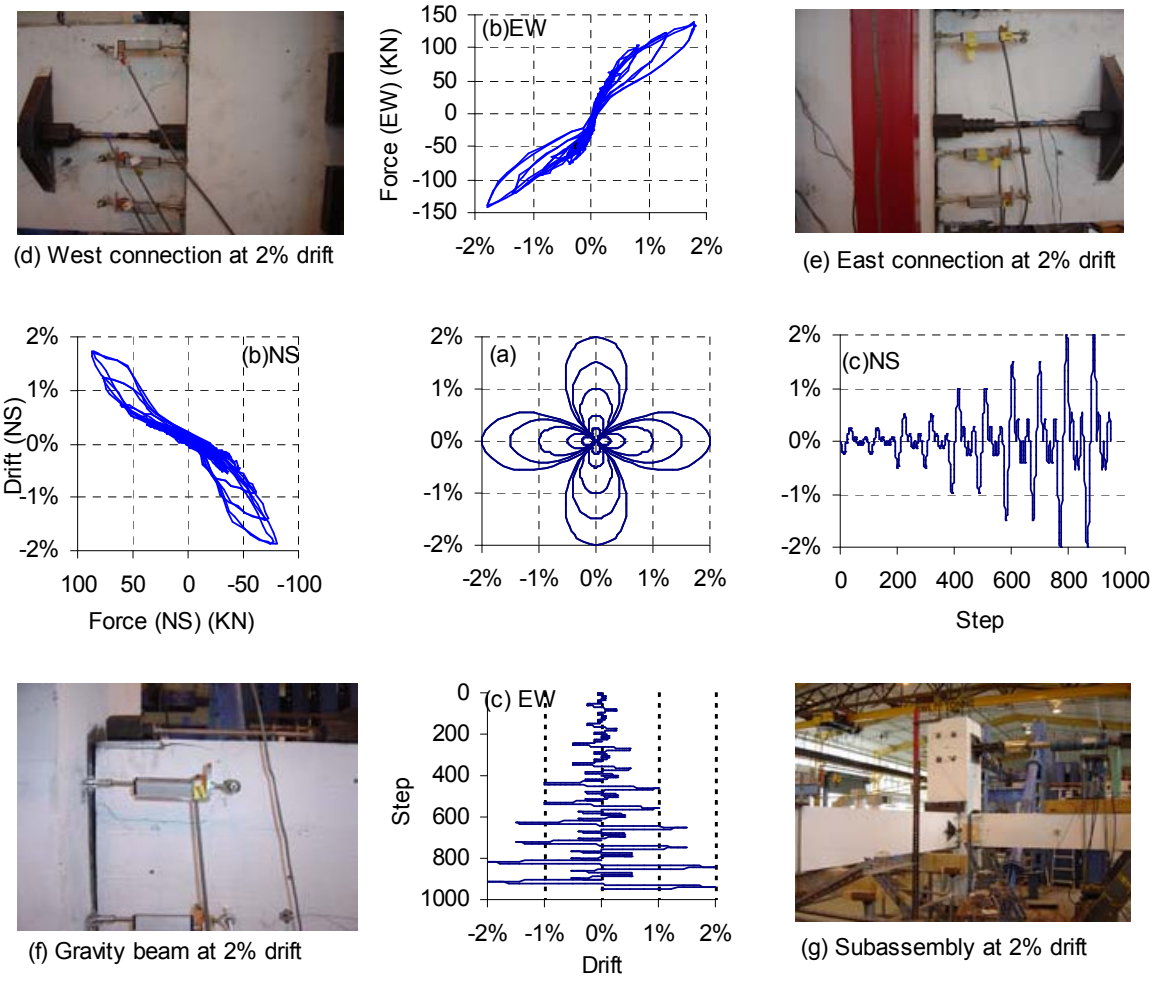

Figure E-4: Experimental results of subassembly tested under bidirectional sine cloves loading with threaded rod energy dissipators showing: (a) Plane view of the bidirectional drift orbit (Sine 4-leaf clove), (b) Force-displacement plots, (c) Displacement inputs and photographs showing (d) West connection at 2% drift, (e) East connection at 2% drift, (f) Gravity beam connection at 2% drift and (g) Subassembly at 2% drift.

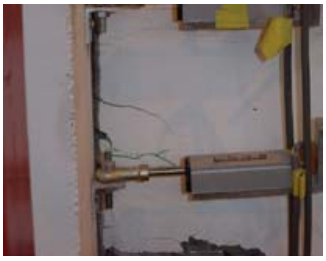

(d) Damage behind steel armour plate

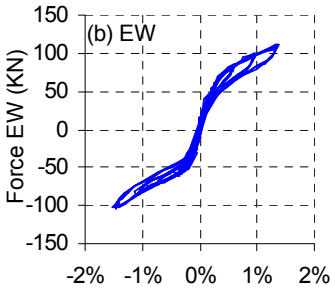

(e) Spalling of concrete

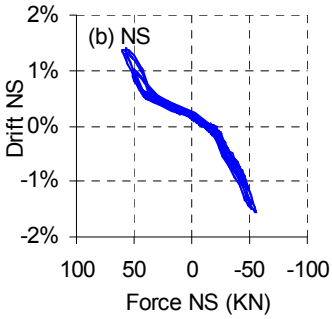

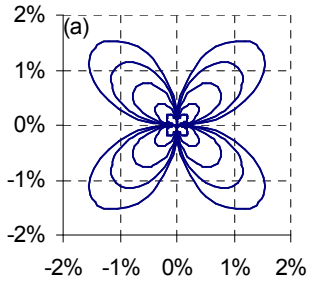

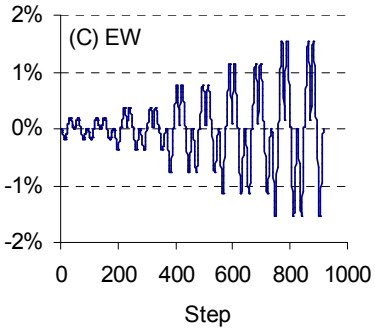

(f) Gravity beam to column Connection opening at 2% drift

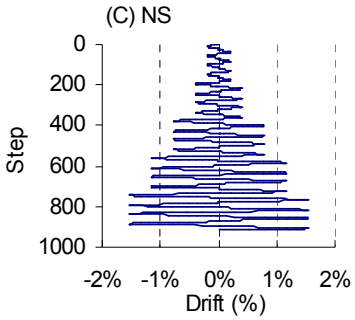

(g) Damage behind top steel armour Plate on the Gravity beam

Figure E-5: Experimental results of subassembly tested under bidirectional cosine cloves loading with prestressing only showing: (a) Plane view of the bidirectional drift orbit (Cosine 4-leaf clove), (b) Force-displacement plots, (c) Displacement inputs and photographs showing (d) Damage behind the angled armour plate on seismic beam, (e) Spalling of concrete on seismic beam, (f) Typical connection at 2% drift , and (g) Damage on top of the gravity beam.

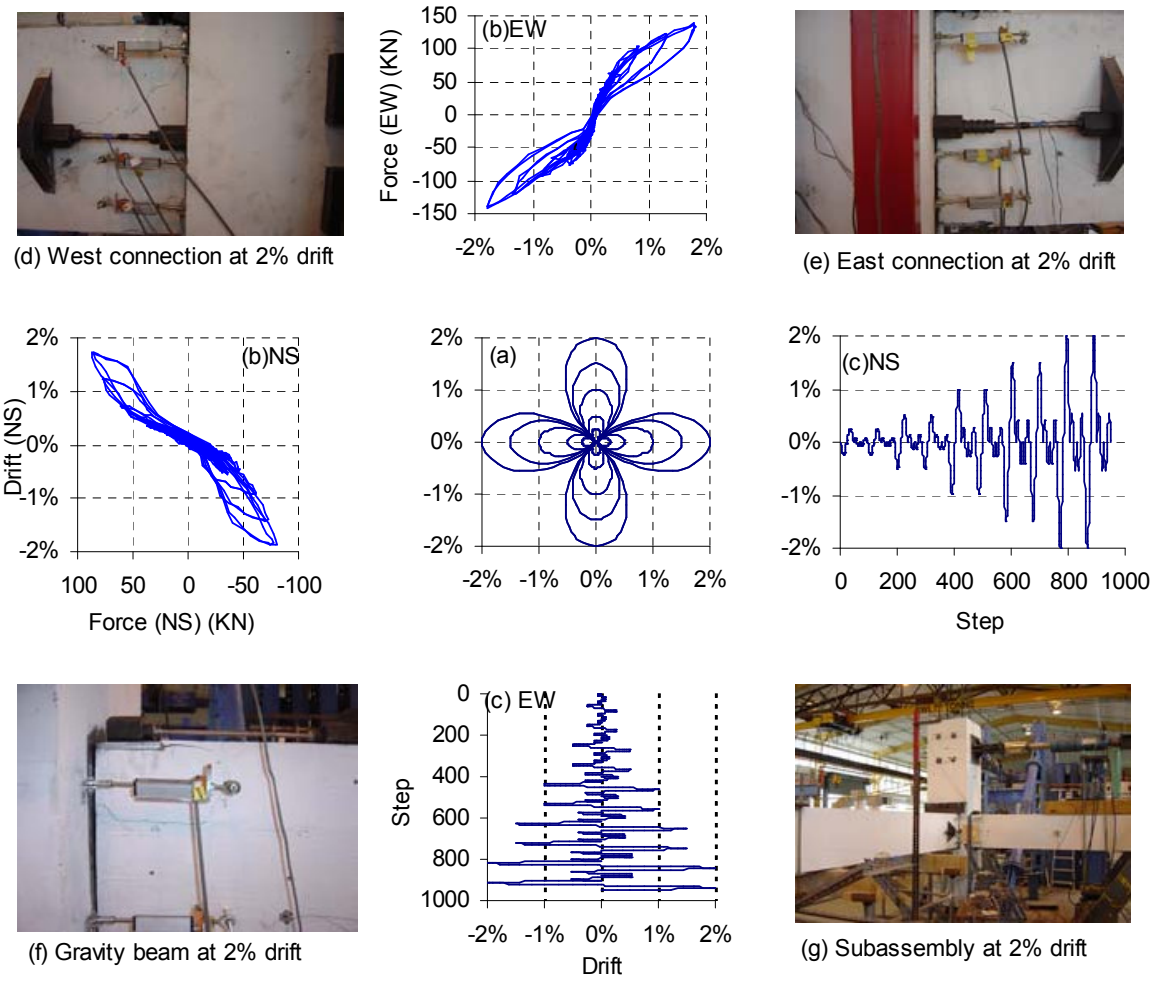

Figure E-6: Experimental results of subassembly tested under bidirectional cosine cloves loading with threaded rod energy dissipators showing: (a) Plane view of the bidirectional drift orbit (Sine 4-leaf clove), (b) Force-displacement plots, (c) Displacement inputs and photographs showing: (d) Bucking of energy dissipator on west seismic beam at 2% drift, (e) Opening of east connection at 2% drift, (f) Threaded rod dissipator on top of gravity beam at 2% drift and (g) Subassembly at 2% drift.

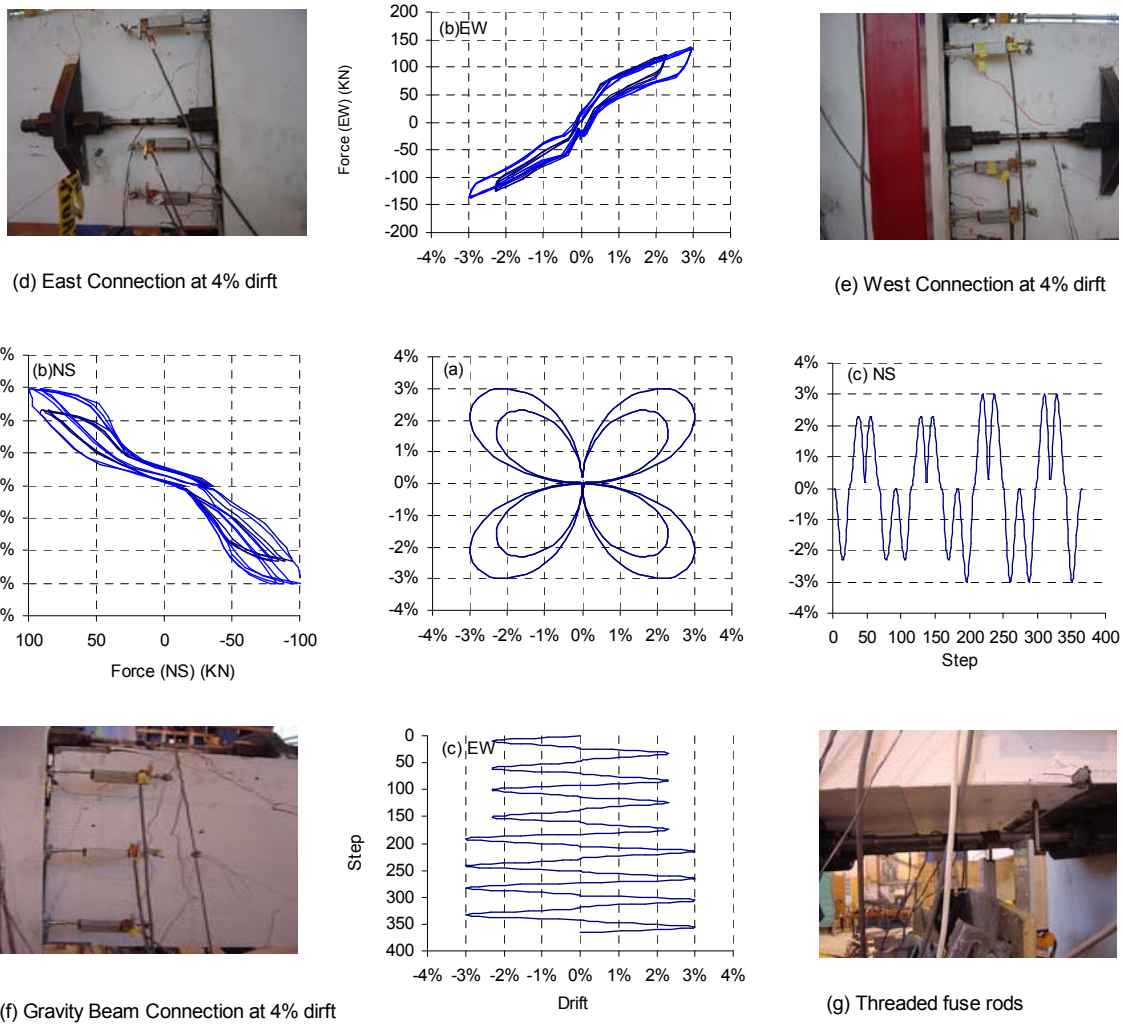

Figure E-7: Experimental results of subassembly tested under bidirectional cosine cloves loading with prestressing only showing: (a) Plane view of the bidirectional drift orbit (Cosine 4-leaf clove), (b) Force-displacement plots, (c) Displacement inputs and photographs showing (d) West beam at 4%, (e) West beam at 4%, (f) Gravity beam at 4%, and (g) Threaded fuse rods under gravity beam.

(d) East Connection at 4% dirft

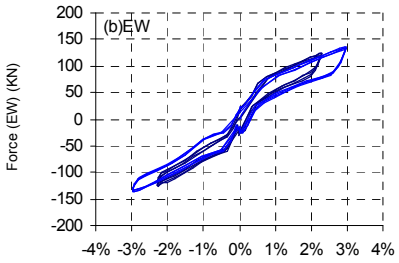

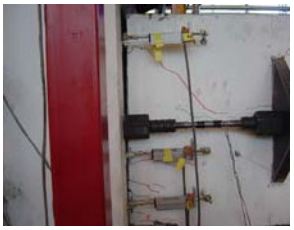

(e) West Connection at 4% dirft

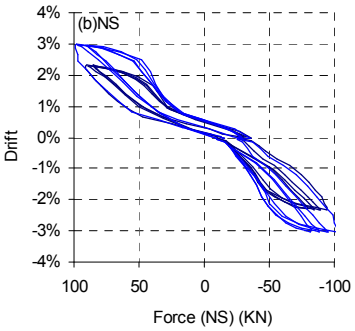

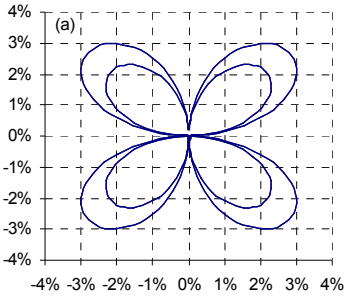

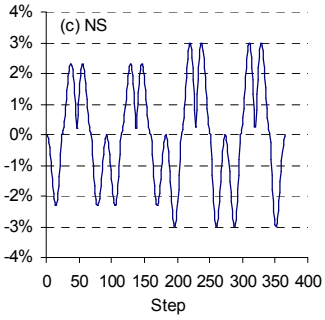

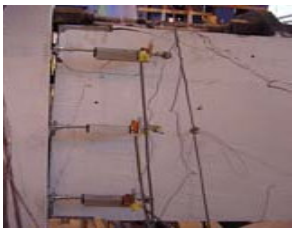

(f) Gravity Beam Connection at 4% dirft

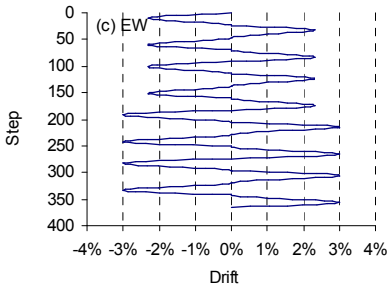

(g) Threaded fuse rods

Figure E-8: Experimental results of subassembly tested under bidirectional cosine cloves loading with threaded rod energy dissipators showing: (a) Plane view of the bidirectional drift orbit (Cosine 4-leaf clove), (b) Force-displacement plots, (c) Displacement inputs and photographs showing (d) Opening of east connection at 4% drift, (e) Opening of west connection at 4% drift, (f) Gravity beam at 4% drift, and (g) Threaded fused rods under the gravity beam.

Appendix F: Construction Drawings.

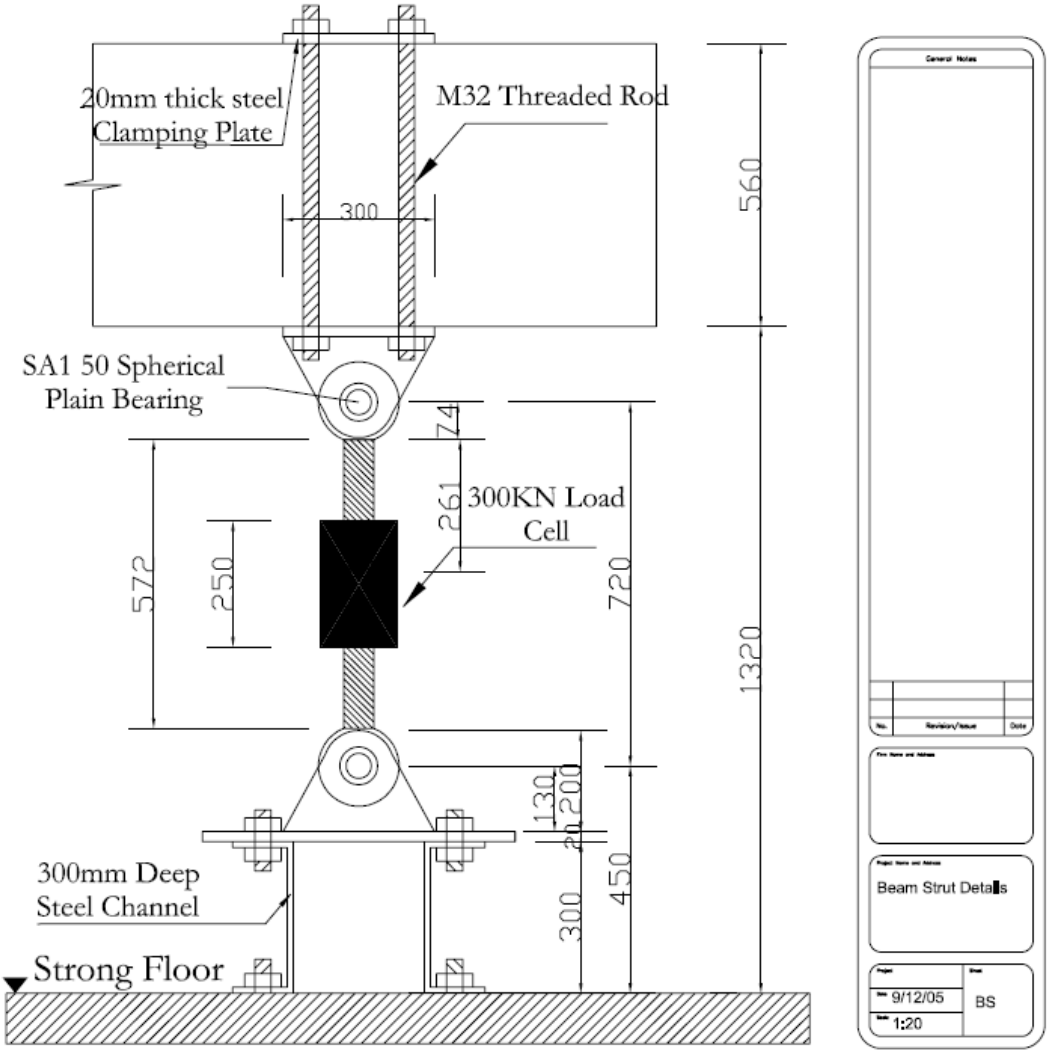

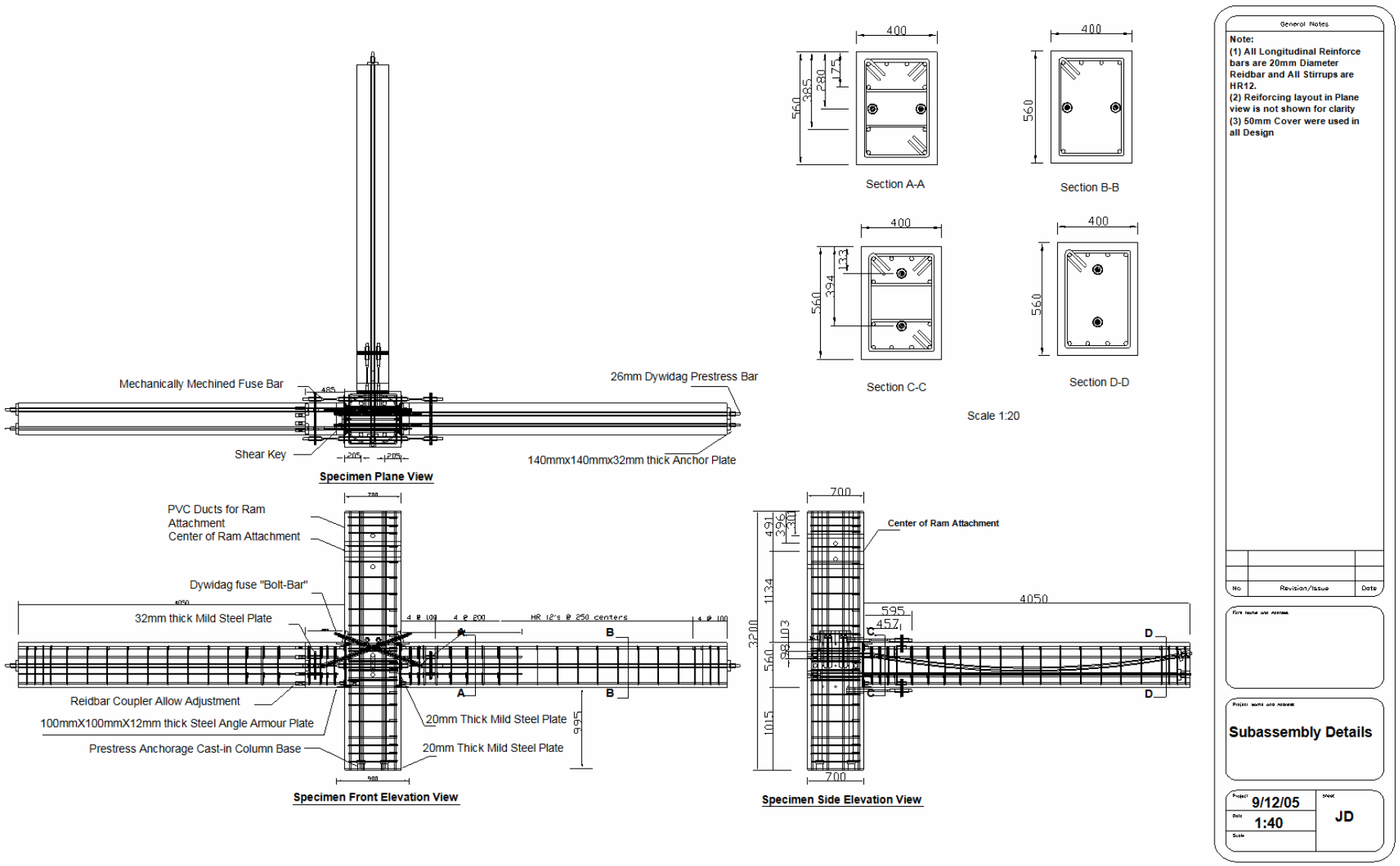
Mechanically Mechined Fuse Bar
26mm Dywidag Prestress Bar
Shear Key
140mmx140mmx32mm thick Anchor Plate
Specimen Plane View
Section A-A
Section B-B
Section C-C
Section D-D
Scale 1:20
PVC Ducts for Ram Attachment
Center of Ram Attachment
Dywidag fuse "Bolt-Bar"
32mm thick Mild Steel Plate
Reidbar Coupler Allow Adjustment
100mmX100mmX12mm thick Steel Angle Armour Plate
Prestress Anchorage Cast-in Column Base
20mm Thick Mild Steel Plate
20mm Thick Mild Steel Plate
HR 12's @ 250 centers
Specimen Front Elevation View
Specimen Side Elevation View
General Notes
Note:
(1) All Longitudinal Reinforce bars are 20mm Diameter Reidbar and All Stirrups are HR12.
(2) Reiforcing layout in Plane view is not shown for clarity
(3) 50mm Cover were used in all Design
No
Revision/Issue
Date
Subassembly Details
9/12/05
1:40
JD

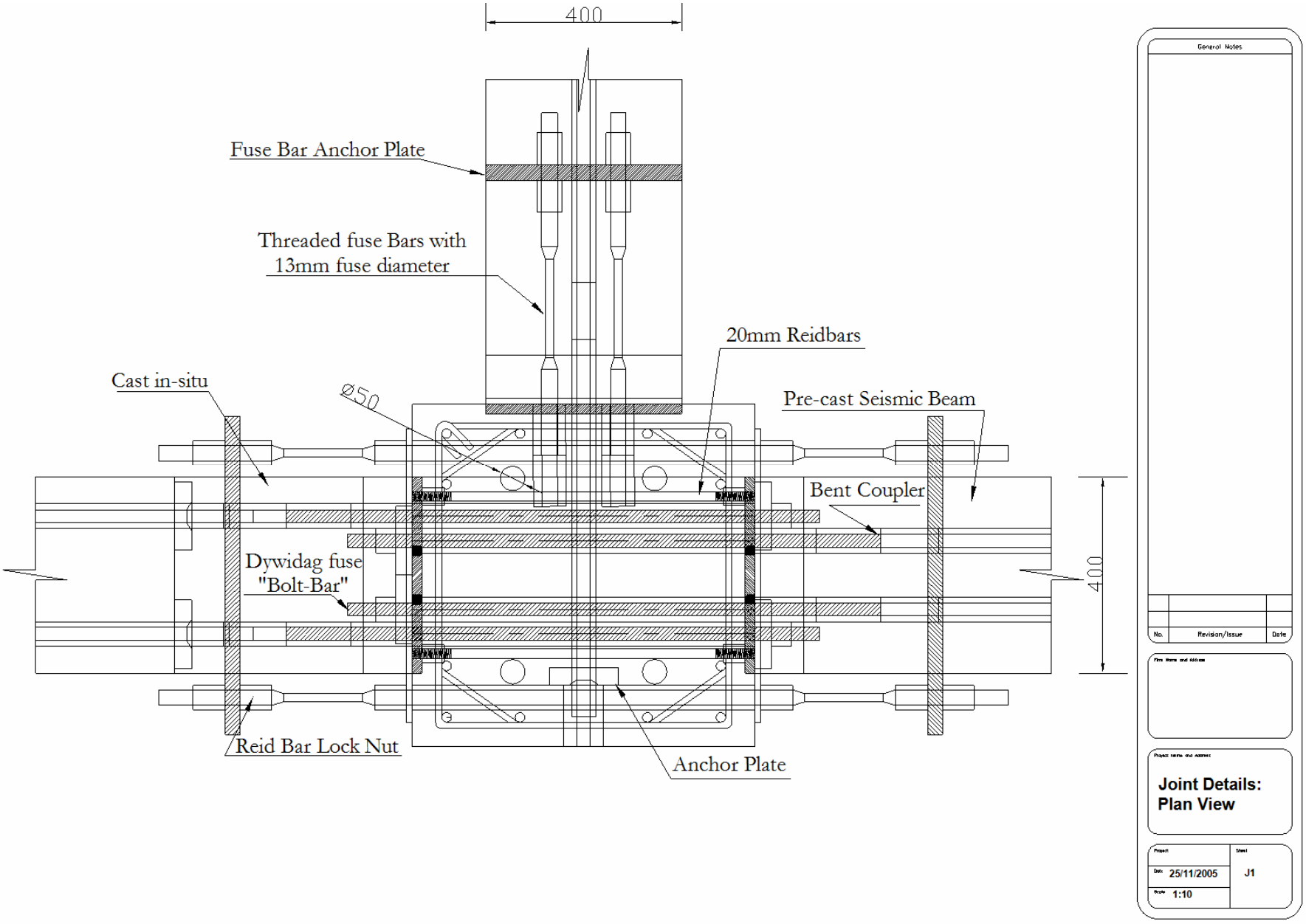
400
Fuse Bar Anchor Plate
Threaded fuse Bars with
13mm fuse diameter
20mm Reidbars
Cast in-situ
Ø50
Pre-cast Seismic Beam
Bent Coupler
Dywidag fuse
"Bolt-Bar"
400
Reid Bar Lock Nut
Anchor Plate
General Notes
No.
Revision/Issue
Date
Joint Details:
Plan View
Date: 25/11/2005
Scale: 1:10
J1

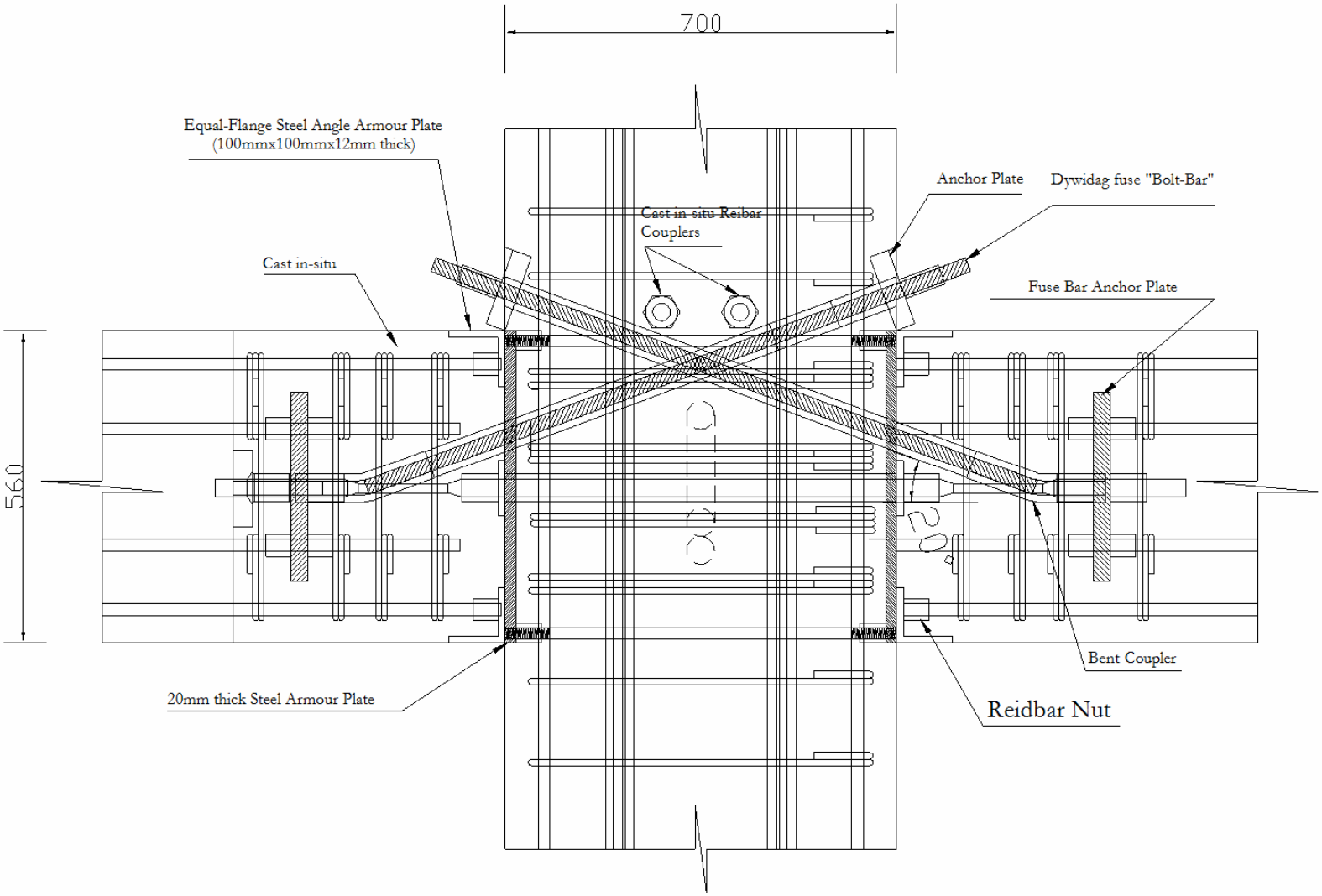

General Notes

No.	Revision/Issue	Date

Project name and address

Joint Details: Front Elevation View

Project	Sheet
Date 25/11/2005	J2
Scale 1:10	

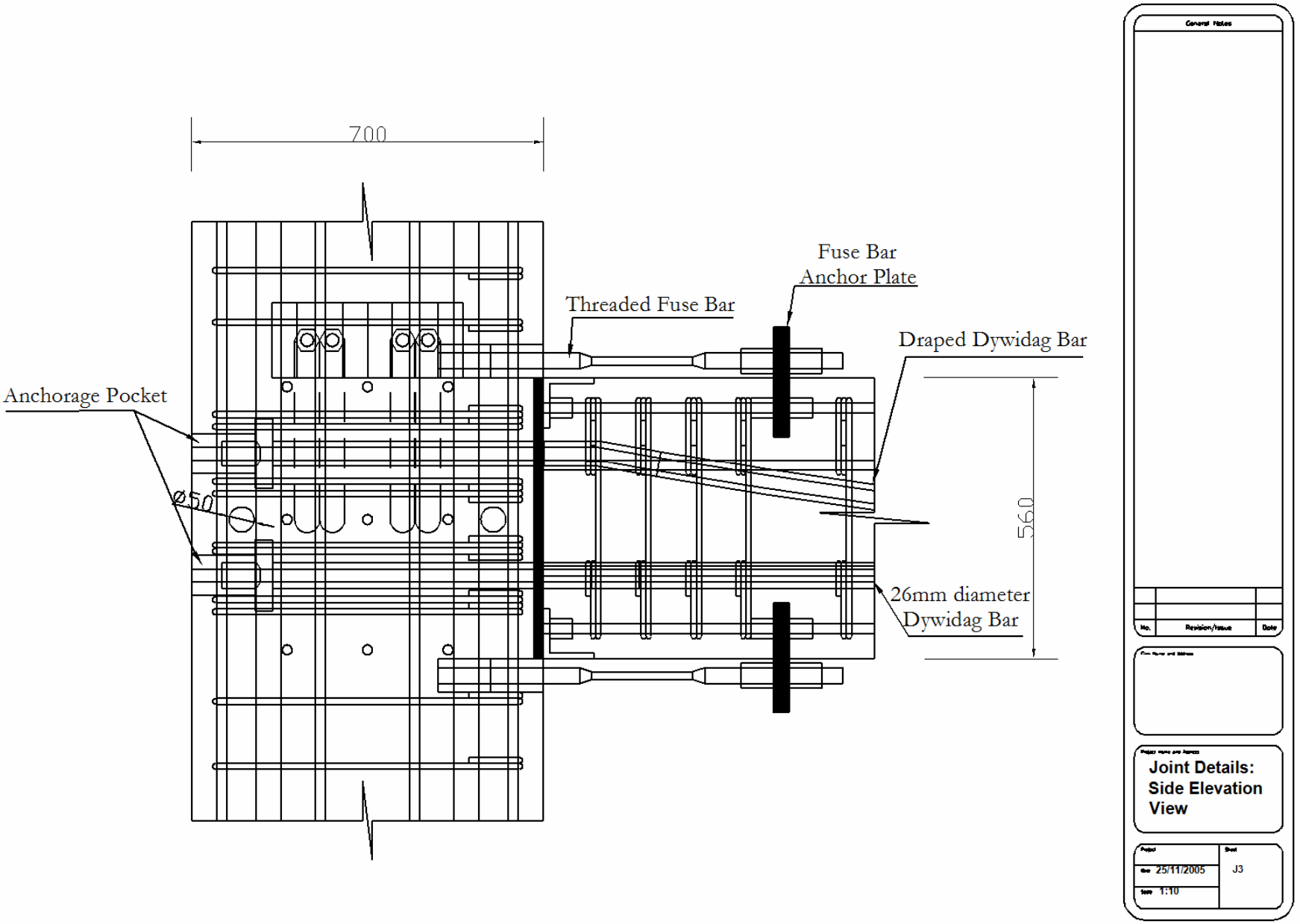
700
Fuse Bar
Anchor Plate
Threaded Fuse Bar
Draped Dywidag Bar
Anchorage Pocket
ø50
560
26mm diameter
Dywidag Bar
General Notes
No.
Revision/Issue
Date
Joint Details:
Side Elevation
View
Project
Sheet
date 25/11/2005
J3
scale 1:10

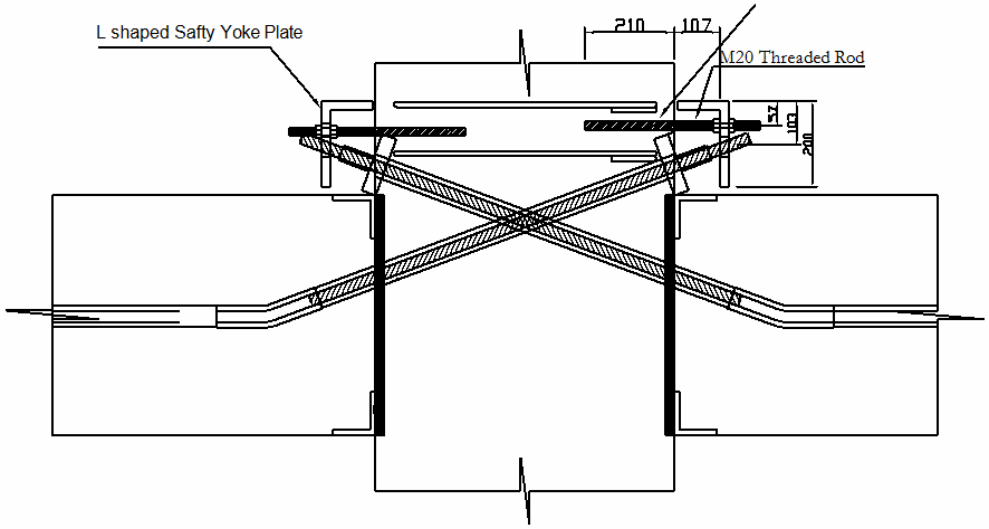

Front Elevation View

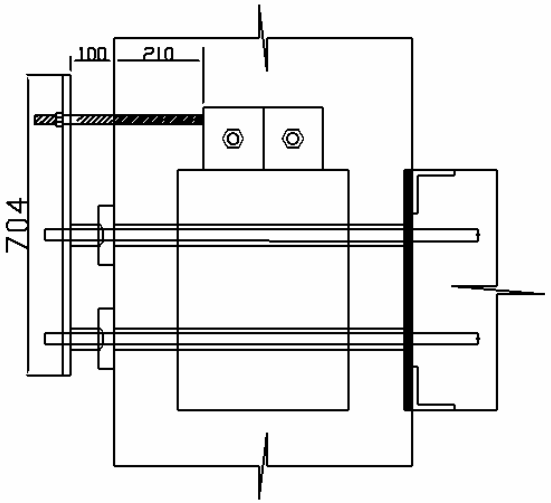

Side Elevation View

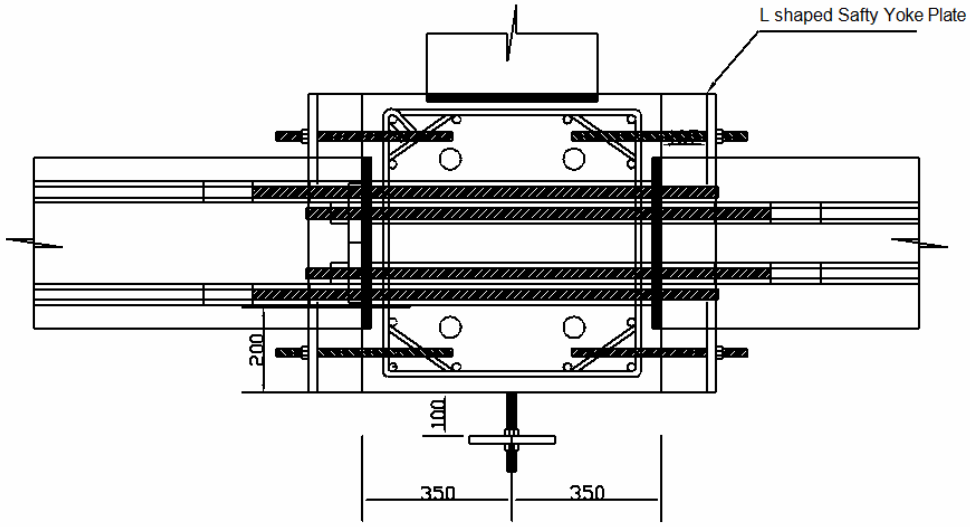

Plane View

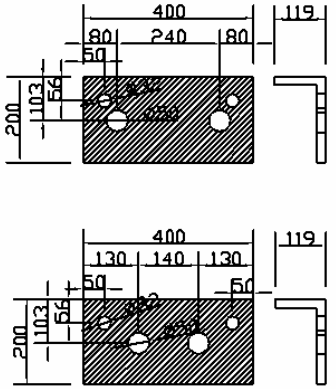

General Notes

(1) All Yoke Plate are 20mm thick mild-steel.
(2) All Anchor Bolts are M20 threaded Rods

No. | Revision/Issue | Date

Safty Yoke Plate Details at the Beam-Column Connections

Date: 9/12/05
Scale: 1:10
Sheet: SY 1

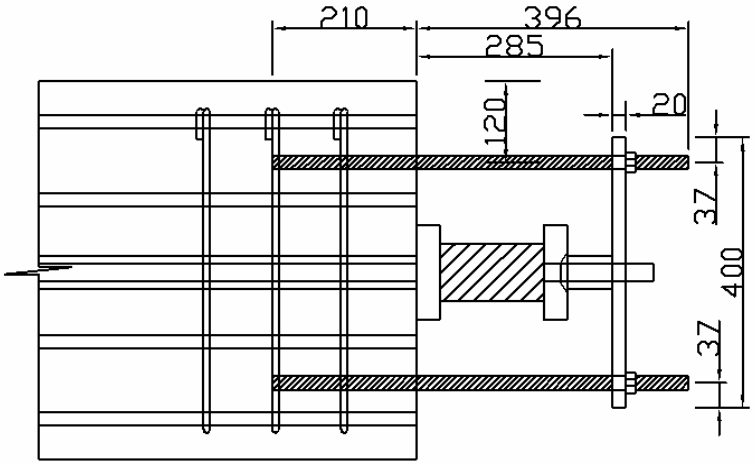

Elevation View

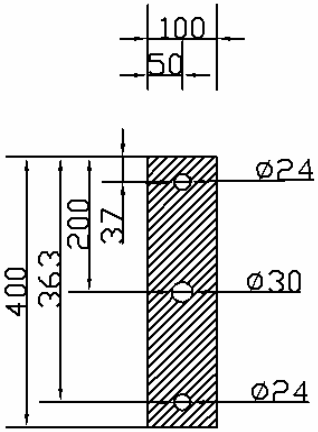

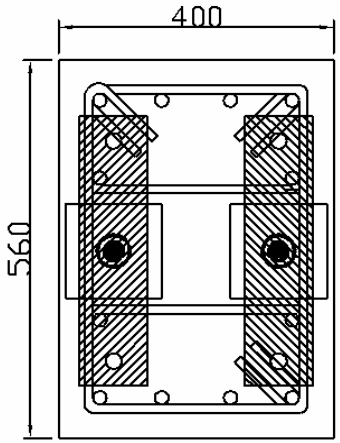

Left Beam End View

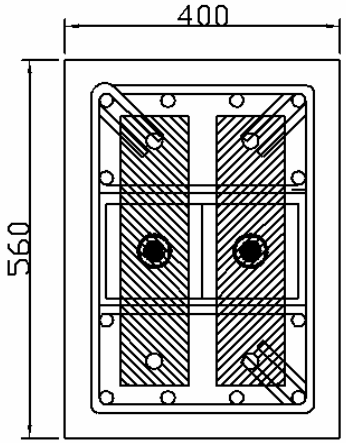

Right Beam End View

General Notes

(1) All Yoke Plate are 20mm thick mild-steel.
(2) All Anchor Bolts are M20 threaded Rods

No.	Revision/Issue	Date

Safty Yoke Plate Details at End of the Seismic Beams

Date 9/12/05	SY 2
Scale 1:10	

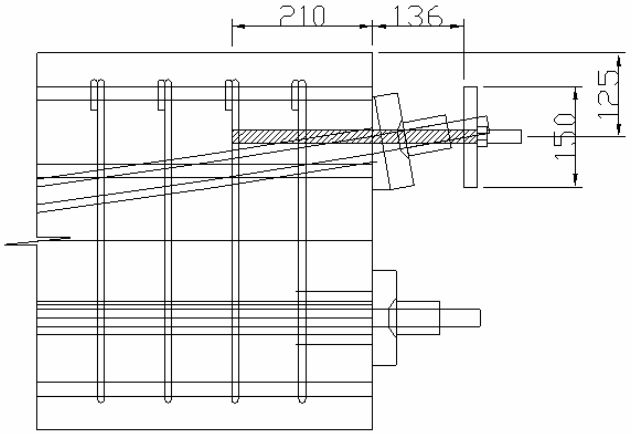

Elevation View

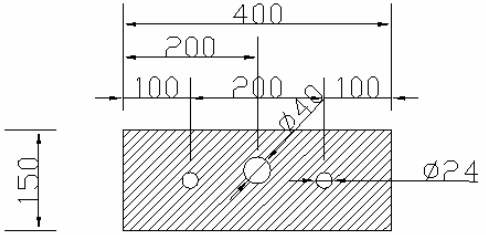

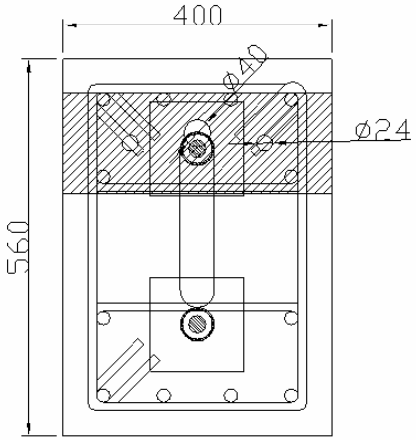

End View

General Notes

(1) All Yoke Plate are 20mm thick mild-steel.
(2) All Anchor Bolts are M20 threaded Rods

No.	Revision/Issue	Date

Firm Name and Address

Project Name and Address

Safty Yoke Plate Details at End of the Gravity Beam

Project	Sheet
Date 9/12/05	SY 3
Scale 1:10	

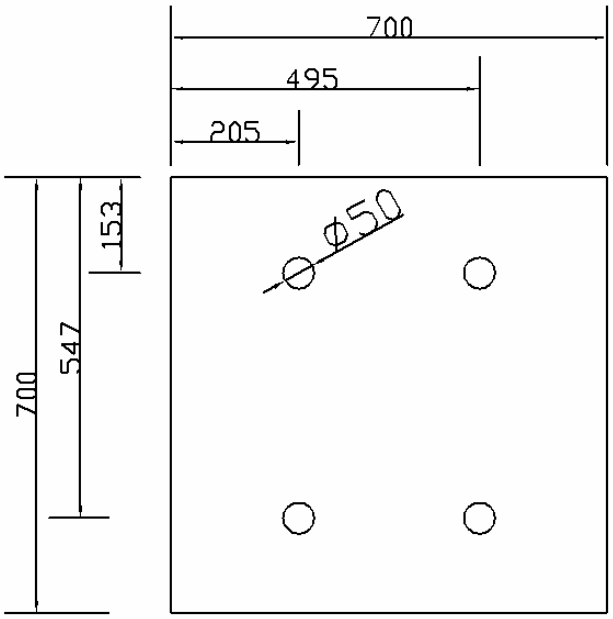

Top Column plate

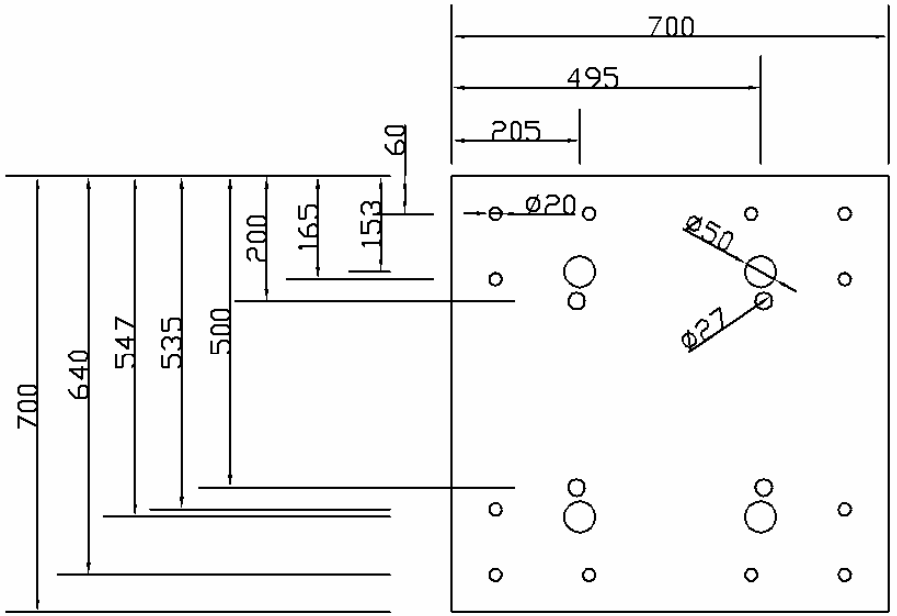

Bottom Column Plate

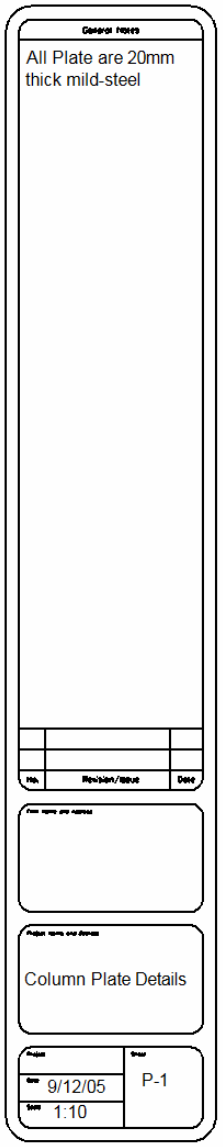

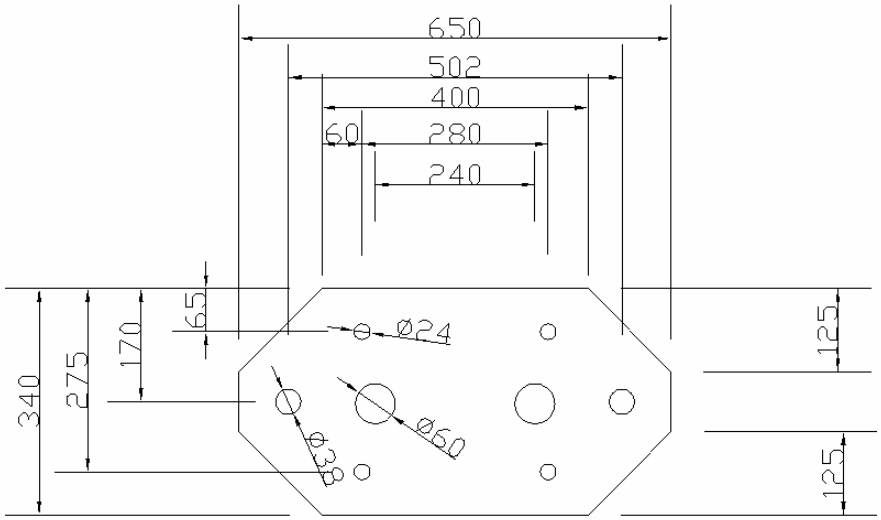

Fuse Rod Anchor Plate in Seismic Beams

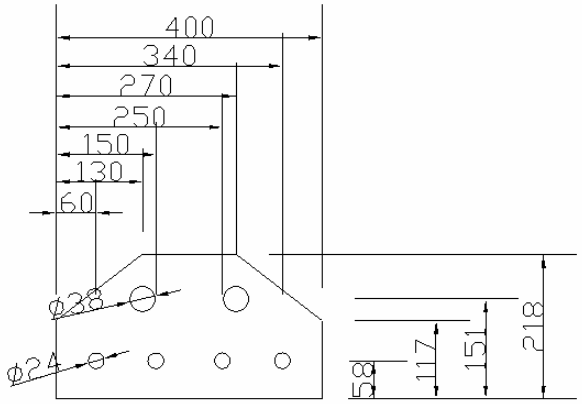

Fuse Rod Anchor Plate in Gravity Beams

General Notes

All Plate are 32mm thick mild-steel

No.	Revision/Issue	Date

File name and address

Threaded Fuse Rod Anchor Plate

Project name and address

Project	Sheet
Date 9/12/05	P-2
Scale 1:10	

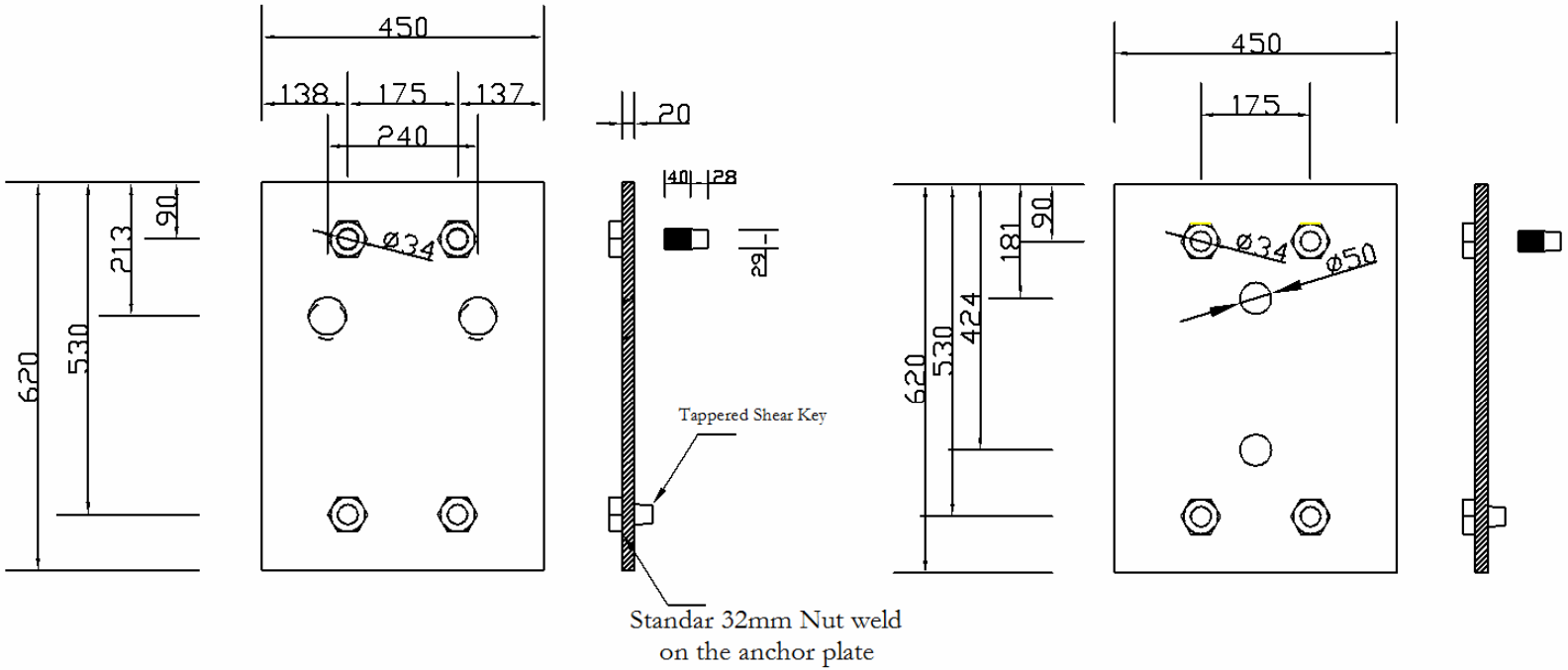

Column Armour Plate at Seismic
Beam-Column Connections

Column Armour Plate at Gravity
Beam -Column Connection

General Notes

No.	Revision/Issue	Date

Connection Armour
Plate at Column Face

9/12/05

1:10

P-3